The London School of Economics and Political Science

Financial Contagion and Instability

Yuliang Zhang

A thesis submitted to the London School of Economics and Political Science for the degree of Doctor of Philosophy. London, 2024

Declaration

I certify that the thesis I have presented for examination for the MPhil/PhD degree of the London School of Economics and Political Science is solely my own work other than where I have clearly indicated that it is the work of others (in which case the extent of any work carried out jointly by me and any other person is clearly identified in it).

I declare that this thesis consists of 111 pages.

Statement of co-authored work

I certify that Chapter 2 of this thesis is based on joint work with Luitgard Veraart. Our working paper is available at SSRN: https://dx.doi.org/10.2139/ssrn.3860262.

Abstract

The thesis contains three chapters on financial contagion and instability. Chapter 1 is devoted to a discussion of financial networks and systemic risk. I provide an overview of the literature that emphasises various channels of shock propagation through network connections, such as networks of contractual obligations or overlapping asset holdings. Two topics are discussed: interconnectedness and liquidity. Chapter 2 is concerned with post-trade netting in derivatives markets. We focus on two types of post-trade risk reduction (PTRR) services that apply multilateral netting techniques: portfolio rebalancing and portfolio compression. We first provide a mathematical characterisation of their netting mechanisms and then analyse the effects from a network perspective by considering contagion arising from defaults on variation margin payments. We provide sufficient conditions for systemic risk reduction and illustrate that post-trade netting can be harmful. We also explore the consequences when institutions strategically react to liquidity stress by delaying their payments. Chapter 3 deals with financial vulnerability. I introduce an index that formulates financial vulnerability from a systemic perspective. It is derived from a model that captures spillover losses in the system caused by deleveraging and joint liquidation of illiquid assets. Using data on U.S. banks around the Great Depression and the Global Financial Crisis, I show that the index is easy to implement and can be used for monitoring financial instability, setting the countercyclical capital buffer, and analysing historical banking crises.

Acknowledgements

I am indebted and immensely grateful to Professor Luitgard Veraart for the supervision, guidance, and support. I have benefited tremendously from discussing with her and learning from her invaluable suggestions. I thank my peers at the Financial Mathematics research group for the memorable time spent together. I thank staff members at the Department of Mathematics for their kind help. The LSE PhD studentship by the London School of Economics and Political Science is gratefully acknowledged.

Contents

Chapter 1

Introduction

In this chapter, I provide an overview of research on financial networks and systemic risk. I discuss two topics: interconnectedness and liquidity.

1.1 Interconnectedness

Most people use the word "systemic" to describe a catastrophic event. The financial world is no exception. While no precise definition exists, the term "systemic risk" has been used to represent many aspects of a crisis. Interconnectedness is one of them. The International Monetary Fund (2009, p. 73) summarises the necessity of assessing the systemic implications of financial linkages as follows:

> While more extensive linkages contribute to economic growth by smoothing credit allocations and allowing greater risk diversification, they also increase the potential for disruptions to spread swiftly across markets and borders. In addition, financial complexity has enabled risk transfers that were not fully recognized by financial regulators or by institutions themselves, complicating the assessment of counterparty risk, risk management, and policy

responses.

Identifying important institutions and exposures is closely related to the abundant academic research on measuring systemic risk. Conceptually, there are two broad categories of importance: systemicness and vulnerability. Measures have different mathematical forms, but both concepts are associated with characteristics such as size, leverage, etc. A fundamental difference is that the former indicates the influence on the rest of the network (contribution to extreme events), whereas the latter reflects the influence by the rest of the network (participation in extreme events). See Bisias et al. (2012) and Benoit et al. (2017) for comprehensive surveys.

The types of methodology depend, to some extent, on the availability of data. Bisias et al. (2012, Section 4) discuss the data issues associated with systemic risk measurement. Centrality measures in social network analysis are intuitive and easy to interpret but need granular exposure data. Popular market-based measures have the advantage of high frequency and public availability for a wide range of institutions. At the same time, they can be noisy. Benoit et al. (2017, p. 134) comment in their survey that market-based approaches can detect changes in market conditions in real time but lack theoretical foundation because they "generally do not permit to clearly identify the source of risk at play." Nevertheless, those measures can be useful as a summary statistic for empirical evaluation.

In short, any measure may be subject to criticism because it neglects the implications of some aspect of systemic risk, depending on the modellers' presumptions and toolkits. None of the proposed measures can be proved superior to all others because, understandably, no uniform criterion for comparison exists. From a practical perspective, the appropriate choice should take into account the policy objective.

The topic of systemic risk measurement is closely related to the mathematical modelling of financial contagion. This thesis builds on the abundant literature that em-

phasises various channels of shock propagation through network connections, such as networks of contractual obligations or overlapping asset holdings (see Glasserman & Young (2016) for a comprehensive review). A distinctive feature of financial network models is that they incorporate a contagion mechanism to reflect real-world features. In the case of interbank liabilities, this can manifest as the equilibrium characterisation via a fixed-point problem which embeds various clearing rules.

Theoretical contributions concentrate on the relationship between network structure and the extent of loss propagation. The development of complicated models and advanced techniques plays a crucial role in this area. The main message is that network fragility is affected by interconnections, shocks, and other potential variables in a nonlinear way. Empirical studies also attempt to understand the network origins of instability. One way is to learn the network topology from data. Another way is to estimate contagion by simulating hypothetical scenarios—for example, using stress tests to investigate the effects of various contagion mechanisms. Upper (2011) summarises the early contributions and provides some insightful comments from a policy perspective. Borio et al. (2014) also provide an assessment of stress testing, with an emphasis on how best to make it useful. Parenthetically, network analysis is only part of the methodologies for macroprudential stress testing, which targets the entire financial system and its interactions with the real economy; see Aikman et al. (2023) for an extensive survey.

1.2 Liquidity

Liquidity was at the heart of the Global Financial Crisis. Some observers interpret liquidity as security. From a theoretical perspective, liquidity has many ramifications in financial markets. The literature on understanding the causes and explaining the eco-

nomic mechanisms underlying liquidity crises is voluminous (see Sufi & Taylor (2022) for a review). One recurring theme is the "vicious spirals" between institutions and asset values. Kindleberger (1978, p. 107), for example, notes that "[t]o the extent that speculators are leveraged with borrowed money, the decline in price leads to further calls on them for margin or cash, and to further liquidation."

Substantial theories and empirical evidence in the academic literature enrich this description. Of particular importance is the financial accelerator hypothesis of Bernanke & Gertler (1989). The basic story is that a drop in asset prices deteriorates the balance sheet condition of borrowers (or lenders), further pushing down asset prices due to some economic constraints. Brunnermeier (2009) provides a clear interpretation of the theoretical underpinnings of potential channels in the case of the Global Financial Crisis.

Asset fire sales are a vivid example of the "illiquidity spirals." When an institution, say a bank, experiences a shock, its equity is eroded. To remain functioning, it may be forced to deleverage by selling assets. Selling under pressure, however, can depress asset prices because the potential buyers may have difficulty absorbing the sales, especially during the market meltdown. Because banks in the system that have incentives for diversification invest in similar assets, the price impact of one bank's selling affects not only itself but also other banks with overlapping portfolios. Moreover, many distressed banks attempt to dump assets during the same period, further exacerbating the spillover.

The phenomenon of fire sales draws much attention in the financial network literature, which uses a bipartite graph as the cornerstone for modelling such price-mediated contagion. The economic constraints are essential to the model. In this regard, behavioural assumptions are made to capture realistic scenarios. Of course, the network of overlapping portfolios and the network of contractual obligations can be treated

simultaneously in a holistic fashion, as stress testing does. In a nutshell, network models allow for treating the system as a whole and therefore can be useful from a macroprudential perspective.

1.3 An integrated perspective

The two topics discussed so far have a long history in academic research. This is not surprising. For example, Leontief (1936) pioneered the input-output models to analyse the economic structure of the United States; in some sense, the literature on financial contagion inherits his spirit. In the following, I briefly introduce the topics of this thesis.

Chapter 2 analyses the implications of Post-trade Risk Reduction (PTRR) services on systemic risk. These services use multilateral netting techniques to mitigate operational and counterparty risks in derivatives markets, leading to a change in the structure of contractual obligations. We model payment networks in the form of variation margin obligations, which should be fulfilled with highly liquid assets within a short time. In this sense, we focus on illiquidity contagion due to margin calls in a systemic context. Partly influenced by stress testing models, we also explore the implications under the assumption that institutions strategically react to liquidity stress by delaying their payments.

Chapter 3 introduces an index of financial vulnerability using a model of fire sales in the banking system. The index is expressed in terms of the size-weighted leverage and the illiquidity-weighted Herfindahl-Hirschman Index, making it easy to implement. Keeping a systemic perspective, I aim to balance theoretical development and practical applications while connecting measurement to instability monitoring, macroprudential regulation, and historical banking crises.

Chapter 2

Post-trade netting and contagion

2.1 Introduction

Recent regulatory reforms to enhance the resilience of over-the-counter (OTC) derivatives markets have provided incentives for market participants to use *post-trade risk reduction (PTRR)* services, which apply multilateral netting techniques to help mitigate risks and manage collateral obligations.[1] PTRR services consist mainly of portfolio compression and portfolio rebalancing. Portfolio compression reduces gross notional positions; portfolio rebalancing reduces counterparty exposures. They share the property of keeping each participant's net position unchanged to ensure market risk neutrality.

With the aim of mitigating operational and counterparty risks in existing derivatives portfolios, PTRR services can reduce the complexity of the intermediation chains. However, this may not imply that they reduce all dimensions of systemic risk stemming from the interconnections. In this work, we will use a network approach to explore the systemic implications of the PTRR services.

[1] See Duffie (2018) for an overview of post-crisis regulatory reforms.

We start by providing a definition of *post-trade netting (PTN-) exercise*. Our mathematical characterisation allows for analysing the PTRR services in a unified way. We focus on contagion in variation margin payment networks, extending the analysis from the previous literature on the relationship between portfolio compression and systemic risk (see below). Following Veraart (2022), we compare the set of defaulting banks under the clearing framework of Veraart (2020) from an ex post point of view. We say that a PTN-exercise reduces systemic risk if there is no default that arises only in the PTN-network but not in the original network—in other words, default is not propagated. Our main result, Theorem 2.4.2, shows that when considering the greatest equilibrium, no default among participants is sufficient for PTN-exercises to reduce systemic risk. Moreover, this insight also holds in an ex ante analysis.

We also consider the least equilibrium, which is particularly relevant in the context of derivatives markets. According to Paddrik et al. (2020) and Bardoscia et al. (2021), financial institutions can react strategically to liquidity stress by delaying their variation margin payments. Bardoscia et al. (2019) develop a clearing framework to capture this feature. We show that its output is mathematically equivalent to the least equilibrium under zero recovery rates (Proposition 2.5.2). Then, we show that some previous results do not carry over to this "worst" equilibrium unless an additional assumption is made. We use an example to illustrate that despite some potential benefits already mentioned, post-trade netting could distort loss propagation and therefore does not guarantee to mitigate contagion risk from a network perspective.

The rest of this chapter is organised as follows. The remainder of this section discusses the related literature. Section 2.2 introduces the PTRR services and the mathematical characterisations. Section 2.3 presents the framework for assessing systemic risk. Sections 2.4 and 2.5 contain the main analyses, followed by the concluding remarks in Section 2.6. Appendix A.1 describes the algorithmic characterisations of

the clearing frameworks mentioned in Section 2.5. Appendix A.2 provides the omitted proofs.

2.1.1 Related literature

The literature on modern netting activities has focused mainly on centralised netting by central counterparties (CCPs). For example, Duffie & Zhu (2011) point out a trade-off in netting efficiency between multilateral central clearing and bilateral clearing; Glasserman et al. (2016) analyse illiquidity associated with netting by multiple CCPs; and Amini et al. (2016) show that partial multilateral netting can have adverse effects on network contagion.

The literature on PTRR services has been scarce. We are unaware of any work exploring the implications of portfolio rebalancing for systemic risk. There are two strands of literature on portfolio compression. The first strand focuses on compression algorithms. O'Kane (2017) proposes several optimisation-based algorithms for portfolio compression and compares their performance in exposure reduction. Similarly, D'Errico & Roukny (2021) study the netting efficiency of portfolio compression under different levels of preference and use a transaction-level data set to demonstrate how much market excess can be eliminated.

The second strand focuses on the risk implications of portfolio compression using network models. Veraart (2022) derives several necessary conditions for portfolio compression to be harmful to the system and shows how the harmfulness can potentially arise. Schuldenzucker & Seuken (2020) apply the Rogers & Veraart (2013) model to investigate compression incentives and when compression can bring adverse effects to the detriment of the system. Amini & Feinstein (2023) formulate an optimal network compression problem in which systemic risk measures are incorporated in the objective function. Amini & Minca (2020) have looked further into the change of seniority

structure of claims induced by central clearing as well as portfolio compression.

2.2 Post-trade netting

2.2.1 The derivatives market

We consider a financial system comprised of institutions $\mathcal{N} = \{1, 2, ..., N\}$ $(N \geq 3)$. These institutions (hereafter called "banks") are typically dealer banks active in global derivatives markets. (Of course, our discussion also applies to a wide range of non-banks that use PTRR services.)

Banks are connected by derivatives contracts, represented by a *notional matrix* $C \in [0, \infty)^{N \times N}$, where C_{ij} denotes the notional amount of liabilities of bank i to bank j, and $C_{ii} = 0$ for all $i \in \mathcal{N}$. The derivatives contracts are fungible and traded over-the-counter (OTC). Consider, for example, single-name Credit Default Swap (CDS) contracts written on the same reference entity with the same maturity date.[2] In this case, C_{ij} can be the notional amount that bank i has promised to bank j if a credit event of the underlying reference entity occurs.

Given a notional matrix C, the *net exposures* of C are given by $C^\top \mathbf{1} - C\mathbf{1}$, where $\mathbf{1}$ is the column vector containing only 1s. The *bilaterally netted notional matrix* associated with C is denoted by C^{bi}, where $C^{bi}_{ij} = \max(C_{ij} - C_{ji}, 0)$ for all $i, j \in \mathcal{N}$. Note that the net exposures of C and C^{bi} are the same.

[2]The derivatives contracts are comparable in the sense that they have the same fundamental characteristics such as maturity and underlying. CDS contracts have been standardised in terms of coupons and maturity dates. Trade positions on these contracts can be bucketed by the reference entity (single name or index) and maturity.

2.2.2 Post-trade risk reduction services

We first provide some background information.[3] Then, we use simple examples to introduce the basic ideas of PTRR services.

Institutional background

A PTRR exercise can be divided into three steps: First, participants submit their portfolio information to a third-party service provider (not a party to the transactions) and specify risk tolerances. Second, the service provider runs its optimisation algorithms and informs each participant of its new portfolio positions. Third, the new positions are established once all participants agree (otherwise, the exercise is void).

The development of PTRR services can be divided into a few stages.[4] Before the Global Financial Crisis, the volume of outstanding derivatives contracts proliferated. Concerns about counterparty risk drove the increase in the CDS market near the crisis. According to Vause (2010), the subsequent fall in notional amounts can be partly attributed to portfolio compression. Following the mandatory clearing of standardised derivatives contracts, services like the triReduce introduced by TriOptima in 2003 for the interest rate swap (IRS) market compresses bilateral swaps and products in the centrally cleared markets.[5] The International Swaps and Derivatives Association (2012) reports that the progress on eliminating outstanding IRS notional positions since 2011 is significant.

[3]Because of the frequent updates, we also refer interested readers to the service providers' websites for the latest information. See, e.g., https://osttra.com/. At the time of writing, CME's TriOptima—one of the leading PTRR service providers—is part of OSTTRA, a joint venture formed on 1st September 2021 between IHS Markit and CME Group. (IHS Markit was acquired by S&P Global on 1st March 2022.)

[4]Post-trade netting mechanisms have been developed throughout Europe since the thirteenth century. Merchants used them in early modern fairs to clear bills of exchange. See Börner & Hatfield (2017) for the historical background.

[5]TriOptima collaborates with LCH.Clearnet on SwapClear; see https://www.lch.com/services/swapclear/enhancements/compression.

Although regulatory reforms are intended to make financial markets more resilient, their implementation is costly. The recent development of PTRR services is attributable to these reforms, such as the Uncleared Margin Rules (UMRs), capital requirements (the SA-CCR and G-SIBs' capital surcharges), and leverage ratio requirements. Because margin and capital costs are often aligned with common risk metrics, portfolio rebalancing that optimises counterparty exposures could potentially reduce the all-in cost of trading derivatives. Meanwhile, technological factors also spur the development of PTRR services. Equipped with advanced optimisation techniques and data processing skills, the Fintech vendors can in principle achieve efficient outcomes by accessing information submitted by a large network of market participants.

Examples

Figure 2.1 shows an example of portfolio rebalancing, also known as counterparty risk rebalancing, which injects market risk-neutral transactions to "reduce counterparty risk by reducing the exposure between two counterparties" (European Securities and Markets Authority, 2020, p. 7). The process of injecting transactions can be illustrated in matrix form as follows:

$$\begin{pmatrix} 0 & 10 & 0 \\ 0 & 0 & 10 \\ 10 & 0 & 0 \end{pmatrix} + \begin{pmatrix} 0 & 0 & 5 \\ 5 & 0 & 0 \\ 0 & 5 & 0 \end{pmatrix} = \begin{pmatrix} 0 & 10 & 5 \\ 5 & 0 & 10 \\ 10 & 5 & 0 \end{pmatrix}.$$

Two observations are in order. First, the initial net exposures of the three banks are $(0, 0, 0)^\top$, which coincide with the net exposures after portfolio rebalancing. Second, portfolio rebalancing increases the gross notional positions from 30 to 45, but it decreases the sum of bilateral exposures from 30 to 15. In this sense, portfolio rebalancing can decrease aggregate variation margin requirements (which are netted bilaterally).

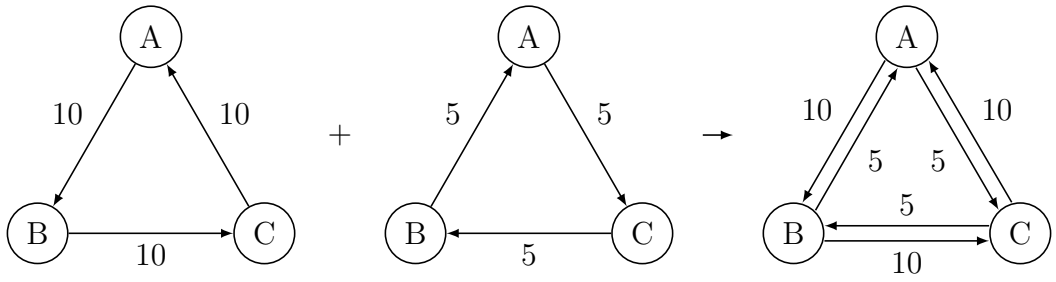

Figure 2.1. Example of portfolio rebalancing.

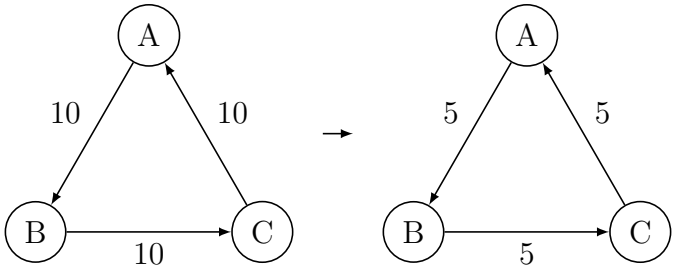

Figure 2.2. Example of portfolio compression.

Figure 2.2 shows an example of portfolio compression, which "aims to reduce the number of contracts and/or the notional amounts of derivatives contracts in a particular asset class/product without changing the market risk of the portfolio" (European Securities and Markets Authority, 2020, p. 7). In our case, the gross notional amounts decrease from 30 to 15.

2.2.3 The mathematical characterisation

Next, we introduce the general mathematical characterisation that embeds the main features of PTRR services.

Definitions

Definition 2.2.1 (Post-trade-netting-exercise)**.** Let $\mathcal{P} \subseteq \mathcal{N}$ and $C, C^{\mathcal{P}} \in [0, \infty)^{N \times N}$. We refer to any element of $\mathcal{P}$ as a *participant* and to $(C, \mathcal{P}, C^{\mathcal{P}})$ as a *post-trade-netting*

exercise (PTN-exercise) if $C^{\mathcal{P}}_{ij} = C_{ij}\ \forall\,(i,j) \notin \mathcal{P}\times\mathcal{P}$ and

$$\sum_{j\in\mathcal{P}}(C^{\mathcal{P}}_{ji} - C^{\mathcal{P}}_{ij}) = \sum_{j\in\mathcal{P}}(C_{ji} - C_{ij}) \quad \forall\, i \in \mathcal{P}. \tag{PTN-constraint}$$

According to the definition, derivatives positions can only change between participants. In addition, the PTN-constraint ensures that the net exposures remain the same after the PTN-exercise.

Remark 2.2.2. $(C, \mathcal{P}, C^{\mathcal{P}})$ is a PTN-exercise if and only if $(C^{\mathcal{P}}, \mathcal{P}, C)$ is a PTN-exercise.

We say a PTN-exercise is a *rebalancing exercise* if $C^{\mathcal{P}} = C + R$ for some rebalancing matrix $R \in [0,\infty)^{N\times N}$, where $R_{ij} = 0$ for all $(i,j) \notin \mathcal{P}\times\mathcal{P}$ and $\sum_{j\in\mathcal{P}} R_{ji} = \sum_{j\in\mathcal{P}} R_{ij}$ for all $i \in \mathcal{P}$. Otherwise, we call the exercise a *compression exercise* and refer to the matrix $C^{\mathcal{P}}$ as the compressed notional matrix. Consequently, the rebalancing matrix represents the transactions to be injected into the original portfolio, while the compressed notional matrix represents the resulting portfolio with some transactions compressed. The result below formalises the relationship between netting by portfolio rebalancing and netting by portfolio compression.

Proposition 2.2.3 (The rebalancing-compression parity)**.** Let C be a notional matrix and $\mathcal{P} \subseteq \mathcal{N}$. For any compressed notional matrix K, define a matrix R by

$$R_{ij} = \max\{0, (K_{ij} - K_{ji}) - (C_{ij} - C_{ji})\} \quad \forall\, i,j \in \mathcal{N}. \tag{2.1}$$

Then R is a rebalancing matrix and satisfies

$$(C + R)^{bi} = K^{bi}. \tag{2.2}$$

Conversely, if R is a rebalancing matrix, then $K = (C + R)^{bi}$ is a compressed notional matrix.

Proof. We first show that R defined by (2.1) is a rebalancing matrix and satisfies equation (2.2). By construction, R is non-negative and satisfies

$$\sum_{j\in\mathcal{P}}(R_{ij} - R_{ji}) = \sum_{j\in\mathcal{P}}(K_{ij} - K_{ji}) - \sum_{j\in\mathcal{P}}(C_{ij} - C_{ji}) = 0 \quad \forall\, i \in \mathcal{P},$$

where the last equality follows from the definition of the compressed notional matrix. In addition, $R_{ij} = R_{ji} = 0$ for all $(i, j) \notin \mathcal{P} \times \mathcal{P}$. Therefore, matrix R is a rebalancing matrix. Moreover, for all $i, j \in \mathcal{N}$,

$$\begin{aligned}(C + R)^{bi}_{ij} &= \max\{0, (C_{ij} - C_{ji}) + (R_{ij} - R_{ji})\} \\ &= \max\{0, (C_{ij} - C_{ji}) + (K_{ij} - K_{ji}) - (C_{ij} - C_{ji})\}\end{aligned}$$

and hence $(C + R)^{bi} = K^{bi}$.

We next show that $K = (C + R)^{bi}$ is a compressed notional matrix if R is a rebalancing matrix. First, K is non-negative. Second, for all $i \in \mathcal{P}$,

$$\begin{aligned}\sum_{j\in\mathcal{P}}(K_{ji} - K_{ij}) &= \sum_{j\in\mathcal{P}}\left[(C + R)^{bi}_{ji} - (C + R)^{bi}_{ij}\right] \\ &= \sum_{j\in\mathcal{P}}(C_{ji} + R_{ji} - C_{ij} - R_{ij}) \\ &= \sum_{j\in\mathcal{P}}(C_{ji} - C_{ij}).\end{aligned}$$

It follows that K is a compressed notional matrix. □

Constraints

Proposition 2.2.3 holds because our mathematical characterisation considers only one constraint on the net exposures. Post-trade netting can certainly include additional constraints. In practice, a diverse set of participants impose risk tolerances according to their preferences. Although a further discussion along this line is beyond the scope of our work and our main results in Section 2.4 do not depend on the additional constraints, we find it useful to discuss some examples below.

First, if the objective is to reduce counterparty risk, the bilateral net exposure is an appropriate metric. The constraint on one counterparty pair could be, for example,

$$|C^{\mathcal{P}}_{ji} - C^{\mathcal{P}}_{ij}| \leq |C_{ji} - C_{ij}|. \tag{2.3}$$

If this holds for all participants, then

$$\sum_{j \in \mathcal{N}} (C^{\mathcal{P}})^{bi}_{ij} \leq \sum_{j \in \mathcal{N}} C^{bi}_{ij} \quad \forall\, i \in \mathcal{P}.$$

As for the notional amount reduction, one constraint could be

$$C^{\mathcal{P}}_{ij} \leq C_{ij}, \tag{2.4}$$

which is similar to the loop compression in O'Kane (2017) and the conservative compression in D'Errico & Roukny (2021).

Note that these constraints need not be applied to all participants. Due to diverse needs, one would expect the delivery of the optimisation services to be a combination of compression and rebalancing. For example, a bank sensitive to the leverage ratio requirement prefers compression, while another bank concerned about the capital requirement chooses rebalancing. The advantage of the service provider is that it can

pool all the information and optimise over several metrics simultaneously.

Consider the example in Figure 2.3. Suppose that bank B only participates in compression. Also, suppose that bank D's portfolio is non-compressible—the reason might be that the transactions belong to a different asset class ineligible for compression. It is straightforward to check that the net exposures remain unchanged, constraints (2.3) and (2.4) are satisfied, and the sum of the bilateral exposures is reduced. In this example, it seems important that banks A and C accept transaction injection; otherwise, the efficiency of exposure optimisation would be hampered.

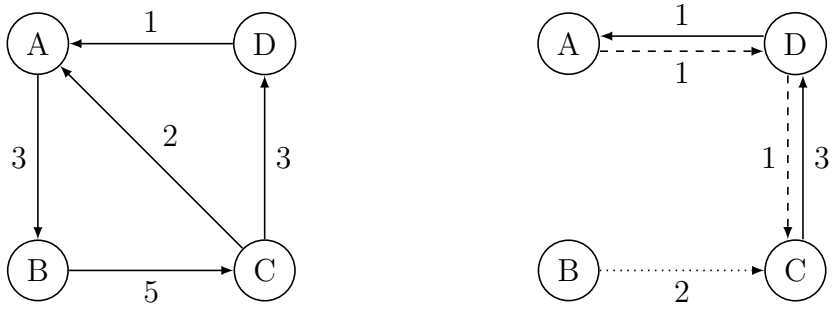

(a) Before. **(b)** After.

Figure 2.3. A combination of portfolio compression and portfolio rebalancing. The numbers next to the arrows represent notional amounts. The dotted and dashed lines indicate the new transactions resulting from compression and rebalancing, respectively.

An optimisation-based characterisation

Lastly, we note that post-trade netting can also be characterised from an optimisation perspective. A natural objective is to minimise the aggregate obligations.

Definition 2.2.4 (Optimal post-trade-netting-exercise)**.** Let $\mathcal{P} \subseteq \mathcal{N}$ and $C \in [0, \infty)^{N \times N}$.

The *PTN-optimisation problem* is defined as

$$\begin{aligned} \min_{\tilde{C}} \quad & \sum_{i\in\mathcal{N}}\sum_{j\in\mathcal{N}} \tilde{C}_{ij} \\ \text{s.t.} \quad & \sum_{j\in\mathcal{P}}(\tilde{C}_{ji} - \tilde{C}_{ij}) = \sum_{j\in\mathcal{P}}(C_{ji} - C_{ij}) && \forall\, i \in \mathcal{P}, \\ & \tilde{C}_{ij} = C_{ij} && \forall\, (i,j) \notin \mathcal{P}\times\mathcal{P}. \end{aligned}$$

Let C^* be a solution to the PTN-optimisation problem. We refer to the triple $(C, \mathcal{P}, C^*)$ as an *optimal* PTN-exercise.

The PTN-optimisation problem is a linear programming problem and admits a solution since the feasible region is non-empty (matrix C satisfies all constraints, and the objective function is bounded from below by zero). In addition, when $\mathcal{P} = \mathcal{N}$, this problem is equivalent to the non-conservative compression problem in D'Errico & Roukny (2021) (see also the method of minimising the l_1-norm in O'Kane (2017)).

2.3 Assessing systemic risk

In this section, we describe the framework for analysing the effects of PTN-exercises on systemic risk.

2.3.1 The payment network

We model the network of payment obligations in the form of variation margins as in Paddrik et al. (2020) and Veraart (2022). Given a notional matrix C, we define the *liabilities matrix* L associated with C by

$$L = \psi C^{bi},$$

where the parameter ψ ($\psi > 0$) can be thought of as capturing the magnitude of variation margins in reduced form. Due to mark-to-market valuations of derivatives contracts, variation margins are exchanged on short notice to protect counterparties from current exposures. We have in mind, for example, the case of American International Group, Inc. (AIG) in the CDS market during the Global Financial Crisis. The protection seller faced tremendous pressure on the margin calls from the protection buyers after a sudden shock to the credit markets.

Remark 2.3.1. A more general definition is $L = f(C)$, where $f : [0,\infty)^{N\times N} \to [0,\infty)^{N\times N}$ could be $f(C) = \psi C^{bi}$ or $f(C) = \psi C$. It can be extended to incorporate multiple assets. Consider, for example, CDS contracts on the same reference entity with k ($k > 1$) different maturity dates and the corresponding notional matrices $C_1, \ldots, C_k$. The liabilities matrix can then be written as $L = f(C_1, \ldots, C_k)$, where $f : [0,\infty)^{N\times N} \times \ldots \times [0,\infty)^{N\times N} \to [0,\infty)^{N\times N}$ maps the notional positions to the variation margin requirements. One simple example is that f is a linear function in all k arguments.

While post-trade netting works on notional positions, we find it mathematically convenient to define the PTN-exercise using matrices representing the associated liabilities (here, the variation margin payment obligations). We will use Lemma 2.3.2 to focus on the liabilities matrices and refer to $(L, \mathcal{P}, L^{\mathcal{P}})$ as a PTN-exercise.

Lemma 2.3.2. Let $(C, \mathcal{P}, C^{\mathcal{P}})$ be a PTN-exercise. Given $\psi > 0$, let $L = \psi C^{bi}$ and $L^{\mathcal{P}} = \psi (C^{\mathcal{P}})^{bi}$. Then, $(L, \mathcal{P}, L^{\mathcal{P}})$ is a PTN-exercise.

Proof. Note that

$$\begin{aligned}\sum_{j\in\mathcal{P}}\left(\psi(C^{\mathcal{P}})^{bi}_{ji}-\psi(C^{\mathcal{P}})^{bi}_{ij}\right) &= \psi\left[\sum_{C^{\mathcal{P}}_{ji}\geq C^{\mathcal{P}}_{ij}}\left(C^{\mathcal{P}}_{ji}-C^{\mathcal{P}}_{ij}\right)-\sum_{C^{\mathcal{P}}_{ji}<C^{\mathcal{P}}_{ij}}\left(C^{\mathcal{P}}_{ij}-C^{\mathcal{P}}_{ji}\right)\right]\\ &= \psi\sum_{j\in\mathcal{P}}\left(C^{\mathcal{P}}_{ji}-C^{\mathcal{P}}_{ij}\right)=\psi\sum_{j\in\mathcal{P}}\left(C_{ji}-C_{ij}\right)\\ &= \sum_{j\in\mathcal{P}}\left(\psi C^{bi}_{ji}-\psi C^{bi}_{ij}\right).\end{aligned}$$

Therefore, the PTN-constraint in Definition 2.2.1 holds for $(\psi C^{bi},\mathcal{P},\psi(C^{\mathcal{P}})^{bi})$. □

We assume that each bank holds a *liquidity buffer* $A^b_i\geq 0$, which may represent cash or high-quality liquid assets to the extent that they can be readily exchanged as variation margins. We summarise banks' liquidity buffers in the N-dimensional vector $A^b=(A^b_1,\ldots,A^b_N)^\top$. We shall refer to the pair (L,A^b) as the *original network* and to the pair $(L^{\mathcal{P}},A^b)$ as the *PTN-network*.

2.3.2 The clearing equilibrium

To characterise the clearing equilibrium, we apply the network model of Veraart (2020), which is used by Veraart (2022) to analyse portfolio compression.

Denote by $\mathbb{1}_{\{\cdot\}}$ the indicator function. The model's key ingredient is a *valuation function* $\mathbb{V}:\mathbb{R}\to[0,1]$ defined by

$$\mathbb{V}(y)=\mathbb{1}_{\{y\geq 1+k\}}+\mathbb{1}_{\{y<1+k\}}r(y),$$

where $k\geq 0$ and $r:(-\infty,1+k)\to[0,1]$ is a non-decreasing and right-continuous function. The specification can summarise various types of asset valuation rules via particular functional forms of $\mathbb{V}$. It conveniently nests several network clearing models

as special cases. For example, Veraart (2020) shows that the clearing vector in the Eisenberg & Noe (2001) model can be expressed using $\mathbb{V}^{\mathrm{EN}}(y) = 1 \wedge y^+$. A definition that will be used later is the *zero recovery rate valuation function* in Veraart (2022):

$$\mathbb{V}^{\mathrm{zero}}(y) = \mathbb{1}_{\{y \geq 1+k\}}.$$

Since a valuation function is used for risk assessment, for any PTN-exercise $(L, \mathcal{P}, L^{\mathcal{P}})$, we also refer to $(L, A^b; \mathbb{V})$ as the *original network* and $(L^{\mathcal{P}}, A^b; \mathbb{V})$ as the *PTN-network*.

The clearing equilibrium is defined by a quantity called *re-evaluated equity*. The underlying idea is that each bank's available assets—the liquidity buffer plus the incoming payments from its counterparties—depend on the payments that other banks in the network can make. As a result, the re-evaluated equity is characterised as a fixed point.

Definition 2.3.3 (Re-evaluated equity)**.** Given the original network $(L, A^b; \mathbb{V})$, let $\mathcal{E} = [-\bar{L}, A^b + \bar{A} - \bar{L}]$, where $\bar{L} = L\mathbf{1}$ and $\bar{A} = \mathbf{1}^\top L$. Define the function $\Phi = \Phi(\cdot; \mathbb{V}) : \mathcal{E} \to \mathcal{E}$ as

$$\Phi_i(E) = \Phi_i(E; \mathbb{V}) = A_i^b + \sum_{j:\bar{L}_j > 0} L_{ji} \mathbb{V}\left(\frac{E_j + \bar{L}_j}{\bar{L}_j}\right) - \bar{L}_i \quad \forall\, i \in \mathcal{N}. \tag{2.5}$$

We refer to a vector $E \in \mathcal{E}$ satisfying $E = \Phi(E)$ as a *re-evaluated equity* in the original network.

Analogously, we can define the re-evaluated equity in the PTN-network, which is provided in Appendix A.2.1 to simplify the exposition. As noted by Veraart (2020), $(\mathcal{E}, \leq)$ is a complete lattice, and the functions Φ is non-decreasing, so the existence of a re-evaluated equity is guaranteed by Tarksi's fixed-point theorem (Theorem 1 in Tarski (1955)). Moreover, one can always find the greatest and the least re-evaluated

equity. In Sections 2.4 and 2.5, we will discuss the implications of post-trade netting under these fixed points.

2.3.3 The default set

A few concepts are necessary before explaining what we mean by systemic risk reduction. Given the original network $(L, A^b; \mathbb{V})$, the *initial equity*, denoted as $E^{\text{initial}}(L)$, is

$$E_i^{\text{initial}}(L) = A_i^b + \sum_{j \in \mathcal{N}} L_{ji} - \bar{L}_i \quad \forall\, i \in \mathcal{N}.$$

The *fundamental default set*, denoted as $\mathcal{F}(L, A^b; \mathbb{V})$, is the set of banks that default even if all banks in the network make their payments in full, i.e.,

$$\mathcal{F}(L, A^b; \mathbb{V}) = \{i \in \mathcal{N} \mid E_i^{\text{initial}}(L) < 0\}.$$

Let E be a re-evaluated equity (i.e., a fixed point of Φ in equation (2.5)). Then, the *default set* is

$$\mathcal{D}(L, A^b; \mathbb{V}) = \mathcal{D}(E) = \{i \in \mathcal{N} \mid E_i < 0\},$$

and the *contagious default set* is $\mathcal{D}(L, A^b; \mathbb{V}) \setminus \mathcal{F}(L, A^b; \mathbb{V})$. Clearly, they both depend on the fixed point.

Remark 2.3.4. The default set in Veraart (2022) is defined as $\{i \in \mathcal{N} \mid E_i < k\bar{L}_i\}$, where k is the parameter in the valuation function (see Remark A.1 in Veraart (2022) for further discussion). Here, we set $k = 0$ and interpret this choice as modelling illiquidity in the context of variation margin payments. Note that each bank's total assets consist only of its liquidity buffer and margin payments received, which are highly liquid assets. In other words, we do not intend to model the full balance sheet.

We analyse from an ex post point of view, as in Veraart (2022). Specifically, we

compare the default set in the original network and the PTN-network, assuming that the PTN-exercise is completed before a shock. (We abstract away from the source of the shock, which is not our focus.)

Definition 2.3.5. For any PTN-exercise, let E be a re-evaluated equity in the original network with default set $\mathcal{D}(E)$ and $E^{\mathcal{P}}$ be a re-evaluated equity in the PTN-network with default set $\mathcal{D}(E^{\mathcal{P}})$. We say that the PTN-exercise (i) *reduces systemic risk* if $\mathcal{D}(E^{\mathcal{P}}) \subseteq \mathcal{D}(E)$; (ii) *strongly reduces systemic risk* if $\mathcal{D}(E^{\mathcal{P}}) \subsetneq \mathcal{D}(E)$; and (iii) is *harmful* if $\mathcal{D}(E^{\mathcal{P}}) \setminus \mathcal{D}(E) \neq \emptyset$.

This definition, consistent with that of Veraart (2022), implies that a PTN-exercise reduces systemic risk if and only if it is not harmful. We leave the discussion about the interpretation of systemic risk reduction to Section 2.6.1.

It is important to note that since there can be more than one re-evaluated equity in a network, Definition 2.3.5 makes sense only if the re-evaluated equities in the original and the PTN-network are comparable. Put differently, we cannot compare the two networks using random fixed points. In what follows, we shall focus on the cases where both re-evaluated equities correspond to the greatest fixed points or the least fixed points.

2.4 Main results

In this section, we analyse when post-trade netting reduces systemic risk. We first consider a special case and then present the general conditions sufficient for risk reduction.

2.4.1 The intermediation chains

We start by looking at the case of optimal PTN-exercise in which all banks are participants. This is unlikely to happen in practice, but the result is useful for providing an

insight about the mechanism of post-trade netting.

Proposition 2.4.1. Consider an optimal PTN-exercise with $\mathcal{P} = \mathcal{N}$. Let $\tilde{E}$ be the greatest re-evaluated equity in the original network with default set $\mathcal{D}(\tilde{E})$ and $\tilde{E}^{\mathcal{P}}$ be the greatest re-evaluated equity in the PTN-network with default set $\mathcal{D}(\tilde{E}^{\mathcal{P}})$. Then, $\mathcal{D}(\tilde{E}^{\mathcal{P}})$ is the fundamental default set in the PTN-network and $\mathcal{D}(\tilde{E}^{\mathcal{P}}) \subseteq \mathcal{D}(\tilde{E})$.

Any default in the PTN-network (if it exists) is a fundamental default, and hence, this optimal PTN-exercise reduces systemic risk under the greatest re-evaluated equity. To prove Proposition 2.4.1, we exploit a result of D'Errico & Roukny (2021), who show in the case of portfolio compression that the graph with the minimum total exposures is bipartite. As a result, the situation in which bank i should pay bank j and bank j should pay a different bank k does not exist.

Figure 2.4 provides a stylised illustration of an optimal PTN-exercise. Banks are simply classified into dealers and end-users. All dealers participate in the exercise. The direction of the arrows indicates the net variation margin owed between counterparties. In Figure 2.4a, feedback loops in the dealers' section may amplify default cascades, whereas they disappear in Figure 2.4b since this PTN-exercise breaks up possible contagion channels between dealers. (Nevertheless, the contagious default of a dealer remains possible when it is hit by a shock from an end-user.)

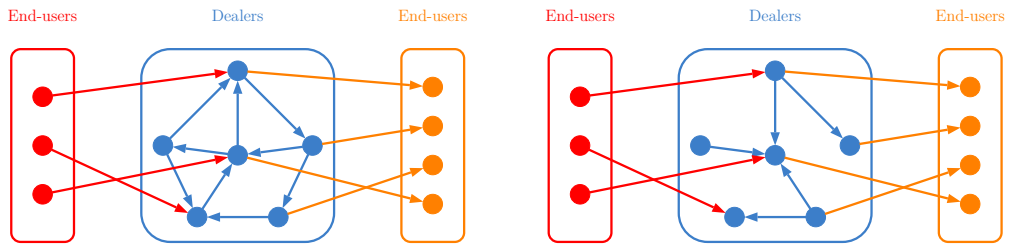

(a) The original network. **(b)** The (optimal) PTN-network.

Figure 2.4. Stylised networks of variation margin flows.

2.4.2 Sufficient conditions for risk reduction

We next provide results on the sufficient conditions for post-trade netting to reduce systemic risk. The first condition assumes that no participant defaults in the original network.

Theorem 2.4.2. Given a PTN-exercise, let $\tilde{E}$ be the greatest re-evaluated equity in the original network that satisfies

$$\{i \in \mathcal{P} \mid \tilde{E}_i < 0\} = \emptyset, \tag{2.6}$$

i.e., no participant defaults in the original network. Then, $\tilde{E}$ is also the greatest re-evaluated equity in the PTN-network. Therefore, the default sets in the two networks are the same. Moreover, the exercise leads to systemic risk reduction, although not a strong reduction.

Remark 2.4.3. In the proof of Theorem 2.4.2, we show that under condition (2.6), any re-evaluated equity in the original network is a re-evaluated equity in the PTN-network. However, if $\tilde{E}$ is the least re-evaluated equity in the original network, it may not be the least re-evaluated equity in the PTN-network (an example can be easily constructed).

Veraart (2022) shows that for portfolio compression which "removes cycles" according to constraint (2.4), condition (2.6) is sufficient for systemic risk reduction under the greatest fixed points. Theorem 2.4.2 above establishes that the statement holds for post-trade netting exercises in general. In particular, it suggests that these exercises are not likely to increase contagion risk in normal times when participants are not likely to default.

Theorem 2.4.2 can also be interpreted using clearing payments. Veraart (2020)

shows that given a re-evaluated equity $\tilde{E}$ in $(L, A^b; \mathbb{V})$, the *clearing payment* of bank i (with positive liabilities) can be written as

$$\tilde{L}_i(\tilde{E}) = \mathbb{V}\left(\frac{\tilde{E}_i + \bar{L}_i}{\bar{L}_i}\right)\bar{L}_i.$$

The following proposition shows the implication of Theorem 2.4.2 on the clearing payments.

Proposition 2.4.4. Given a PTN-exercise $(L, \mathcal{P}, L^{\mathcal{P}})$, let $\tilde{E}$ be a re-evaluated equity in the original network that satisfies (2.6). Then for all $i \in \mathcal{N}$,

$$\tilde{L}_i^{\mathcal{P}}(\tilde{E}) + (\bar{L}_i - \bar{L}_i^{\mathcal{P}}) = \tilde{L}_i(\tilde{E}), \tag{2.7}$$

where $\tilde{L}(\tilde{E})$ and $\tilde{L}^{\mathcal{P}}(\tilde{E})$ are the clearing payments in the original and the PTN-network, respectively.

Proof. By the proof of Theorem 2.4.2, $\tilde{E}$ is also a re-evaluated equity in the PTN-network. In addition, for all $i \in \mathcal{N}$ with $\bar{L}_i^{\mathcal{P}} > 0$,

$$\tilde{L}_i^{\mathcal{P}}(\tilde{E}) = \mathbb{V}\left(\frac{\tilde{E}_i + \bar{L}_i^{\mathcal{P}}}{\bar{L}_i^{\mathcal{P}}}\right)\bar{L}_i^{\mathcal{P}}.$$

First, equation (2.7) holds for all $i \in \mathcal{N} \setminus \mathcal{P}$ because non-participants have the same payment obligations in both networks. Second, the result follows immediately for $i \in \mathcal{P}$ with $\bar{L}_i \times \bar{L}_i^{\mathcal{P}} = 0$. Third, for $i \in \mathcal{P}$ with $\bar{L}_i \times \bar{L}_i^{\mathcal{P}} > 0$,

$$\mathbb{V}\left(\frac{\tilde{E}_i + \bar{L}_i}{\bar{L}_i}\right) = 1 = \mathbb{V}\left(\frac{\tilde{E}_i + \bar{L}_i^{\mathcal{P}}}{\bar{L}_i^{\mathcal{P}}}\right)$$

by condition (2.6). Therefore, equation (2.7) holds for all $i \in \mathcal{N}$. □

Proposition 2.4.4 says that as long as no participant defaults in the original net-

work, clearing the PTN-network is equivalent to clearing the original network and then subtracting $(\bar{L} - \bar{L}^{\mathcal{P}})$ from the clearing payments in the original network. This means that under condition (2.6), the order of clearing and netting does not matter—the difference in payments is equal to the amount of reduced liabilities.

Proposition 2.4.5. Given a PTN-exercise, let $\tilde{E}^{\mathcal{P}}$ be the greatest re-evaluated equity in the PTN-network that satisfies

$$\{i \in \mathcal{P} \mid \tilde{E}_i^{\mathcal{P}} < 0\} = \emptyset, \tag{2.8}$$

i.e., no participant defaults in the PTN-network. Then, $\tilde{E}^{\mathcal{P}}$ is also the greatest re-evaluated equity in the original network. Therefore, the default sets in the two networks are the same. Moreover, the exercise leads to systemic risk reduction, although not a strong reduction.

Proof. Since $(L^{\mathcal{P}}, \mathcal{P}, L)$ is a PTN-exercise (see Remark 2.2.2), Proposition 2.4.5 follows immediately by applying Theorem 2.4.2 to $(L^{\mathcal{P}}, \mathcal{P}, L)$. □

Proposition 2.4.5 states the second sufficient condition for systemic risk reduction. Combined with Theorem 2.4.2, the result implies that if the PTN-exercise *strongly* reduces systemic risk, then both the original and the PTN-network contain defaulting participant(s). More importantly, this implies that the exercise cannot eliminate existing default(s) among participants. In such a case, at least one participant is in fundamental default.

2.4.3 Ex ante analysis

In the following, we present an ex ante analysis. It relies on the work of Glasserman & Young (2015), who build on the Eisenberg & Noe (2001) model to estimate the

magnitude of contagion based on three bank characteristics: (i) net worth; (ii) outside leverage; and (iii) financial connectivity.

Net worth, denoted as w, coincides with our definition of initial equity. (It is assumed that $w_i > 0$ for all $i \in \mathcal{N}$.) Outside leverage is defined as the ratio of liquidity buffer and net worth:

$$\lambda_i = \frac{A_i^b}{w_i} \quad \forall\, i \in \mathcal{N}.$$

For the last characteristic, suppose that the entity indexed by N is an external node such that the liabilities matrix L in the original network satisfies $L_{Nj} = 0$ for all $j \in \mathcal{N}$ (so this external node can be interpreted as banks' customers), then the financial connectivity of bank i is defined by

$$\theta_i = \frac{\bar{L}_i - L_{iN}}{\bar{L}_i},$$

i.e., the proportion of bank i's total liabilities to other banks in the network. (We set $\theta_i = 0$ if $\bar{L}_i = 0$.) Note that if the PTN-exercise satisfies

$$\bar{L}_i^{\mathcal{P}} \leq \bar{L}_i \quad \forall\, i \in \mathcal{N}, \tag{2.9}$$

then it reduces the financial connectivity of all banks. On the other hand, post-trade netting can affect neither net worth nor outside leverage.

Next, we explain how to apply the results of Glasserman & Young (2015) in our context. Their first result (Proposition 1) says that if the aggregate net worth of a fixed set of banks is larger than the contagion index for the single shocked bank, say bank i, defined as $w_i\theta_i(\lambda_i - 1)$, then contagion from bank i to that set is impossible, regardless of the assumption on the shock distribution. The implication is that once condition (2.9) is satisfied, contagion is impossible in the original network *and* the PTN-network.

To some extent, our assumption of whether there exists a default in $\mathcal{P}$ is similar in spirit to the condition based on the bank characteristics mentioned above.

Similarly, we can apply other results of Glasserman & Young (2015), which account for some specific shock distributions. The takeaway is that because the amount of total liabilities is reduced for every bank (i.e., condition (2.9)), the sufficient condition satisfied in the original network also holds in the PTN-network.

2.4.4 Numerical example

Having discussed the conditions for systemic risk reduction, we now show a harmful PTN-exercise in Figure 2.5.

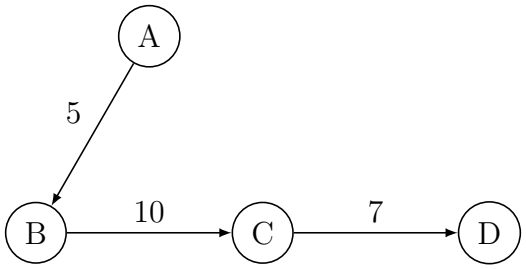

(a) The original network.

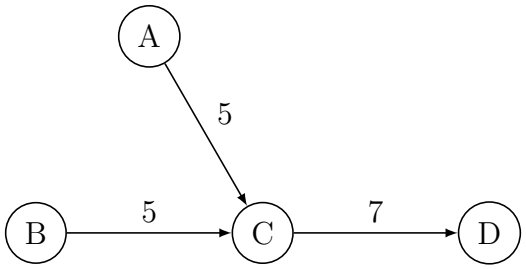

(b) The PTN-network.

Figure 2.5. A PTN-exercise under zero recovery rate. The liabilities are next to the arrows. The liquidity buffers are $(1, 10, 1, 0)^\top$.

It is straightforward to check that $\tilde{E} = (-4, 0, 4, 7)^\top$ is the unique re-evaluated equity in the original network and $\tilde{E}^{\mathcal{P}} = (-4, 5, -1, 0)^\top$ is the unique re-evaluated equity in the PTN-network. Hence, this PTN-exercise is harmful. In the original

network, bank A is the only bank in fundamental default, which does not lead to additional defaults. In contrast, bank A's default triggers the contagious default of bank C in the PTN-network. This difference is due to the fact that after shortening the intermediation chains, bank C now faces bank A directly and receives no payment from A. In short, the example illustrates that post-trade netting can be harmful by reallocating the risk-sharing relationships.

2.5 The worst equilibrium

In this section, we move on to analyse post-trade netting under a special case of the least re-evaluated equity, which can be interpreted as the worst equilibrium.

2.5.1 The least fixed point

So far, we have made comparisons using the greatest re-evaluated equities. The literature on network clearing often focuses on the greatest fixed point, which reflects the best possible outcome for the system. However, multiplicity can be a concern to the extent that it contributes to network instability. Theoretically, Rogers & Veraart (2013) distinguish between the greatest and the least fixed points by interpreting the difference as spreading insolvency versus spreading solvency.[6] In a similar setting, Csóka & Herings (2018) rationalise the least fixed point with a decentralised clearing procedure.

[6]The greatest fixed point can be derived by considering a fixed point iteration starting with the assumption that every bank satisfies its payment obligations in full, and then tracking whether there are any fundamental defaults that then might cause contagious defaults. Hence, the greatest fixed point is the result of a spread of insolvency that started from the best possible situation. However, if one starts with the assumption that initially no banks receive any payments from others, then they can only use their liquidity buffers to make payments. If these are enough to satisfy the payment obligations, then solvency starts to spread through the network, and potentially some banks can avoid default. Hence, the least fixed point is the result of a spread of solvency that started from the worst possible situation.

In the context of derivatives markets, Paddrik et al. (2020) and Bardoscia et al. (2021) point out that there are situations in which financial institutions under stress can take defensive actions not to meet their payment obligations in a timely manner. Bardoscia et al. (2019) introduce the Full Payment Algorithm (FPA) to embed such a phenomenon. They assume that banks with insufficient liquidity buffers wait for potential payments from their counterparties and only make payments in full once they receive enough liquid assets. This dictates that even if a bank can obtain extra liquidity to fulfil its obligations, it would do nothing but wait. In this sense, payments are made in sequence: at each iteration, each bank either pays in full or pays nothing. The algorithm ends if no more banks can make any payment. The vector of cumulative payments is the *output of the FPA*. (The formal definition is provided in Appendix A.1.) Theorem 2.5.1 is useful for relating the FPA to our framework.

Theorem 2.5.1. For any given financial network, the output of the FPA is the least clearing vector in the Rogers & Veraart (2013) model with default cost parameters equal to zero.

Given a financial network (L, A^b), the relative liabilities matrix Π is defined by $\Pi_{ij} = L_{ij}/\bar{L}_i$ if $\bar{L}_i > 0$, and $\Pi_{ij} = 0$ otherwise for all $i, j \in \mathcal{N}$. A *clearing payment vector* in the Rogers & Veraart (2013) model with default cost parameters $\alpha, \beta \in [0, 1]$ is a fixed point of the function $\Psi^{RV} : [0, \bar{L}] \to [0, \bar{L}]$ defined by

$$\Psi_i^{RV}(\tilde{L}) = \begin{cases} \bar{L}_i, & \text{if } A_i^b + \sum_{j \in \mathcal{N}} \Pi_{ji} \tilde{L}_j \geq \bar{L}_i, \\ \alpha A_i^b + \beta \sum_{j \in \mathcal{N}} \Pi_{ji} \tilde{L}_j, & \text{otherwise.} \end{cases}$$

By Theorem 2.5.1, the least fixed point in the Rogers & Veraart (2013) model under zero recovery rates can be interpreted as *the worst equilibrium* as a result of a strategic response to stress. Proposition 2.5.2 gives the corresponding re-evaluated equity, which

is directly related to our framework.

Proposition 2.5.2. For any given financial network (L, A^b), the re-evaluated equity under the worst equilibrium, denoted as E^w, can be written as

$$E_i^w = A_i^b + \sum_{j:\bar{L}_j>0} L_{ji}\frac{L_j^*}{\bar{L}_j} - \bar{L}_i \quad \forall\, i \in \mathcal{N},$$

where L^* is the output of the FPA.

Proof. We omit the proof of this result because it is a minor variation on the proof of Theorem 2.9 in Veraart (2020), which shows how the clearing payment vector in the Rogers & Veraart (2013) model can be rewritten in terms of the re-evaluated equity. □

2.5.2 Conservative netting

Having shown why the least fixed point under zero recovery rates is relevant to our analysis, we introduce a constraint important for the following result. We refer to a PTN-exercise $(L, \mathcal{P}, L^{\mathcal{P}})$ as *conservative* if

$$L_{ij}^{\mathcal{P}} \leq L_{ij} \quad \forall\, i, j \in \mathcal{N}. \tag{2.10}$$

The constraint means that counterparty relationships are preserved so that if one bank is a net seller to (or a net buyer from) another bank, this remains after the exercise.

Theorem 2.5.3. Suppose that $\mathbb{V} = \mathbb{V}^{\text{zero}}$. For any conservative PTN-exercise that satisfies (2.10),

$$E^* \leq E^{\mathcal{P};*}, \tag{2.11}$$

where E^* and $E^{\mathcal{P};*}$ are the greatest re-evaluated equity in the original and the PTN-network, respectively. The inequality also holds when E^* and $E^{\mathcal{P};*}$ are the correspond-

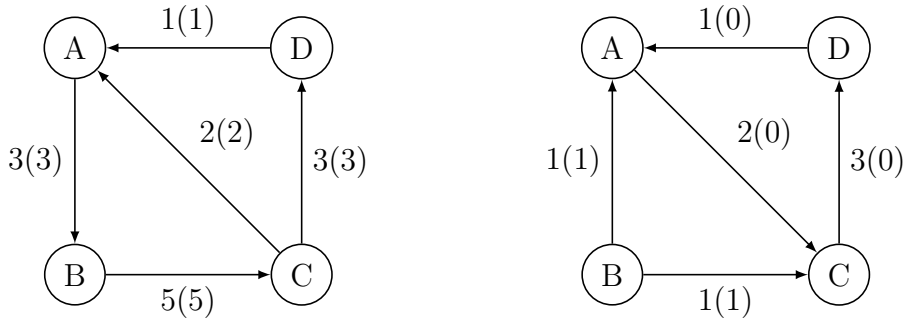

(a) The original network. **(b)** The PTN-network.

Figure 2.6. A harmful PTN-exercise under the worst equilibrium. The liabilities are next to the arrows. The liquidity buffers are $(0.5, 5.5, 1.5, 0.5)^\top$. The numbers in brackets represent the clearing payments.

ing least re-valuated equities.

Theorem 2.5.3 for PTN-exercises under the greatest equilibrium is a general version of Proposition 4.12 in Veraart (2022) which considers compression cycles. Moreover, the result suggests that in situations where banks react strategically to liquidity stress by delaying their payments, conservative PTN-exercises bring systemic risk reduction. However, this does not generally apply to non-conservative exercises. To illustrate, consider the example of a harmful PTN-exercise in Figure 2.6. Although there is no default in the original network, three banks default in the PTN-network. This outcome is impossible under the greatest re-evaluated equities (by Theorem 2.4.2). The example suggests that in a worst-case situation, simply reducing overall exposures (through rewiring the network) while neglecting how the liquidity flows is insufficient to mitigate contagion.

2.6 Concluding remarks

While an enriched framework is outside the scope of the present work, we hope to suggest some alternative perspectives on the topic of post-trade netting.

2.6.1 Risk measurement

Our definition of the default set allows for a meaningful comparison between two networks of different sizes. It tells who defaults and not just the number of defaults. As discussed in Veraart (2022), a strong reduction in systemic risk can be interpreted as a Pareto improvement: the PTN-exercise does not cause any new default, while at least one bank that defaults in the original network becomes better off in the PTN-network. In this sense, our definition of risk reduction does not favour a trade-off—for example, an exercise that significantly reduces the number of defaults but also introduces a small number of new defaults. Since market participants can decide on which services to use and proposals to accept, we believe it is reasonable to take a conservative view and define risk reduction in the spirit of mitigating the extent of risk propagation.

In addition to our risk measurement based on the re-evaluated equity, it is also of interest to compare the clearing payments, as mentioned in Section 2.4. However, since PTN-exercises can increase or decrease total payment obligations, we need to ensure that the risk measure is suitably normalised. For this, one can use the actual payments made to the external node (see also Amini & Feinstein (2023)). Since the external node does not participate in the PTN-exercise, the total liabilities to the external node cannot change. Therefore, the payments it receives can also be used as a normalised measure. More specifically, the total payments made to the external node in the original network and the PTN-network, respectively, are given by

$$\sum_{i\in\mathcal{N}:\bar{L}_i>0} \mathbb{V}\left(\frac{\tilde{E}_i+\bar{L}_i}{\bar{L}_i}\right) L_{iN}, \qquad \sum_{i\in\mathcal{N}:\bar{L}_i^{\mathcal{P}}>0} \mathbb{V}\left(\frac{\tilde{E}_i^{\mathcal{P}}+\bar{L}_i^{\mathcal{P}}}{\bar{L}_i^{\mathcal{P}}}\right) L_{iN}.$$

Therefore, it boils down to comparing $\mathbb{V}\left(\frac{\tilde{E}_i+\bar{L}_i}{\bar{L}_i}\right)$, which models the proportion of bank i's repayment in the original network under re-evaluated equity $\tilde{E}$, to $\mathbb{V}\left(\frac{\tilde{E}_i^{\mathcal{P}}+\bar{L}_i^{\mathcal{P}}}{\bar{L}_i^{\mathcal{P}}}\right)$,

which models the proportion of bank i's repayment in the PTN-network under re-evaluated equity $\tilde{E}^{\mathcal{P}}$. See Veraart (2020, 2022) for further details.

2.6.2 Margin requirements

Our analysis has focused on illiquidity propagation triggered by defaults on variation margin calls. These margin calls are intended to reduce counterparty risk, but the fact that they are inherently procyclical can increase the stress on market participants in adverse market conditions (European Systemic Risk Board, 2017). With this in mind, PTRR services might be useful in mitigating the procyclicality of margin requirements. In particular, these services can reduce the magnitude of the variation margins that must be exchanged when market conditions change. In March 2020, the COVID-19 pandemic caused significant liquidity stress in financial markets, with considerable variation margins due precisely when liquidity was already under strain (International Swaps and Derivatives Association, 2022). The results in Section 2.4 suggest that PTRR services could reduce parts of these pressures without increasing contagion risk at normal times.

Our analysis does not touch on the initial margins. In the event that a counterparty has defaulted, the entity to the defaulting counterparty would replace the transactions with the defaulter using the collected initial margins to mitigate the adverse change in the value of contracts. Replacement loss occurs if the replacement cost under volatile market conditions exceeds the margin received from the defaulting counterparty. As introduced in the beginning, portfolio rebalancing allows market participants to alleviate the pressure of tightened collateral requirements. However, reducing cost is not equivalent to reducing risk. The consultation paper of the European Securities and Markets Authority (2020) asks: provided that market participants are incentivised to use PTRR services to optimise their use of collateral, would these services cause the

market to be "under collateralised" or increase any risk? In this regard, the framework of Jackson & Manning (2007) may be useful to assess PTRR services while capturing pre-settlement risk. In addition, Ghamami et al. (2022) build a clearing framework in the spirit of Eisenberg & Noe (2001) to study contagion in networks with collateral requirements. Veraart (2022) also proposes a valuation function to model payment obligations protected by initial margins. In any case, more information on the netting algorithms is needed to better understand the risk implications of collateral optimisation.

Chapter 3

Financial vulnerability

3.1 Introduction

Monitoring financial vulnerability is crucial for financial stability. In 2008, the G20 initiated the Early Warning Exercise jointly conducted by the International Monetary Fund (IMF) and the Financial Stability Board (FSB) to identify vulnerabilities and provide policy recommendations (see IMF (2010)). The first input into the assessment framework of the FSB (2021) is a set of surveillance indicators. In this chapter, I introduce an index of financial vulnerability for the banking sector through the lens of fire sales, motivated by two well-known observations: first, forced asset liquidation is a common feature of crisis episodes, and second, bank failures have devastating effects on the economy.

Substantial efforts have been made to use various indicators to analyse the causes of economic crises, such as the currency and banking crises in the 1990s (e.g., Kaminsky & Reinhart (1999)). Although there is obviously no single choice of a suitable indicator, identifying vulnerabilities is not straightforward (see Borio & Drehmann (2009) and Adrian et al. (2015)). Composite indicators based mainly on asset prices are good at

reflecting concurrent market conditions, but are unlikely to reveal vulnerabilities in advance (e.g., Shin, 2014). In addition, the definition of vulnerability by the Financial Stability Board (2021, p. 5) concerns systemic disruption and therefore warrants taking into account propagation mechanisms.

Measurement is essential for economic analysis and is involved in many traditions of the macroeconomic literature (e.g., Burns & Mitchell (1946); Friedman & Schwartz (1963)). Given the orientation towards financial vulnerability, this work follows the tradition from Leontief (1936), who analyses structural changes of the system by input-output tables. In my view, the perspective of treating the system as a whole is particularly relevant. Moreover, the idea is pragmatic. It was developed by Stone (1947) into the Social Accounting Matrix and applied in a wide range of areas (such as regional science and managerial science).

Methodologically, this work takes advantage of recent advances in systemic risk measurement, following the spirit of Koopmans (1947, p. 162), who advocates for "fuller utilization of the concepts and hypothesis of economic theory [...] as part of the process of observation and measurement." I use the "vulnerable banks" model of Greenwood, Landier & Thesmar (2015), who assume that banks offset exogenous shocks by selling assets and derive an aggregate vulnerability (AV) measure for spillover losses in the system as a consequence of joint liquidation.[1] By decomposing the measure, I construct a Financial Vulnerability Index (FVI):

$$\text{FVI} = \text{Leverage} \times \text{Illiquidity}.$$

[1]See, for example, Acharya et al. (2017) for a model-based systemic risk measure and Bisias et al. (2012) for a review of the literature. For network models on fire sales, see Cifuentes et al. (2005), Cont & Schaanning (2019), among many others. This work approaches fire sales from a fundamentally different angle: it focuses on deleveraging and price impact, the causes of contagion as described by Kiyotaki & Moore (2002), rather than how losses propagate through the overlapping portfolios.

The former refers to the degree of banks' deleveraging; the latter arises from assets' illiquidity, whereby fire-selling illiquid assets leads to spillover losses. The distinguishing feature of the FVI is the expression in terms of size-weighted leverage and illiquidity-weighted Herfindahl-Hirschman Index, while the link with contagion is underpinned by the model. The index brings computational simplicity, which is advantageous in practice, and is intuitively appealing in the sense that monitoring leverage and illiquidity jointly and severally is consistent with crisis policies.

To illustrate the empirical feasibility and informativeness, I apply the index to the large U.S. bank holding companies (BHCs) from 1996Q1 to 2021Q4 (Section 3.3). Retrospectively, the FVI issues signals ahead of vulnerabilities materialise in the run-up to the Global Financial Crisis (GFC) and aligns with the turmoil during the COVID-19 pandemic. The index is well suited for monitoring purposes by conveying information about vulnerability in a relatively concise form and can be interpreted jointly with other indicators of sources of systemic risk.

In addition to monitoring instability, the identification of vulnerabilities is also useful for the implementation of macroprudential instruments, such as buffer requirements. The Basel Committee on Banking Supervision (2017, p. 2) notes that "the link between the indicators selected and how they contribute to assessments of 'excess' credit giving rise to systemic risk is not always clearly spelled out." Regarding this, the theoretical rationale for using the FVI stems from its relevance to pecuniary externalities (e.g., Lorenzoni (2008)). Consequently, the index satisfies the three criteria for the selection of indicators listed in the report by the Committee on the Global Financial System (2012): (i) relevance for macroprudential instruments; (ii) ease of data availability; and (iii) simplicity. In Section 3.4, I compare the FVI with the credit-to-GDP gap and demonstrate that it can be helpful to set the countercyclical capital buffer.

Lastly, this work contributes to research on historical banking crises (see Frydman &

Xu (2023) for a literature review). Historical accounts of fire sales are often accounted for by studies on financial crises (e.g., Kindleberger (1978)). Theories of fire sales date at least to Irving Fisher's (1933) debt-deflation explanation of the Great Depression; similar amplification mechanisms have been extensively studied in the macro-finance literature (e.g., Bernanke & Gertler (1989)). Based on above, the FVI that provides a proxy for financial vulnerability can be expected to be used in empirical research. In Section 3.5, I implement the index for national banks in the United States in 1928 and 1933 and discuss the related academic research.

The remainder of this chapter is organised as follows. Section 3.2 describes the derivation of the FVI. Section 3.3 conducts the empirical analysis for the U.S. banking system during 1996–2021, followed by some validation exercises. Section 3.4 further discusses operationalising the index for policy purposes. Section 3.5 illustrates an implementation in the context of banking panics during the Great Depression. Finally, Section 3.6 concludes.

3.2 The Financial Vulnerability Index

3.2.1 Insight from the Great Fire of London in 1666

I find it instructive to draw an analogy before introducing my index. In my view, a burning house resembles a deleveraging bank. The house's vulnerability to catching fire depends largely on the material—a wooden house is more vulnerable than a brick house. Likewise, a bank with higher leverage is more likely to suffer from fire-sale losses. Asset illiquidity can be interpreted as street width: Wide streets insulate the spreading flames. Adequate liquidity absorbs shocks to the market. In addition, the structure of asset portfolios is analogous to the city layout (which differs from the street width). The houses are connected by streets that can spread fires. Banks are

connected by asset holdings that can incur indirect losses. In both cases, the structure affects how the losses propagate.

On 2 September 1666, a fire broke out in a baker's house in Pudding Lane, a narrow street of wooden houses in the City of London, causing severe damage. A Rebuilding Act was passed in the following year, requiring the building of brick houses and the widening of streets. Nevertheless, London was rebuilt according to the old layout—none of the new designs were adopted. The rebuild predominantly addressed London's fundamental weakness, a tinderbox full of wooden houses and narrow streets. Ideally, it provided an opportunity to redesign the layout to better prevent future fires. However, in reality, many factors impeded new proposals and prompted a quick rebuild.

The lesson for fire sales in financial markets, perhaps, is that addressing leverage and illiquidity separately promotes making timely decisions in response to changing conditions. At least, this is consistent with crisis policies such as capital injection and liquidity provision during the GFC.

3.2.2 Measurement with theory

Leverage and illiquidity are preponderant in the discussion of fire sales in finance and macroeconomics (for an overview, see Shleifer & Vishny (2011)). In deriving my index, I think of these vulnerabilities as corresponding to externalities: banks create fire-sale externalities when they do not internalise the effects of their behaviours and make investments in illiquid assets via taking on excessive leverage.

Specifically, I use the model of Greenwood et al. (2015) under the following assumptions: (i) banks respond to exogenous asset shocks by selling assets proportionally to return to the pre-shock leverage; (ii) the selling of illiquid assets has a linear price impact on the same asset class; and (iii) banks holding the fire-sold assets are exposed to spillover losses caused by the deleveraging. Greenwood et al. (2015) justify the leverage

targeting by referring to the empirical findings of Adrian & Shin (2010). In addition, while selling assets proportionally is a simplifying theoretical assumption, the precise form of asset shrinkage is undetermined at the empirical level and does not invalidate the mathematical model.

Most importantly, the objective of this work is to introduce an index, not to model contagion. Studies quantifying fire-sale losses must take a stance on the modelling assumptions; how seriously the estimates are taken depends on the specific perspective on the model. It is worth noting the distinction between measuring vulnerability and assessing systemic risk: the former formalises the concept by providing an analytical structure; the latter applies a modelling framework to quantify the effect of changes in model inputs. In summary, this work aims to identify vulnerabilities from a systemic perspective with an accounting framework that incorporates bank and asset heterogeneity.[2]

At time t, there are N banks and K asset classes; each bank has total assets a_{nt} and equity e_{nt}. Leverage b_{nt} is defined as the debt-to-equity ratio. The assets and equity of the system are given by $a_t = \sum_n a_{nt}$ and $e_t = \sum_n e_{nt}$, respectively. The asset matrix $M_t = (m_{nkt})$ is the $N \times K$ matrix of portfolio weights, i.e., m_{nkt} is the fraction of asset k in bank n's total assets. The total value of asset k is thus $v_{kt} = \sum_n a_{nt} m_{nkt}$. The asset shock is characterised by $F_t = (f_{1t}, \ldots, f_{Kt})^\top$. The aggregate vulnerability (AV) defined by Greenwood et al. (2015) is

$$\mathrm{AV}_t = \frac{\mathbf{1}^\top A_t M_t L_t M_t^\top B_t A_t M_t F_t}{e_t},$$

[2]Despite the mathematical structure, different models can lead to similar messages. For example, Calomiris & Wilson (2004) incorporate adverse selection between banks and depositors into the model of Black & Scholes (1973) to identify the dynamic process of balance sheet adjustment, where banks choose the level of asset risk (defined as the standard deviation of asset returns) through risky loans. By assuming that banks target the riskiness of deposits (i.e., default premiums), they show that the deposit risk increases with asset risk and decreases with capital ratio.

where $A_t = \text{diag}(a_{1t}, \ldots, a_{Nt})$, $B_t = \text{diag}(b_{1t}, \ldots, b_{Nt})$, and $\mathbf{1}$ is the column vector containing only 1s. More specifically, $A_t M_t F_t$ translates the shock into losses so that $B_t A_t M_t F_t$ tells the amounts to be sold to return to the target leverage. The vector is then premultiplied by $M_t^\top$, which means that banks sell assets proportionately to their original holdings. For each asset class, the sale has a linear price impact that depends on its illiquidity, which is captured by L_t. Finally, AV_t calculates the fraction of aggregate equity lost as spillover losses beyond the direct impact of the shock.

I assume that the price impact is inversely proportional to the wealth of outside investors to capture the idea that the industry peers of distressed institutions may be financially constrained themselves and that there are outside investors with deep pockets to absorb liquidations (Shleifer & Vishny, 1992). (Consider, for example, a mortgage-backed security that has limited potential buyers upon the default of some mortgages because only a few institutions have the expertise to evaluate it accurately.) Formally, the k-th diagonal entry of L_t is l_k/w_t, where w_t is the outside wealth at time t, and l_k represents the illiquidity of asset k. I will normalise the measure and focus on the trend to facilitate comparison. While a shortcoming due to data constraints is that the admittedly imprecise time-varying trend of aggregate liquidity is imputed as the size of potential buyers, the magnitude of the price impact is less of a concern here than it might be elsewhere.[3]

In addition, I apply a constant shock to all assets, i.e., $f_{kt} = f$, and drop f from the expression henceforth. This setting is strong but appropriate because it is essential to ensure the consistency of identification over time. Moreover, the focus is on vulnerabilities, not shocks or triggers of the crisis, which are inherently challenging to forecast (FSB, 2021).

[3]To the extent that there have been changes across asset classes over time, it is better to consider time-varying l_k. However, estimating price impacts remains a challenging empirical question that requires a wide range of data. In Greenwood et al. (2015), all asset classes have the same price impact—$10 billions of asset sales generate a price change of 10 basis points.

3.2.3 Index construction

Banks' common exposures can be described heuristically by a bipartite graph: the two sets of nodes are banks and assets, and the edges represent portfolio allocations. The goal is to isolate the nodes from the edges.

The key step is to construct a counterfactual AV measure by assuming that all banks have the same allocation of portfolio weights, i.e.,

$$m_{nkt}^{\mathrm{H}} = \frac{v_{kt}}{\sum_j v_{jt}} \quad \forall\, k.$$

The aggregate vulnerability of the hypothetical system is immediately given by

$$\mathrm{AV}_t^{\mathrm{H}} = \frac{\sum_n a_{nt} b_{nt}}{\sum_n e_{nt}} \times \sum_k \frac{l_k}{w_t/a_t} m_{kt}^2,$$

while the total value of each asset does not change ($\sum_n a_{nt} m_{nkt}^{\mathrm{H}} = v_{kt}$). The ratio $\mathrm{AV}_t/\mathrm{AV}_t^{\mathrm{H}}$ can be thought of as portfolio diversity in the sense of Wagner (2011), who assumes that investors tend to hold diverse portfolios to differentiate themselves from each other and mitigate the impact of joint liquidation. Moreover, $\mathrm{AV}_t^{\mathrm{H}}$ yields the following expression for AV_t:

$$\mathrm{AV}_t = \underbrace{\sum_n \frac{a_{nt}}{e_t} b_{nt}}_{\text{leverage}} \times \underbrace{\sum_k \frac{l_k}{w_t/a_t} m_{kt}^2}_{\text{illiquidity}} \times \underbrace{\frac{\mathrm{AV}_t}{\mathrm{AV}_t^{\mathrm{H}}}}_{\text{heterogeneity}}.$$

This decomposition breaks down the contagious effect of fire sales into three factors identified by the three terms on the right. Next, I elaborate on each of these factors.

The first factor, which can be rewritten as the product of a size-weighted average leverage ($\sum_n (a_{nt}/a_t) b_{nt}$) and system leverage ($a_t/e_t$), reflects the vulnerability that arises when large banks carry the most excessive leverage. Accounting for this cross-

sectional dimension of risk build-up is compatible with the concern of so-called "too-big-to-fail": the reaction by complex big banks could foster deleveraging during market downturns, causing larger effects than smaller banks.[4]

The second factor measures the overall level of system illiquidity, which is high when the system portfolio is made up of relatively illiquid assets of large size and/or aggregate liquidity (w_t/a_t) is low. It has a conventional interpretation in terms of the illiquidity-weighted Herfindahl-Hirschman Index (HHI) and therefore captures illiquidity concentration at the asset class level.[5] Indeed, there are broad interests from regulators and academics on measuring risk concentration; for example, the European System Risk Board (ESRB) lists the HHI of asset classes as a metric for measuring the structural systemic risk stemming from amplification channels (see Table 4.4 and Annex 4.2 in ESRB (2018)).

The third factor, the AV ratio, indicates the effect of portfolio heterogeneity. Arguably, it is an important aspect in explaining fire-sale contagion, but the factor is not underlined here due to two drawbacks. First, banks' portfolio choice (m_{nkt}) plays a negligible role in affecting the level of aggregate vulnerability.[6] Second, the ratio

[4]This perspective is akin to the analysis in Adrian & Brunnermeier (2016) and Brownlees & Engle (2017), where larger size and higher leverage predict systemic risk. Bernanke (2012) notes that the cause of the disproportionate effects in the mortgage markets during the subprime crisis, in contrast to the dot-com bubble, is that the losses were not dispersed as desired—they concentrated on several prominent institutions, which engaged in disorderly liquidation and precipitated abrupt plummet of market confidence.

[5] An alternative decomposition of the AV measure in the sense of Duarte & Eisenbach (2021) leads to

$$\mathrm{AV}_t = \frac{a_t}{w_t} \times (b_t + 1)\bar{b}_t \times \sum_k m_{kt}^2 l_k \sum_n \mu_{nkt}\beta_{nt}\alpha_{nt},$$

where $b_t = a_t/e_t - 1$, $\bar{b}_t = (1/N)\sum_n b_{nt}$, $\mu_{nkt} = m_{nkt}/m_{kt}$, $\beta_{nt} = b_{nt}/\bar{b}_t$, and $\alpha_{nt} = a_{nt}/a_t$. They interpret the last term as capturing "illiquidity concentration." However, it is conceptually the same as the definition of aggregate vulnerability in Greenwood et al. (2015) because extracting aggregate terms from the cross-sectional AV measure does not qualitatively alter its information content. (The logic of this argument is not affected by the fact that Duarte & Eisenbach (2021) incorporate an additional factor into the Greenwood et al. (2015) model.)

[6] Note that by definition, $M_t F_t = f\mathbf{1}$ if $f_{kt} = f$ for all k. In Section 3.3, Figure 3.4 shows that the FVI captures the change in AV almost precisely, verifying that the AV ratio (which is of value around one) cannot determine the evolution of aggregate vulnerability by introducing meaningful variation.

does not clearly tell where the vulnerability emerges, making it less appropriate for identification over time.

Having explained the individual factors, I now define the Financial Vulnerability Index (FVI) as

$$\text{FVI}_t = \sum_n \frac{a_{nt}}{e_t} b_{nt} \times \sum_k \frac{l_k}{w_t/a_t} m_{kt}^2.$$

The index needs only aggregate bank-specific and asset-specific variables—it does not require knowing the asset holding at any individual bank. This is an attractive feature and benefits implementation with data from different sources. Moreover, the FVI can be interpreted as a model-free index in that financial factors such as leverage and illiquidity largely contributed to the disruption of intermediation during financial crises, as informed by empirical studies (for discussions, see Calomiris (1993); Gertler & Gilchrist (2018)).

3.2.4 Remarks

I conclude this section with two remarks. The takeaway is that the FVI can be adapted to incorporate other instability risks.

Funding illiquidity. Banks create liquidity by financing illiquid assets with liquid liabilities. However, funding may be unstable—consider the run on repo during the GFC (see, e.g., Gorton & Metrick (2012)). As a result, borrowers who lack sufficient short-term funding often have to sell illiquid assets rapidly. This funding illiquidity can be reinforced by market illiquidity, leading to the "margin spiral" coined by Brunnermeier & Pedersen (2009). The FVI can account for the liability side of the balance sheet by changing the assumption; for example, the more liquid the liabilities, the less

price impact.[7]

Non-bank financial institutions. Despite the pivotal role of the banking sector, it is important to identify emerging risks from structural changes to the financial system.[8] The FVI can be adapted to capture vulnerabilities from non-banks where the general principle of the illiquidity spirals applies. In Appendix B.1, I show how to construct a vulnerability index for mutual funds in a similar way.

3.3 Financial instability monitoring

Balance-sheet leverage and illiquidity are determinants of financial instability in the hypothesis of Minsky (1964). Although they are not sufficiently representative of financial instability, the latter is more complex to measure. This section demonstrates the plausibility of the FVI for monitoring financial instability. I first describe the data and present the time series. Then, I investigate the information content of the FVI and compare it with related indicators, aiming to distinguish the role of quantity and price from an operational perspective.

3.3.1 Data

I obtain the balance sheet data at a quarterly frequency for U.S. BHCs that file a FR Y-9C report with the Federal Reserve (I will refer to them as banks for convenience). The sample covers the top one hundred banks (by total assets) each quarter from

[7]Berger & Bouwman (2009) and Brunnermeier et al. (2012) (see also Bai et al. (2018)) propose measures of liquidity mismatch by assigning different weights to items on both sides of the balance sheet.

[8]Of course, it is important to also track household debt (see, e.g., the U.S. debt-income ratios in Mason & Jayadev (2014)). Mishkin (1978) points out that household balance sheets can help explain the severity of the Great Depression. For more empirical evidence on the relation between household debt and output growth, see Mian & Sufi (2018) and the references therein.

1996Q1 to 2021Q4. It does not consist of a fixed sample of banks and in particular, excludes banks which report negative equity.[9]

Total assets and equity (Tier 1 capital) are directly available from the data. The outside wealth is the difference between the total assets in financial sectors obtained from the Financial Accounts of the United States and the total assets in the sample subtracted by cash. Following Duarte & Eisenbach (2021), I use the net stable funding ratio (NSFR) to capture varying degrees of asset illiquidity (l_k), which are listed in Table 3.1.[10] The value of l_k for the U.S. Treasuries is normalised to 1. The details of the mapping between asset categories and codes in FR Y-9C are relegated to Appendix B.2.

3.3.2 Trends

Figure 3.1 shows the evolution of the FVI. It started rising noticeably in early 2004 and expanded for four years before its peak, reflecting that a build-up of vulnerability had accompanied the banking system before the 2007–2008 financial turmoil. Between 2008Q3 and the end of 2009, the index plunged considerably, with a magnitude comparable to the surge. The prolonged decline was substantial, and the FVI flattened out from 2015. The FVI increased sharply near 2020Q1, but the magnitude was much lower than that during the GFC, presumably because the distress during the COVID-

[9]TAUNUS CORPORATION (RSSD ID: 2816906) is excluded from the data during 1999Q2–2011Q4 for consistency reason, although it was one of the top ten banks (by total assets) in that period. It reported thin equity during 1999Q2–2001Q1 and negative equity during 2001Q2–2011Q4. TD BANKNORTH (RSSD ID: 1249196), which reported negative equity throughout 2008, is excluded from the data in 2009Q1 due to thin equity. As a result, the average fraction of total assets of all BHCs covered by the sample during 1996Q1–2011Q4 and 2012Q1–2021Q4 is 0.88 and 0.93, respectively. In addition, the leverage of BARCLAYS GROUP US (RSSD ID: 2914521) in the sample is capped at 32. This large bank reported very thin capital during 2004Q4–2010Q3.

[10]The NSFR requires banks to maintain a sustainable funding structure to reduce risks resulting from short-term liquidity outflows (Basel Committee on Banking Supervision, 2014). Note that using these estimates is imperfect because the categories for the NSFR do not correspond exactly to those shown in the table.

Table 3.1. Asset illiquidity

Asset class	l_k
Cash	0
U.S. Treasuries	1
Repo & fed funds sold	2
Agency securities	3
Agency mortgage-backed securities	3
Agency-backed securities & other debt securities	7
Equities & other securities	11
Municipal securities	12
Residential real estate loans	12
Nonagency mortgage-backed securities	13
Commercial real estate loans	15
Other real estate loans	15
Commercial and industrial loans	15
Consumer loans	15
Lease financings	15
Residual loans	15
Residual securities	20
Residual assets	20

19 pandemic did not originate from within the banking sector. The trend returned to the pre-pandemic level in 2021, consistent with normalising market conditions.

Figure 3.2 shows the evolution of the two factors. As one would expect, both were elevated in the run-up to the GFC. Illiquidity increased steadily, while leverage built up slowly and then rose sharply. Leverage peaked at the end of 2007, coinciding with the crisis, before falling precipitously in 2008. It then rebounded, but fell persistently from 2010 onwards. (The fluctuation in 2009 comes partly from the fact that some banks close to failure reported very low equity.) Illiquidity exhibited a relatively moderate decline until 2014 when it started to level off. (The temporary increase in 2009 is due to an artefact of the composition of banks in the sample: several large investment banks became BHCs in 2008.) In contrast, leverage has slightly trended upward since 2016. In the wake of the pandemic, the upward trend of leverage remained, whereas system

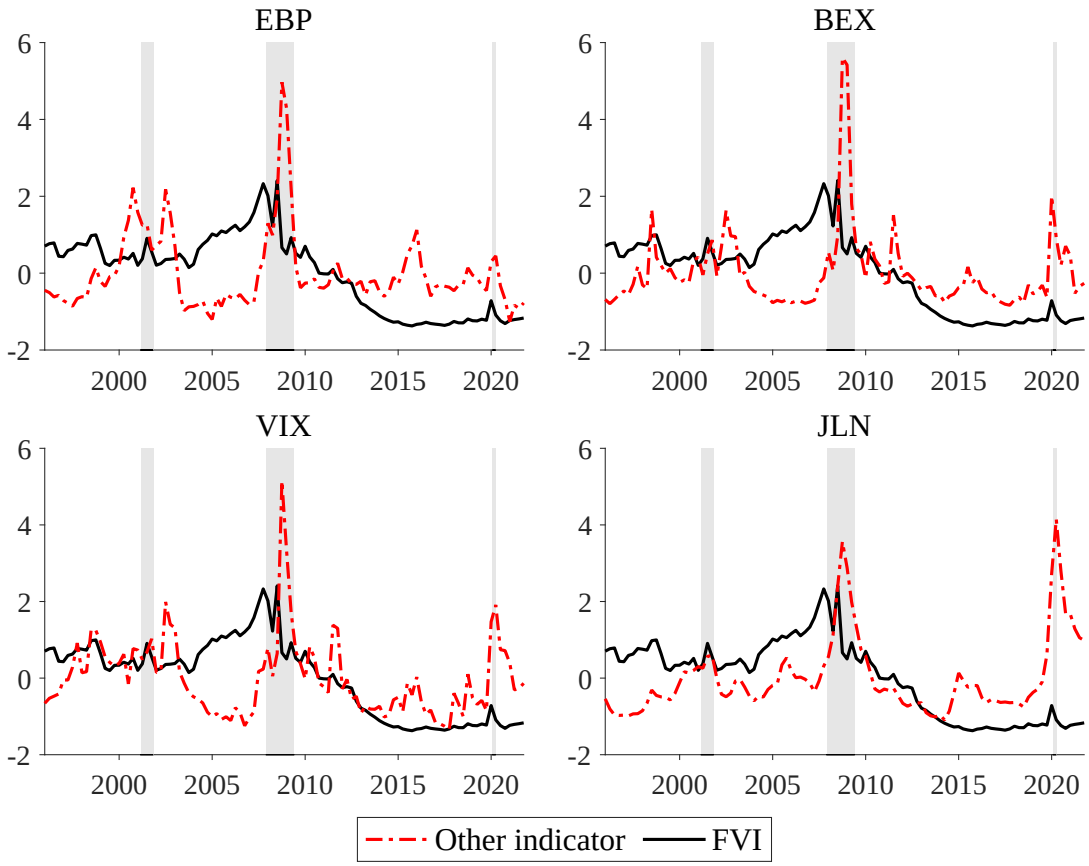

Figure 3.1. Crisis indicators. The figure shows the FVI (solid line) together with another crisis indicator (dashed line): EBP, BEX, VIX, and JLN (see text). All time series are normalised to have zero mean and unit standard deviation. The EBP is Gilchrist & Zakrajšek's (2012) excess bond premium updated in Favara et al. (2016) (available for download at https://www.federalreserve.gov/econres/notes/feds-notes/updating-the-recession-risk-and-the-excess-bond-premium-20161006.html). The BEX is Bekaert, Engstrom & Xu's (2022) risk aversion index obtained from Xu's website (https://www.nancyxu.net/risk-aversion-index). The VIX is the CBOE Volatility Index obtained from Federal Reserve Economic Data (https://fred.stlouisfed.org/series/VIXCLS). The JLN is Jurado, Ludvigson & Ng's (2015) 3-month ahead macroeconomic uncertainty index obtained from Ludvigson's website (https://www.sydneyludvigson.com/macro-and-financial-uncertainty-indexes). The sample period is 1996Q1–2021Q4. The monthly indicators are averaged within the quarter to obtain a quarterly time series. Shaded areas correspond to the National Bureau of Economic Research (NBER) recession dates (available at https://www.nber.org/research/data/us-business-cycle-expansions-and-contractions).

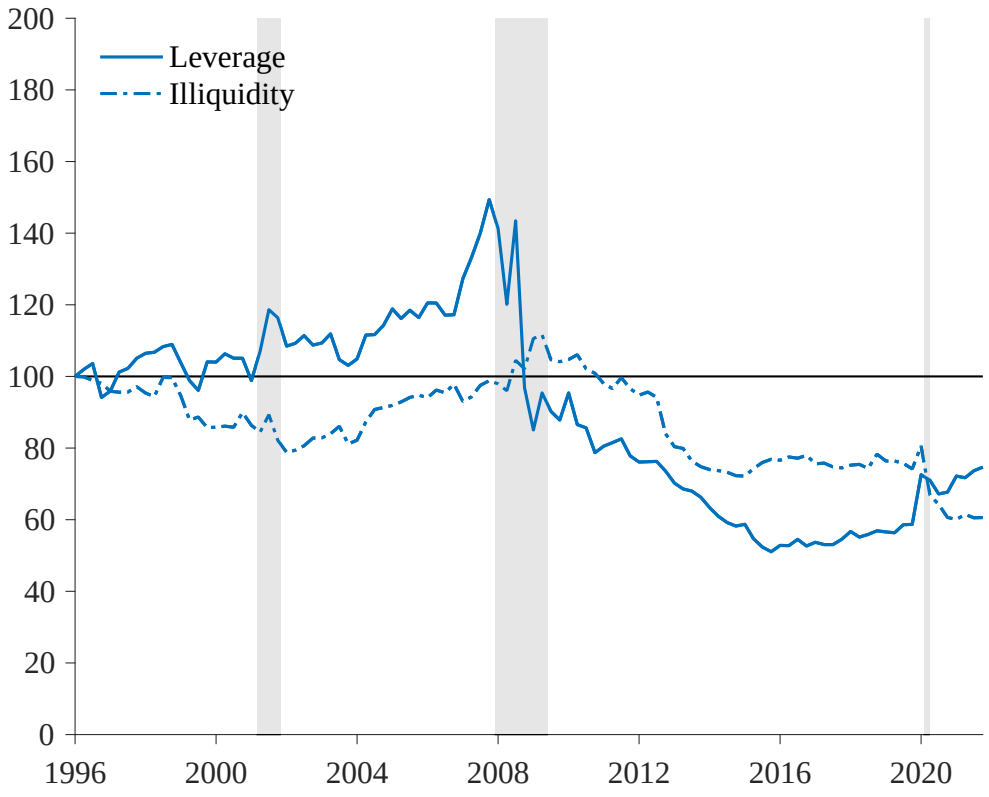

Figure 3.2. Vulnerability evolution during 1996Q1–2021Q4. The figure shows the time series of leverage and illiquidity in the FVI. They are normalised to 100 at the start of the sample period. Shaded areas correspond to the NBER recession dates.

liquidity was enhanced. In addition, rapid stabilisation reflects substantial intervention through the banking system.

To quantify the relative contribution of the two factors, I apply a variance decomposition:

$$\text{var}(\log \text{FVI}_t) = \text{var}(\log \text{LEV}_t) + \text{var}(\log \text{ILLIQ}_t) + 2\text{cov}(\log \text{LEV}_t, \log \text{ILLIQ}_t).$$

I compare between two sub-periods outside the GFC: 2002Q1–2006Q4 (pre-crisis) and 2010Q1–2014Q4 (post-crisis). Figure 3.3 presents the result. The pre-crisis effect of

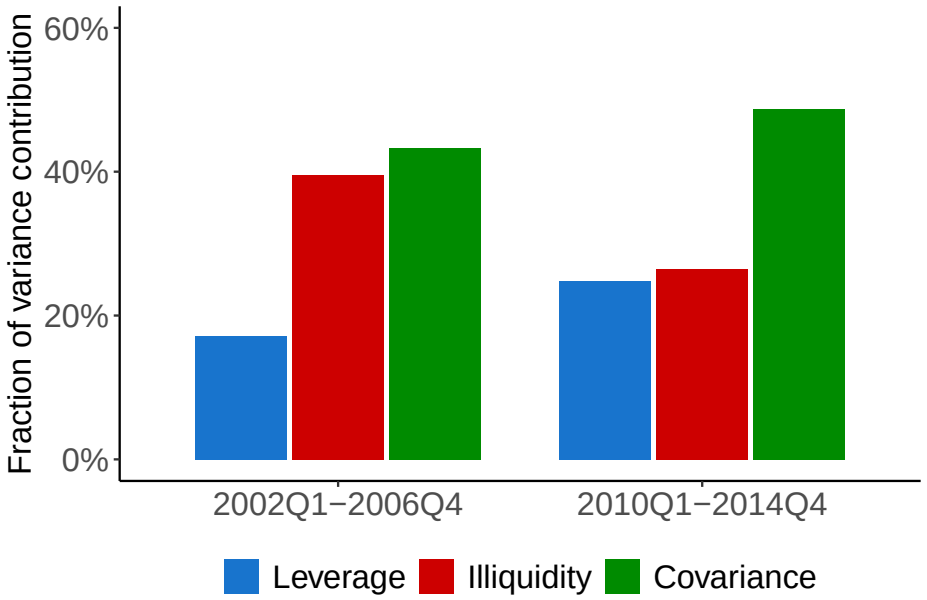

Figure 3.3. Variance decomposition.

illiquidity is pronounced, with the change accounting for a considerable share (about 40%). In the post-crisis period, the contribution of leverage is approximately equal to that of illiquidity (about 25%), which might be attributed to a stringent leverage regulation under the Basel III framework. In contrast, illiquidity plays a relatively less role in the second period. The correlation between leverage and illiquidity also matters, explaining about half of the total variation in both periods. Overall, the results are consistent with the patterns shown in the figure.

Figure 3.4 plots the FVI with the AV measure. The AV ratio (not shown) fluctuates around its mean of 0.98, so on average the aggregate vulnerability is 2% lower due to heterogeneous portfolio allocations. The figure makes clear that the variation in AV_t is substantially determined by the distributions of bank and asset characteristics (leverage and illiquidity), while the distribution of bank-level portfolio composition (portfolio heterogeneity) plays essentially no role.[11] Reassuringly, the comparison reveals that

[11] This argument also applies to the framework of Duarte & Eisenbach (2021) which assumes constant asset shock. See Footnote 6.

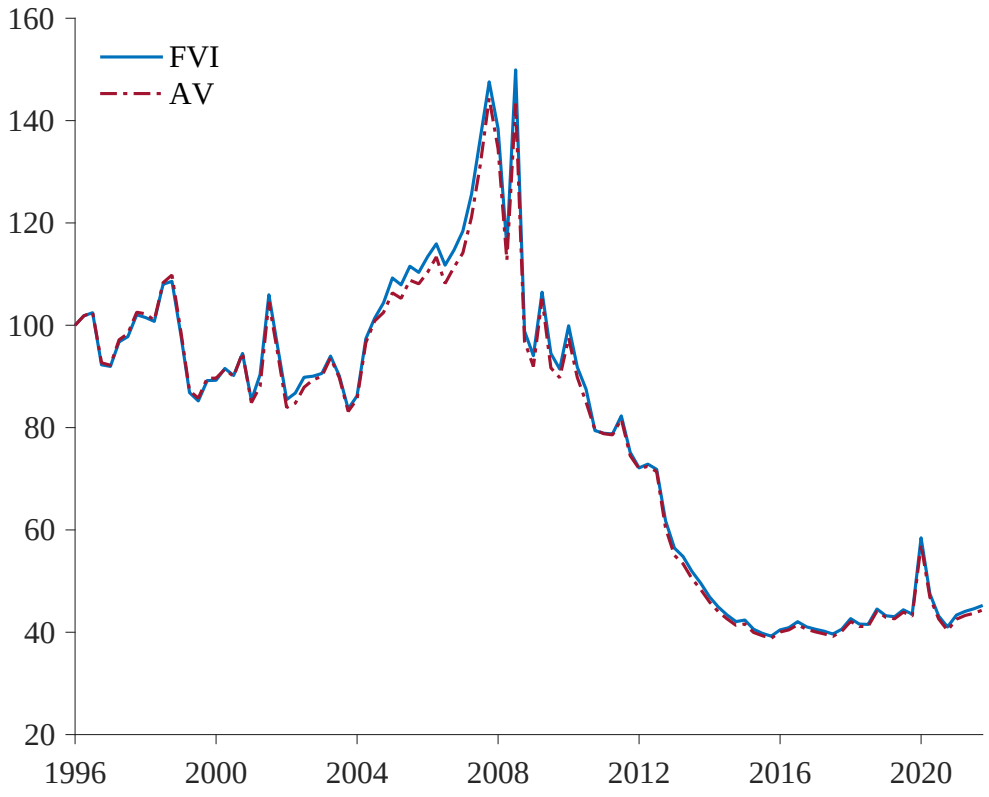

Figure 3.4. FVI and AV.

the simple FVI is a reasonably good candidate for monitoring aggregate vulnerability in lieu of the AV measure.

Despite the benchmark setting, it may be plausible to be concerned about the robustness to other specifications. Does the index continue to yield a similar pattern of vulnerability evolution when the model assumptions change? Two points arise. First, the asset matrix, which connects the assumption of selling behaviour (liquidation rules) with the AV measure.[12] Second, the level of asset illiquidity at any time (mentioned

[12]Selling assets proportionately is a simplifying assumption at the theoretical level. Presumably, banks are forced against several binding constraints (such as the risk-weighted capital requirement) and find it notoriously hard to raise equity in times of distress. In this case, they have incentives to deleverage through selling assets with greater risk weights, for example. It is also plausible that banks may be inclined to sell liquid assets first, given that this will lead to less price decline.

previously), which determines the price impact. The question can be addressed by noting that Duarte & Eisenbach (2021) have conducted a battery of comprehensive robustness checks, showing that the trends would not be significantly affected by various assumptions (see Section I in their Internet Appendix for details). I have shown and explained that the FVI approximates AV remarkably well in the benchmark setting of Greenwood et al. (2015). Therefore, the alternative model specifications do not change the qualitative patterns of the FVI, and similar checks do not need to be repeated.

3.3.3 The financial frictions

Abundant theories have been developed to explain the asymmetry and nonlinearity associated with financial frictions and the macroeconomy. Motivated by this line of research, I investigate the conditional relationship between future economic growth and current financial vulnerability, using the quantile regression of Koenker & Bassett (1978). Relatedly, the approach is applied by Giglio et al. (2016) to study the recession-relevant information content of systemic risk measures, and by Adrian et al. (2019) to propose a framework of "vulnerable growth" to quantify downside risks to GDP growth. Unlike their use of composite indices constructed from a large number of measures with predictive power, I focus on the FVI as a "pure" proxy for vulnerability and examine the link between "vulnerable banks" and "vulnerable growth."

I use the pre-2020 sample and follow the specification of Adrian et al. (2019).[13] Denote the annualised average growth rate of GDP between t and $t+h$ by y_{t+h} and the vector containing the predictive variable(s) and a constant by $x_t \in \mathbb{R}^k$. The goal

[13]The regression stops at 2019Q4 to avoid the substantial swings in growth during the COVID-19 pandemic. The data on real GDP is downloaded from Federal Reserve Economic Data (https://fred.stlouisfed.org/series/A191RL1Q225SBEA).

is to estimate the quantile function of y_{t+h} conditional on x_t:

$$\hat{\mathcal{Q}}_\tau(y_{t+h} \,|\, x_t) = x_t^\top \hat{\beta}_\tau.$$

The regression coefficient, $\hat{\beta}_\tau$, is obtained by minimising the sum of absolute errors weighted by τ:

$$\underset{\beta_\tau \in \mathbb{R}^k}{\arg\min} \sum_{t=1}^{T-h} \left(\tau \cdot \mathbb{1}_{\{y_{t+h} \geq x_t^\top \beta_\tau\}} |y_{t+h} - x_t^\top \beta_\tau| + (1-\tau) \cdot \mathbb{1}_{\{y_{t+h} < x_t^\top \beta_\tau\}} |y_{t+h} - x_t^\top \beta_\tau| \right),$$

where $\mathbb{1}_{\{.\}}$ is the indicator function.

As a first look, the left plot in Figure 3.5 shows the ordinary least squares (OLS) regression line and the univariate quantile regression lines for the fifth, fiftieth, and ninety-fifth quantiles. The regression slopes appear to differ from the OLS slope at $\tau = 5\%$ and $\tau = 95\%$. At high quantiles, the FVI is positively associated with (one-quarter-ahead) GDP growth, suggesting that an increase in FVI predicts an increase in GDP growth. This makes sense during the booms. The relationship becomes negative at low quantiles, suggesting that increased vulnerability may be followed by severe recessions.

To more formally evaluate the information content of the FVI, the right plot in Figure 3.5 shows the coefficients for the quantile regression where conditioning variables are the FVI and the current GDP growth. The estimates are flat over a large range of quantiles. Estimated coefficients outside the confidence bounds would suggest a nonlinear relationship between GDP growth and the FVI.[14] Therefore, the result implies that the estimated slope is significantly different from the OLS slope only at $\tau = 95\%$.

[14] As in Adrian et al. (2019), the confidence bounds are computed under the hypothesis of constant slopes, using 1000 bootstrapped samples generated by a vector autoregression with 4 lags, Gaussian errors, and a constant, fitted to the sample of the FVI and GDP growth.

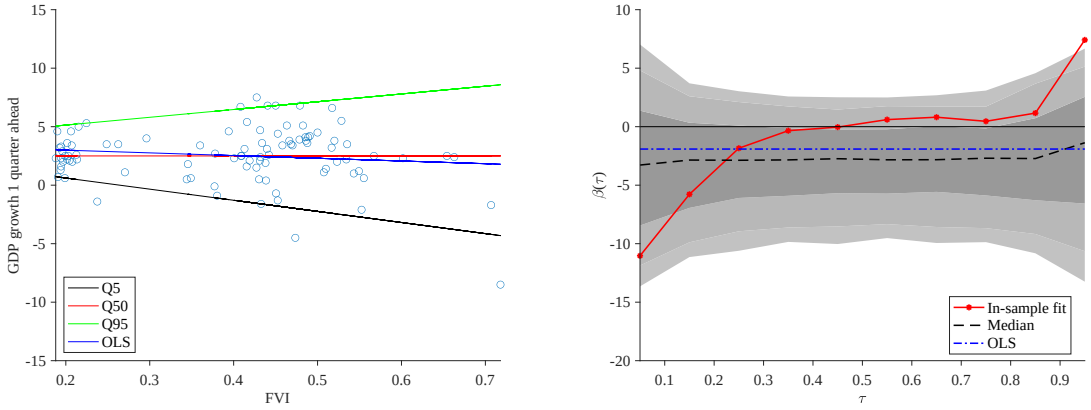

Figure 3.5. Quantile regressions (FVI). The sample period is 1996Q1–2019Q4. The left plot shows the one-quarter-ahead GDP growth against the FVI, along with the OLS regression line and the fitted univariate quantile regression lines for the fifth, fiftieth, and ninety-fifth quantiles. The right plot shows the estimated quantile regression coefficients in regressions of one-quarter-ahead GDP growth on the FVI and current GDP growth. As in Adrian et al. (2019), the confidence bounds (at the 75%, 90%, and 95% level) are obtained under the hypothesis of constant slopes and computed from 1000 bootstrapped samples, which are generated using a vector autoregression with 4 lags fitted to the sample of the FVI and GDP growth.

For comparison, I also use the Chicago Fed's National Financial Conditions Index (NFCI) as the predictive variable.[15] The NFCI uses a weighted average of about one hundred indicators of financial activity to reflect financial conditions in the U.S. banking system (Brave & Butters, 2012). Based on the sample from 1973Q to 2015Q4, Adrian et al. (2019) find that the nonlinear relationship between the NFCI and GDP growth is statistically significant at both the high and low quantiles. Figure 3.6 shows that during 1996Q1–2019Q4, it is above the significance level only at low quantiles. In addition, the figure suggests negative effects on the GDP growth at both low and high quantiles. This is different from the observation in Adrian et al. (2019), where there is a positive effect at high quantiles.

In conclusion, the quantile effect of vulnerability on GDP growth is weak. How-

[15]The NFCI at the quarterly frequency is obtained by averaging the weekly observations. The data is available for download from Federal Reserve Economic Data (https://fred.stlouisfed.org/series/NFCI).

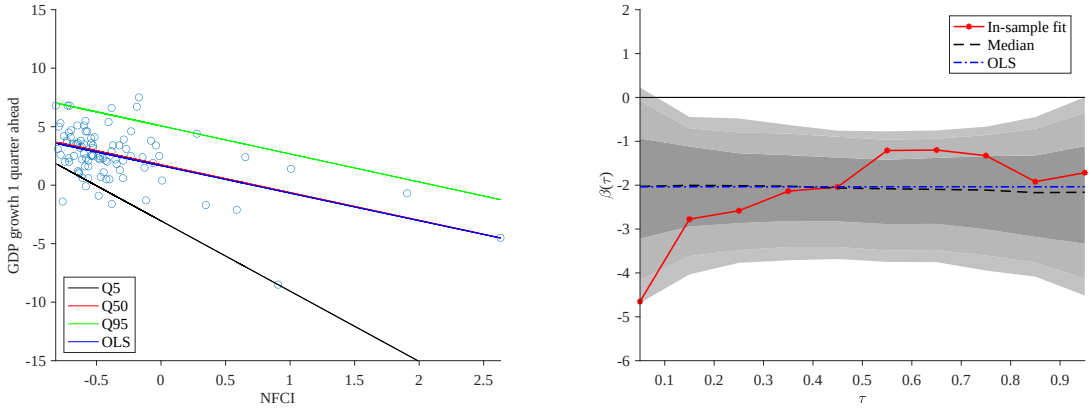

Figure 3.6. Quantile regressions (NFCI). This figure shows the results on quantile regressions when using the NFCI as the predictive variable. See text.

ever, the interpretation deserves some caution because the regressions seem sensitive to the sample period and a long time span is important when evaluating the predictive ability of financial indicators for macroeconomic outcomes. In addition, balance sheet measures generally have difficulty in generating enough statistical power. For these reasons, I cannot say much more.

3.3.4 Comparison with other indicators

There are various explanations for the increasing vulnerability. In general, a higher risk appetite should induce intermediaries to take on more risk, and higher risk taking is associated with larger balance sheets and higher leverage.[16] Next, I confront the FVI to U.S. proxies of stress and uncertainty, which capture risk appetite in credit markets in different dimensions. The Gilchrist & Zakrajšek's (2012) excess bond premium is a measure of risk appetite in the corporate bond market with high information content for future economic developments; it captures variation in corporate credit spreads beyond the compensation for expected defaults. The Bekaert, Engstrom & Xu's (2022) risk

[16]Theories predict a causal link between risk taking and risk appetite, although an exploration of this issue is beyond the scope of this work. See the literature on the risk-taking channel of monetary policy transmission (Borio & Zhu (2012)).

Table 3.2. Correlations among the indicators

	FVI	EBP	BEX	VIX	JLN
FVI	1.00				
EBP	0.17*	1.00			
BEX	0.17*	0.79***	1.00		
VIX	0.25***	0.74***	0.91***	1.00	
JLN	0.08	0.48***	0.63***	0.59***	1.00

Notes: The table shows the correlation coefficients between the FVI and the indicators mentioned in the main text (data sources are mentioned in Figure 3.1). The monthly indicators are averaged within the quarter to obtain a quarterly time series. The sample period is 1996Q1–2021Q4. * $p < .1$; ** $p < .05$; *** $p < .01$.

aversion index is based on the equity variance risk premium. The VIX is constructed using the implied volatilities of a broad range of S&P 500 index options and often used as a proxy for uncertainty. The Jurado, Ludvigson & Ng's (2015) macroeconomic uncertainty index is an aggregate of the conditional volatility of the unforecastable component of a series of economic variables.

The dashed lines in Figure 3.1 show these four market-based indicators, normalised using the full-sample mean and standard deviation. They were low in the boom period before the GFC and spiked simultaneously. In addition, they are comparatively more volatile than the FVI. Table 3.2 reports the correlations. The FVI is moderately correlated with VIX at 0.25, but the correlations with others are generally low and not statistically significant. On the other hand, the cross correlations among the four market-based indicators are high and statistically significant, although they are derived from different methods. (The notions of risk appetite and uncertainty are difficult to distinguish semantically and are sometimes used as synonyms in measuring "financial strains.") In short, the FVI is not directly related to the larger economy and exhibits independent variation compared to popular measures of stress and uncertainty.

The comparison has implications for decision making. Consider two analogies between measurement in atmospheric science and economics: first, atmospheric chem-

istry analyses the interaction between the atmosphere and organisms by tracing the composition of the atmosphere, as tracing the composition of financial accounts; second, measuring atmospheric temperature and pressure for weather forecasting can be thought of as measuring financial stress for forecasting macroeconomic activity. Following this logic, quantities tell latent vulnerabilities, while asset prices help signal distress.[17] From the perspective of operationalising macroprudential regulation, the use of indicators depends largely on the objective, a point that will be revisited in the next section.

3.4 Countercyclical capital buffer

This section demonstrates that the FVI can be used to set the countercyclical capital buffer (CCyB), an instrument designed to protect the banking sector from periods of excessive growth associated with a build-up of systemic risk.

3.4.1 Comparison with the benchmark

According to the reference guide (Basel Committee on Banking Supervision (2010)), the benchmark buffer rate of CCyB varies between 0 and 2.5% and increases linearly when the value of the credit-to-GDP gap (henceforth the "gap"), defined as the deviation of the credit-to-GDP ratio from its long-term trend, exceeds a threshold. Specifically, it

[17]This dichotomy is consistent with the literature (Borio & Lowe (2002)): Schularick & Taylor (2012) show that bank-loan growth is a near-universal precursor of financial crises; Baron et al. (2021) show that substantial declines in returns provide information on the timing of banking crises. Along this line, Greenwood et al. (2022) define an indicator by looking at excess credit growth and booming asset prices. This line of early warning literature relies on predictive power in a statistical model to explain the causes of crises (see, e.g., Demirgüç-Kunt & Detragiache (2005) for a review). The FVI starts from an accounting perspective and addresses vulnerabilities in the evolving financial structure, which consists of assets and liabilities, rather than asset prices that are more related to macroeconomic conditions. Benoit et al. (2017, p. 134), for example, note that market-based approaches may lack a theoretical foundation and "generally do not permit to clearly identify the source of risk at play".

is computed as

$$\text{Buffer}_t^{\text{GAP}}(\%) = \begin{cases} 0, & \text{if } \text{GAP}_t < \text{GAP}^{\text{low}}, \\ 2.5 \times \left(\frac{\text{GAP}_t - \text{GAP}^{\text{low}}}{\text{GAP}^{\text{high}} - \text{GAP}^{\text{low}}} \right), & \text{if } \text{GAP}^{\text{low}} \leq \text{GAP}_t \leq \text{GAP}^{\text{high}}, \\ 2.5, & \text{if } \text{GAP}_t > \text{GAP}^{\text{high}}, \end{cases}$$

where GAP^{low} and GAP^{high} equal to 2% and 10%, respectively. Using historical data from a wide range of countries, Drehmann et al. (2011) show that the gap presents good signalling properties without generating large noise and can perform well in setting the CCyB.

Because the CCyB is designed to restrict risk build-up among banks, the FVI can reasonably be expected to play a role in the task. For comparison, I set the buffer rate based on the FVI as follows:

$$\text{Buffer}_t^{\text{FVI}}(\%) = \begin{cases} 0, & \text{if } \text{FVI}_t < \text{FVI}_t^{\text{low}}, \\ 2.5 \times \left(\frac{\text{FVI}_t - \text{FVI}_t^{\text{low}}}{\text{FVI}_t^{\text{high}} - \text{FVI}_t^{\text{low}}} \right), & \text{if } \text{FVI}_t^{\text{low}} \leq \text{FVI}_t \leq \text{FVI}_t^{\text{high}}, \\ 2.5, & \text{if } \text{FVI}_t > \text{FVI}_t^{\text{high}}, \end{cases}$$

where $\text{FVI}_t^{\text{low}}$ and $\text{FVI}_t^{\text{high}}$ are the 65th percentile and the 80th percentile of FVI_t up to time t, respectively. Note that only the information available up to that date is used. Also note that the result depends on the thresholds. The exercise is merely for illustrative purposes, so I will not address robustness but rather refer to the work of the ESRB (Detken et al., 2014, Section 5) for practical challenges and alternative analytical methods.

The top plot of Figure 3.7 shows the estimated buffers from 2004Q1 to 2021Q4. $\text{Buffer}_t^{\text{FVI}}$ is triggered in 2004Q2, then reaches maximum in 2004Q4 and remains high

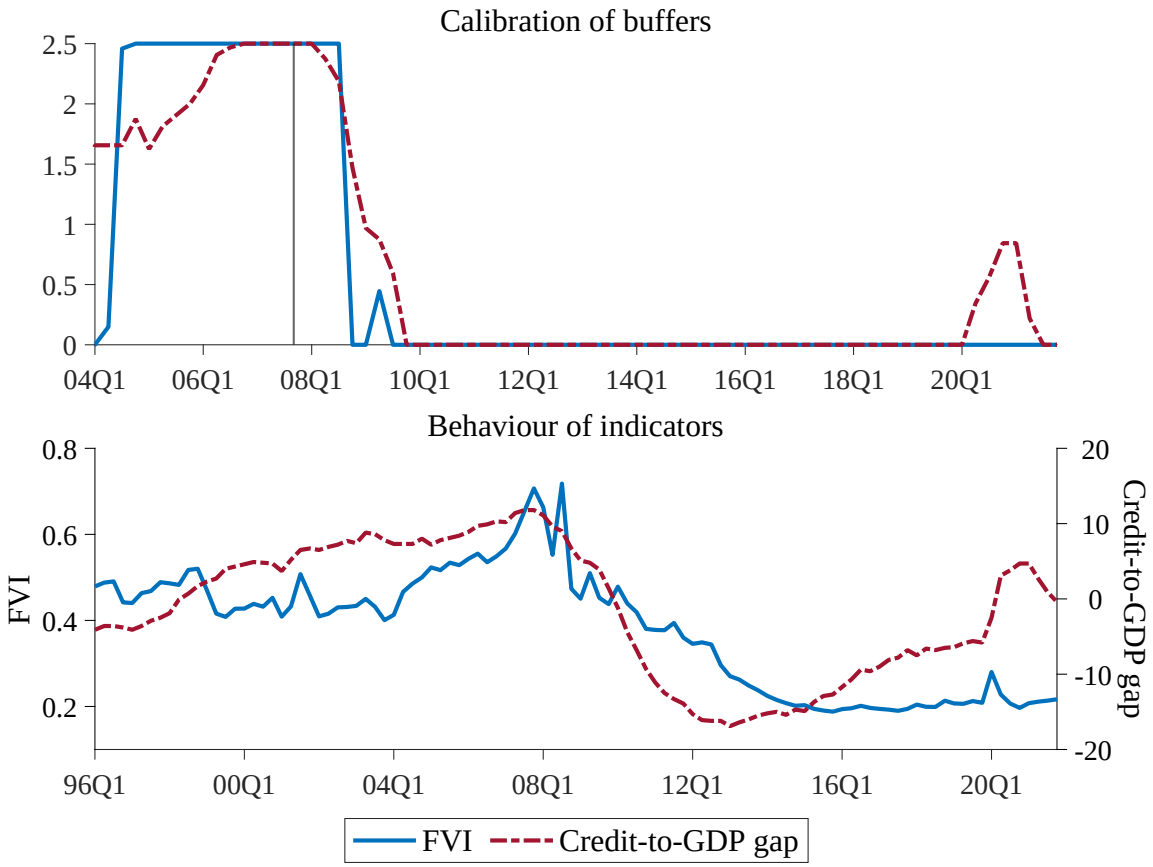

Figure 3.7. Mapping indicators into buffers. The vertical line indicates the start date of the crisis according to the chronology of Laeven & Valencia (2020). The credit-to-GDP data are available from the BIS website (https://data.bis.org/topics/CREDIT_GAPS).

for nearly four years. It drops to zero in 2008Q4, increases temporarily in 2009Q2, and is constant thereafter. $\text{Buffer}_t^{\text{GAP}}$ rises steadily from 2005Q1 and reaches maximum in 2006Q4. It decreases from 2008Q2 and drops to zero in 2009Q4. The two indicators demonstrate comovement (see the bottom plot of Figure 3.7), and both could trigger buffer requirements before the GFC. The results suggest that given banks' active adjustments, the FVI could reflect changes in the banking sector in a timely fashion and, therefore, could be one of the potential anchors to build macroprudential capital buffers in good times.

However, both indicators are worse at signalling the proper timing of the release. The vertical line indicates the start date of the crisis. $\text{Buffer}_t^{\text{FVI}}$ responds with a delay (due to changes in the composition of banks in the sample) before dropping to zero in one quarter. $\text{Buffer}_t^{\text{GAP}}$ decreases promptly but falls to zero only after two years when the crisis is less pronounced. Drehmann et al. (2011), for example, show that market indicators are better at signalling the proper timing of the release. In a nutshell, quantities that reflect sources of weakness and prices that capture market stress can work jointly for different phases of financial cycles.

Turning to the end of the sample period, $\text{Buffer}_t^{\text{FVI}}$ does not respond because the abrupt change in FVI is mild, while the gap surges in 2020Q1 and triggers $\text{Buffer}_t^{\text{GAP}}$ by attaining a level that almost parallels 2004Q1. However, unlike the GFC, the economic crisis during the COVID-19 pandemic is caused by an exogenous shock. Moreover, the gap's soar is mainly the consequence of the contraction in GDP and increased lending due to the policy response (which also causes the FVI to rise). The upward trend of the gap does not last long and is close to zero in 2021Q3. In reality, the Basel Committee on Banking Supervision (2021, p. 33) finds that the accumulated CCyBs among most of its member jurisdictions were limited at the onset of the pandemic.

3.4.2 Comments

The current CCyB policy framework differs between jurisdictions; it is implemented in a manner of "guided discretion" that combines evaluating indicators to identify systemic risk build-up with expert judgement (Basel Committee on Banking Supervision, 2017). For example, the Financial Policy Committee at the Bank of England (2023) chooses the CCyB buffer rate in two stages: (i) assessing financial vulnerabilities and (ii) assessing banks' resilience to potential shocks. In this context, the FVI can be helpful for decision-making in the first stage before further analytical approaches are applied

(such as macroprudential stress tests).

Meanwhile, an emphasis on indicators comes with caveats. First, the selection of indicators in an early warning system can change over time and depends on the development of the financial system. Second, the index lacks a cost-benefit analysis, which requires additional parameter estimation. Simple measures do not help to assess the appropriate level and effectiveness of the CCyB. In this regard, Van Oordt (2023) uses a statistical approach based on systemic risk measures to calibrate the magnitude of CCyB for six advanced economies, and Elenev et al. (2021) apply a general equilibrium model to study the welfare gains of the buffer requirements.

3.5 Historical banking crises

The starting point of this work is to formulate financial vulnerability from a systemic perspective. The construction of the index suggests that it transcends implementation restricted to a specific period. So far, attention has been focused on the current banking system. This section illustrates an implementation for the United States in 1928 and 1933.

3.5.1 Empirical implementation

I digitalise balance sheet data in the Annual Report of the Office of the Comptroller of the Currency (OCC). The sample consists of all nationally chartered banks in 48 states (excluding Alaska and Hawaii) recorded in the report. Equity is the sum of capital, surplus and undivided profits (see Figure 3.8), and there are 15 asset classes (see Figure 3.9).[18]

[18]The leverage factor of the FVI uses Table No. 97 in the 1928 annual report and Table K in the 1933 annual report. The illiquidity factor of the FVI uses Table No. 60 in the 1929 annual report and Table No. 66 in the 1934 annual report. "U.S. Government securities" and "Securities fully guaranteed by U.S. Government" in Table No. 66 are combined to make the asset classes in the two years identical.

by reports of condition December 31, 1928—Continued

PENNSYLVANIA—Continued

DISTRICT NO. 3—Continued

Cash and exchange, including lawful reserve with Federal reserve bank	Other assets	Total resources and liabilities	Capital	Surplus and undivided profits	Circulation	Due to banks	Demand deposits (including United States deposits)	Time deposits	Other liabilities	
$418,958	$28,530	$2,897,402	$200,000	$240,255	$49,050	$32,863	$1,192,992	$1,059,844	$122,398	1
787,410	51,557	8,734,357	400,000	680,352	197,750	101,062	3,102,616	3,675,569	577,008	2
150,943	3,436	1,511,404	200,000	51,098		9,104	590,892	635,310	25,000	3
8,493,289	3,500,339	58,463,130	3,300,000	5,188,059	500,000	4,699,300	25,231,958	8,357,653	11,196,160	4

Figure 3.8. Excerpt from the OCC Annual Report, 1928.

Abstract of reports of condition of national banks at date of each call during year ended October 31, 1929 (arranged by States and reserve cities)—Continued

PENNSYLVANIA

[In thousands of dollars]

	Dec. 31, 1928	Mar. 27, 1929	June 29, 1929	Oct. 4, 1929
	822 banks	821 banks	820 banks	817 banks
RESOURCES				
Loans and discounts (including rediscounts)	901,764	909,946	927,215	941,044
Overdrafts	223	254	242	305
United States Government securities owned	152,115	152,606	151,339	149,682
Other bonds, stocks, securities, etc., owned	515,411	512,680	502,506	495,043
Customers' liability account of acceptances	788	961	831	858
Banking house, furniture and fixtures	63,319	63,799	64,616	66,147
Other real estate owned	8,635	9,426	10,117	10,055
Reserve with Federal reserve bank	64,496	62,856	63,177	62,271
Cash in vault	31,794	29,702	24,133	28,638
Due from banks	75,724	61,796	66,628	74,213
Outside checks and other cash items	2,177	1,442	2,243	1,817
Redemption fund and due from United States Treasurer	3,082	3,092	3,122	3,144
Acceptances of other banks and bills of exchange or drafts sold with indorsement	33	51	23	62
Securities borrowed	249	299	323	324
Other assets	2,549	3,074	3,650	3,582
Total	1,822,359	1,811,984	1,820,165	1,837,185

Figure 3.9. Excerpt from the OCC Annual Report, 1929.

Due to the lack of data, the parameter l_k is omitted from the mathematical expression. In addition, the price impact is assumed to be inversely proportional to aggregate liquidity, which is defined as the sum of vault cash, reserves with the Federal Reserve banks, outside checks, and other cash items. These liquid assets are relatively easy to meet withdrawal demands, so the assumption can be interpreted as being consistent with "cash-in-the-market" pricing (Allen & Gale, 1994). Of course, alternative assumptions are worth further exploration, given that different definitions of illiquidity are possible, but the one used here can be seen as a plausible benchmark.

Table 3.3 reports the result. Four Mountain states (Arizona, Utah, Idaho, and Montana) had high FVI on the eve of the Great Depression. This is mainly because, in each of these states, a few large banks dominated the local market. On average, the FVI was high in the West, followed by the Midwest, South, and Northeast. The comparison between 1928 and 1933 indicates deleveraging in most states. A more obvious observation is the widespread reduction of illiquidity. Asset concentration, measured as the HHI, decreased in all states (results not shown). According to the study of Wicker (1996), banking panics during the Great Depression were concentrated in a few regions; Chicago, for example, experienced a wave of bank suspensions in 1931. The table shows that the liquidity condition in Illinois was significantly improved as of December 1933. To check the association between distress and change in illiquidity, I calculate the bank suspension rate by state as the ratio of total number of banks suspended during 1929–33 and the total number of banks in 1928.[19] The OLS regression shows that the degree of suspension during 1929–33 is statistically significant in explaining the cross-sectional percentage decrease in illiquidity in the same period (the

The files are available for download on the St. Louis Fed website (Federal Reserve Archival System for Economic Research).

[19]The *Federal Reserve Bulletin* (September 1937) contains the statistics of bank suspensions, which "comprise all banks closed to the public, either temporarily or permanently by supervisory authorities or by the banks' boards of directors on account of financial difficulties."

t-statistic is 3.49 with adjusted R^2 of 0.192).

Table 3.3. Financial vulnerability by states

State	1928			1933		
	Leverage	Illiquidity	FVI	Leverage	Illiquidity	FVI
AL	49.1	5.5	270.0	25.3	2.8	70.8
AZ	239.5	3.2	766.4	107.7	2.3	247.7
AR	70.7	4.7	332.3	51.9	2.0	103.8
CA	77.3	5.2	402.0	68.5	4.7	322.0
CO	136.0	3.3	448.8	101.5	1.7	172.5
CT	37.6	6.5	244.4	47.3	4.0	189.2
DE	23.6	5.5	129.8	14.4	5.9	85.0
FL	69.0	3.9	269.1	66.1	2.6	171.9
GA	59.1	5.4	319.1	61.4	3.6	221.0
ID	159.6	4.1	654.4	99.5	1.2	119.4
IL	81.3	4.6	374.0	86.6	1.1	95.3
IN	62.9	4.5	283.0	62.1	1.6	99.4
IA	99.2	4.5	446.4	79.6	1.7	135.3
KS	85.8	3.9	334.6	63.7	2.1	133.8
KY	65.6	6.5	426.4	58.2	3.2	186.2
LA	77.0	5.8	446.6	99.1	2.6	257.7
ME	66.9	7.1	475.0	60.5	1.4	84.7
MD	61.0	4.8	292.8	75.8	1.8	136.4
MA	66.6	5.1	339.7	44.1	2.5	110.2
MI	83.1	5.2	432.1	65.7	2.2	144.5
MN	103.9	3.8	394.8	84.3	2.6	219.2

Table 3.3 Continued

State	1928			1933		
	Leverage	Illiquidity	FVI	Leverage	Illiquidity	FVI
MS	89.1	5.3	472.2	66.1	1.9	125.6
MO	77.3	4.8	371.0	104.2	1.6	166.7
MT	142.1	4.0	568.4	68.7	1.8	123.7
NE	120.9	4.7	568.2	80.0	2.2	176.0
NV	106.4	5.0	532.0	215.8	2.2	474.8
NH	39.9	4.3	171.6	33.6	3.1	104.2
NJ	65.0	6.3	409.5	60.0	4.0	240.0
NM	158.1	3.5	553.4	82.7	1.4	115.8
NY	78.3	4.0	313.2	40.6	2.3	93.4
NC	48.5	6.6	320.1	33.4	2.0	66.8
ND	123.8	4.3	532.3	61.7	3.0	185.1
OH	51.8	5.3	274.5	48.4	3.2	154.9
OK	152.4	3.5	533.4	68.7	2.0	137.4
OR	100.2	3.7	370.7	124.2	2.3	285.7
PA	40.4	5.4	218.2	34.5	3.6	124.2
RI	30.0	5.5	165.0	20.0	4.8	96.0
SC	72.0	5.7	410.4	57.2	1.8	103.0
SD	113.8	3.8	432.4	60.3	3.2	193.0
TN	73.4	6.2	455.1	67.8	2.9	196.6
TX	76.4	4.4	336.2	62.1	1.9	118.0
UT	158.7	4.1	650.7	82.4	2.5	206.0
VT	59.6	7.0	417.2	29.5	3.7	109.2

Table 3.3 Continued

State	1928			1933		
	Leverage	Illiquidity	FVI	Leverage	Illiquidity	FVI
VA	45.9	8.5	390.1	47.1	4.0	188.4
WA	114.6	3.9	446.9	63.3	2.5	158.2
WV	42.8	6.8	291.0	37.3	3.7	138.0
WI	87.5	6.1	533.8	58.9	2.7	159.0
WY	97.2	3.9	379.1	67.4	1.7	114.6

The OCC Annual Report also allows for implementing the FVI for each Federal Reserve district, shown in Table 3.4. Consistent with the state-level result, districts in the West and Midwest had high FVI in 1928, and the seventh district saw a big improvement in liquidity. In addition to different disaggregation, extending the sample using similar balance sheet information is also possible. Exploring structural changes in the banking system from a long-run perspective can be the next step.

Table 3.4. Financial vulnerability by Federal Reserve districts

District	1928			1933		
	Leverage	Illiquidity	FVI	Leverage	Illiquidity	FVI
1	58.8	5.4	317.5	43.3	2.8	121.2
2	77.7	4.1	318.6	43.2	2.7	116.6
3	35.2	6.0	211.2	32.9	4.1	134.9
4	51.7	4.9	253.3	42.5	3.6	153.0
5	51.8	6.2	321.2	52.4	2.9	152.0
6	62.5	5.3	331.2	57.6	3.0	172.8
7	82.0	4.9	401.8	78.7	1.8	141.7

Table 3.4 Continued

District	1928			1933		
	Leverage	Illiquidity	FVI	Leverage	Illiquidity	FVI
8	70.7	5.0	353.5	75.9	2.5	189.8
9	108.2	3.9	422.0	77.3	3.3	255.1
10	124.3	3.8	472.3	82.5	2.2	181.5
11	78.8	4.4	346.7	64.9	2.8	181.7
12	86.5	4.8	415.2	71.7	4.5	322.7

3.5.2 Discussion

I now discuss the connection with the literature. The potential improvement and application mentioned are left for future research.

Influenced in part by theoretical models of financial contagion through contractual obligations (e.g., Allen & Gale (2000)), researchers have rekindled interest in the role of interbank networks in historical crises. They have attempted to apply network analysis to contexts where a common thread is the pyramid structure and the propagation of withdrawal through the correspondence relationship (see, e.g., White (1983) for an introduction to the American banking system in the early 20th century). An example is the work of Anderson et al. (2019), who use an interbank clearing model to study the effect of the National Banking Acts on financial stability. The accounting structure of the FVI does not appear to speak prima facie to contagion but its elements are implicitly invoked in many contagion models. The index can be blended with more institutional details as a next step. For example, the definition of liquid assets can include interbank assets of country banks to incorporate the assumption that they

withdraw deposits at reserve city banks and central reserve city banks during panics.[20]

Meanwhile, abundant literature has studied the role of financial frictions in financial crises.[21] It is well-established that severe recessions are often preceded by credit expansions (e.g., Reinhart & Rogoff, 2009). Rajan & Ramcharan (2015), for example, study the role of leverage in asset price inflation in the 1920s. The FVI is related to the line of research on how well vulnerability and shock can account for the severity of financial crises (Krishnamurthy & Muir (2020)). Provided data availability, the index could be extended to cross-country studies along the lines of Jordà et al. (2021), which explores the relationship between bank capital and crisis risk via balance sheet ratios. In sum, the FVI could be used as a proxy for financial vulnerability while providing a systemic perspective on the anatomy of financial crises.

3.6 Conclusion

I have introduced an index of financial vulnerability based on a general law of economic motion, for which voluminous theories have been discussed for a long time. I have also used U.S. data to show the empirical implementation in different areas. The demonstration of indicators is widespread in media and policy reports. Against the background of macroprudential regulation, the FVI adds value from both the systemic and operational perspectives. While the index is not, of course, perfect, it could be preferred because of its simplicity and communicability.

[20] For example, see Mitchener & Richardson (2019) for empirical evidence on the behaviour of banks in different locations during the Great Depression.

[21] See Sufi & Taylor (2022) for a recent survey and Calomiris & Gorton (1991) for an earlier discussion on the origins of banking panics.

Appendix A

Appendix for Chapter 2

A.1 Algorithmic equilibrium characterisations

This section presents the two algorithmic equilibrium characterisations for the models discussed in Section 2.5.

Algorithm 1 Full Payment Algorithm (FPA) in Bardoscia et al. (2019)

1: Set $e(0) := A^b$, $l(0) := \mathbf{0}$, and $\mathcal{A}(0) := \emptyset$. Set $t = 1$.
2: For all $i \in \mathcal{N}$, set

$$e_i(t) = e_i(t-1) + \sum_{j \in \mathcal{N}} l_j(t-1)\Pi_{ji} - l_i(t-1). \tag{A.1.1}$$

3: Determine

$$\mathcal{A}(t) = \{i \in \mathcal{N} \,|\, e_i(t) \geq \bar{L}_i\} \setminus \bigcup_{s=0}^{t-1} \mathcal{A}(s). \tag{A.1.2}$$

4: **if** $\mathcal{A}(t) \equiv \emptyset$ **then**
5: **return** $\tilde{l}_* = \sum_{s=0}^{t-1} l(s)$.
6: **else**
7: set $l_i(t) = \bar{L}_i$ for all $i \in \mathcal{A}(t)$, and $l_i(t) = 0$ otherwise.
8: **end if**
9: Set $t = t + 1$ and go back to step 2.

Algorithm 1 corresponds to the Full Payment Algorithm (FPA) by Bardoscia et al.

(2019). It computes a vector $\tilde{l}_*$ that corresponds to the payments made by all banks in the network. The mechanism can be understood as follows. At time t, $e(t)$ consists of the available liquid assets (including received payments), and $\mathcal{A}(t)$ is the set banks that can pay in full. Step 7 incorporates the assumption that banks either make full payment or pay nothing.[1] Therefore, the modelling assumption results in a sequence of payments, and banks can only pay in full if they have received sufficient liquidity.

Algorithm 2 Least Clearing Vector Algorithm (LA) for Rogers & Veraart (2013) model with $\alpha = \beta = 0$

1: Set $t = 0$, $l^{(0)} := \mathbf{0}$, and $\mathcal{D}^{(-1)} := \mathcal{N}$.
2: For all $i \in \mathcal{N}$, determine

$$v_i^{(t)} := A_i^b + \sum_{j \in \mathcal{N}} l_j^{(t)} \Pi_{ji} - \bar{L}_i. \tag{A.1.3}$$

3: Define

$$\mathcal{D}^{(t)} := \{i \in \mathcal{N} \,|\, v_i^{(t)} < 0\} \text{ and } \mathcal{S}^{(t)} := \{i \in \mathcal{N} \,|\, v_i^{(t)} \geq 0\}. \tag{A.1.4}$$

4: **if** $\mathcal{D}^{(t)} \equiv \mathcal{D}^{(t-1)}$ **then**
5: **return** $l_* = l^{(t-1)}$.
6: **else**
7: set $l_i^{(t+1)} = \bar{L}_i$ for all $i \in \mathcal{S}^{(t)}$, and $l_i^{(t+1)} = 0$ for all $i \in \mathcal{D}^{(t)}$.
8: **end if**
9: Set $t = t + 1$ and go back to step 2.

Algorithm 2 corresponds to the least clearing vector in the Rogers & Veraart (2013) model with $\alpha = \beta = 0$, in which case the defaulting banks make zero payments. We refer to Algorithm 2 as the Least Clearing Vector Algorithm (LA). The algorithm starts by assuming that initially there is no solvent bank that would be able to make any payment. $\mathcal{S}^{(0)}$ is the set of banks that would be able to pay liabilities in full even if all other banks did not meet their obligations. Similar to the construction in Rogers &

[1] Note that an important difference between the FPA and the hard default in Paddrik et al. (2020) is that in the former setting, it is assumed that—unlike the Eisenberg & Noe (2001) model in finding an equilibrium payment vector—there is no coordination among banks in the FPA to determine the payments.

Veraart (2013, Theorem 3.7), the output of the algorithm is the least clearing vector.

A.2 Proofs

This section provides the remaining proofs for Chapter 2.

A.2.1 Preliminaries

The following definition is a continuation of Section 2.3.2.

Definition A.2.1. Let $(L^{\mathcal{P}}, A^b; \mathbb{V})$ be the PTN-network. Define the function $\Phi^{\mathcal{P}} = \Phi^{\mathcal{P}}(\cdot; \mathbb{V}) : \mathcal{E}^{\mathcal{P}} \to \mathcal{E}^{\mathcal{P}}$ as

$$\Phi_i^{\mathcal{P}}(E) = \Phi_i^{\mathcal{P}}(E; \mathbb{V}) = A_i^b + \sum_{j:\bar{L}_j^{\mathcal{P}}>0} L_{ji}^{\mathcal{P}} \mathbb{V}\left(\frac{E_j + \bar{L}_j^{\mathcal{P}}}{\bar{L}_j^{\mathcal{P}}}\right) - \bar{L}_i^{\mathcal{P}} \quad \forall\, i \in \mathcal{N}, \tag{A.2.1}$$

where $\mathcal{E}^{\mathcal{P}} = [-\bar{L}^{\mathcal{P}}, A^b + \bar{A}^{\mathcal{P}} - \bar{L}^{\mathcal{P}}]$, $\bar{L}^{\mathcal{P}} = L^{\mathcal{P}}\mathbf{1}$, and $\bar{A}^{\mathcal{P}} = \mathbf{1}^\top L^{\mathcal{P}}$. We refer to a vector $E \in \mathcal{E}^{\mathcal{P}}$ satisfying $E = \Phi^{\mathcal{P}}(E)$ as a re-evaluated equity in the PTN-network.

We use the following lemmas to prove the main results in Section 2.4.

Lemma A.2.2. For any PTN-exercise $(L, \mathcal{P}, L^{\mathcal{P}})$, $\bar{L}_i = \bar{L}_i^{\mathcal{P}}$ for all $i \in \mathcal{N} \setminus \mathcal{P}$ and

$$\sum_{j\in\mathcal{P}} L_{ji} - \bar{L}_i = \sum_{j\in\mathcal{P}} L_{ji}^{\mathcal{P}} - \bar{L}_i^{\mathcal{P}} \quad \forall\, i \in \mathcal{N}. \tag{A.2.2}$$

Proof of Lemma A.2.2. The first result is a direct consequence of Definition 2.2.1. In addition, equation (A.2.2) is equivalent to

$$\sum_{j\in\mathcal{P}} L_{ji} - \bar{L}_i + \sum_{j\in\mathcal{N}\setminus\mathcal{P}} L_{ji} = \sum_{j\in\mathcal{P}} L_{ji}^{\mathcal{P}} - \bar{L}_i^{\mathcal{P}} + \sum_{j\in\mathcal{N}\setminus\mathcal{P}} \underbrace{L_{ji}^{\mathcal{P}}}_{=L_{ji}},$$

which holds because of the PTN-constraint in Definition 2.2.1. □

Lemma A.2.3. Given a PTN-exercise $(L, \mathcal{P}, L^{\mathcal{P}})$, let $E^{(0)} = E^{\text{initial}}(L)$ and $E^{\mathcal{P}(0)} = E^{\text{initial}}(L^{\mathcal{P}})$ be the initial equity in the original network and the PTN-network, respectively. For $n \in \mathbb{N}$, we define two sequences recursively by

$$E^{(n)} = \Phi\left(E^{(n-1)}\right), \quad E^{\mathcal{P}(n)} = \Phi^{\mathcal{P}}\left(E^{\mathcal{P}(n-1)}\right), \tag{A.2.3}$$

where the functions Φ and $\Phi^{\mathcal{P}}$ are defined in (2.5) and (A.2.1), respectively. Then

1. $E^{(0)} = E^{\mathcal{P}(0)}$;
2. the sequences $\left(E^{(n)}\right)$ and $\left(E^{\mathcal{P}(n)}\right)$ are non-increasing, i.e., for all $n \in \mathbb{N}_0$,

$$E^{(n)} \geq E^{(n+1)}, \qquad E^{\mathcal{P}(n)} \geq E^{\mathcal{P}(n+1)};$$

3. the sequences $\left(E^{(n)}\right)$ and $\left(E^{\mathcal{P}(n)}\right)$ converge to the greatest re-evaluated equities, i.e.,

$$\lim_{n\to\infty} E^{(n)} = E^{*}, \qquad \lim_{n\to\infty} E^{\mathcal{P}(n)} = E^{\mathcal{P};*},$$

where E^{*} and $E^{\mathcal{P};*}$ are the greatest fixed point of Φ and $\Phi^{\mathcal{P}}$, respectively.

Proof of Lemma A.2.3. For all $i \in \mathcal{N}$, the initial equities in the two networks can be written as

$$\begin{aligned} E_i^{(0)} &= A_i^b + \sum_{j\in\mathcal{N}\setminus\mathcal{P}} (L_{ji} - L_{ij}) + \sum_{j\in\mathcal{P}} (L_{ji} - L_{ij}), \\ E_i^{\mathcal{P}(0)} &= A_i^b + \sum_{j\in\mathcal{N}\setminus\mathcal{P}} (L_{ji} - L_{ij}) + \sum_{j\in\mathcal{P}} (L_{ji}^{\mathcal{P}} - L_{ij}^{\mathcal{P}}). \end{aligned}$$

Therefore, $E^{(0)} = E^{\mathcal{P}(0)}$ follows from the PTN-constraint in Definition 2.2.1. The second statement follows from Theorem 2.6 in Veraart (2020) because the functions Φ

and $\Phi^{\mathcal{P}}$ are non-decreasing by Lemma A.1 in Veraart (2020). The third statement also follows from Theorem 2.6 in Veraart (2020). □

A.2.2 Proof of Proposition 2.4.1

We use Lemma A.2.4 (similar to Lemma B.4 in Veraart (2022)) to prove Proposition 2.4.1.

Lemma A.2.4. For any PTN-exercise $(L, \mathcal{P}, L^{\mathcal{P}})$, let $\mathcal{F} = \{i \in \mathcal{N} \,|\, E_i^{\text{initial}}(L) < 0\}$ and $\mathcal{F}^{\mathcal{P}} = \{i \in \mathcal{N} \mid E_i^{\text{initial}}(L^{\mathcal{P}}) < 0\}$ be the fundamental default set in the original network and the PTN-network, respectively. Let $\tilde{E}$ be the greatest re-evaluated equity in the original network with default set $\mathcal{D}(\tilde{E})$ and $\tilde{E}^{\mathcal{P}}$ be the greatest re-evaluated equity in the PTN-network with default set $\mathcal{D}(\tilde{E}^{\mathcal{P}})$. Then $\mathcal{F} = \mathcal{F}^{\mathcal{P}}$, $\mathcal{F} \subseteq \mathcal{D}(\tilde{E})$, and $\mathcal{F}^{\mathcal{P}} \subseteq \mathcal{D}(\tilde{E}^{\mathcal{P}})$.

Proof of Lemma A.2.4. First, by Lemma A.2.3, $E^{\text{initial}}(L) = E^{\text{initial}}(L^{\mathcal{P}})$, so $\mathcal{F} = \mathcal{F}^{\mathcal{P}}$. Second, fix $i \in \mathcal{F}$ and consider the sequence $\left(E^{(n)}\right)$ defined by (A.2.3). Then Lemma A.2.3 implies that $\forall\, m \in \mathbb{N}$, $0 > E_i^{(0)} \geq E_i^{(m)} \geq \lim_{n\to\infty} E_i^{(n)} = \tilde{E}_i$, where $\tilde{E}$ is the greatest fixed point of Φ. Therefore, $i \in \mathcal{D}(\tilde{E})$. Finally, $\mathcal{F}^{\mathcal{P}} \subseteq \mathcal{D}(\tilde{E}^{\mathcal{P}})$ can be proved similarly by considering the sequence $(E^{\mathcal{P}(n)})$. □

Proof of Proposition 2.4.1. Given the fundamental default set in the PTN-network, denoted as $\mathcal{F}^{\mathcal{P}}$, we know from Lemma A.2.4 that $\mathcal{F}^{\mathcal{P}} \subseteq \mathcal{D}(\tilde{E}^{\mathcal{P}})$. We prove $\mathcal{F}^{\mathcal{P}} = \mathcal{D}(\tilde{E}^{\mathcal{P}})$ by showing that $\mathcal{D}(\tilde{E}^{\mathcal{P}}) \subseteq \mathcal{F}^{\mathcal{P}}$. Let $i \in \mathcal{D}(\tilde{E}^{\mathcal{P}})$. Then

$$0 > \tilde{E}_i^{\mathcal{P}} = A_i^b + \sum_{j \in \mathcal{M}^{\mathcal{P}}} L_{ji}^{\mathcal{P}} \mathbb{V}\left(\frac{\tilde{E}_j^{\mathcal{P}} + \bar{L}_j^{\mathcal{P}}}{\bar{L}_j^{\mathcal{P}}}\right) - \bar{L}_i^{\mathcal{P}}.$$

Hence, $\bar{L}_i^{\mathcal{P}} > 0$. Since $\mathcal{P} = \mathcal{N}$, the graph corresponding to the optimal PTN-network

is bipartite by Lemma 1 in D'Errico & Roukny (2021).[2] This implies that $L^{\mathcal{P}}_{ji} = 0$ for all $j \in \mathcal{M}^{\mathcal{P}}$. It follows that

$$\sum_{j \in \mathcal{M}^{\mathcal{P}}} L^{\mathcal{P}}_{ji} \mathbb{V}\left(\frac{\tilde{E}^{\mathcal{P}}_j + \bar{L}^{\mathcal{P}}_j}{\bar{L}^{\mathcal{P}}_j}\right) = 0 = \sum_{j \in \mathcal{N}} L^{\mathcal{P}}_{ji},$$

and hence

$$0 > \tilde{E}^{\mathcal{P}}_i = A^b_i - \bar{L}^{\mathcal{P}}_i = E^{\text{initial}}_i(L^{\mathcal{P}}).$$

Therefore $\mathcal{F}^{\mathcal{P}} = \mathcal{D}(\tilde{E}^{\mathcal{P}})$. Furthermore, $\mathcal{F}^{\mathcal{P}} = \mathcal{D}(\tilde{E}^{\mathcal{P}}) \subseteq \mathcal{D}(\tilde{E})$ by Lemma A.2.4 □

A.2.3 Proof of Theorem 2.4.2

Proof. Given the PTN-exercise $(L, \mathcal{P}, L^{\mathcal{P}})$, set

$$\mathcal{M} = \{i \in \mathcal{N} \mid \bar{L}_i > 0\}, \qquad \mathcal{M}^{\mathcal{P}} = \{i \in \mathcal{N} \mid \bar{L}^{\mathcal{P}}_i > 0\}.$$

1. Recall that for $(L, A^b; \mathbb{V})$ and $(L^{\mathcal{P}}, A^b; \mathbb{V})$ we consider the functions

$$\Phi_i(E) = A^b_i + \sum_{j \in \mathcal{M}} L_{ji} \mathbb{V}\left(\frac{E_j + \bar{L}_j}{\bar{L}_j}\right) - \bar{L}_i \quad \forall\, i \in \mathcal{N},$$
$$\Phi^{\mathcal{P}}_i(E) = A^b_i + \sum_{j \in \mathcal{M}^{\mathcal{P}}} L^{\mathcal{P}}_{ji} \mathbb{V}\left(\frac{E_j + \bar{L}^{\mathcal{P}}_j}{\bar{L}^{\mathcal{P}}_j}\right) - \bar{L}^{\mathcal{P}}_i \quad \forall\, i \in \mathcal{N}$$

   on $\mathcal{E} = [-\bar{L}, A^b + \bar{A} - \bar{L}]$, and $\mathcal{E}^{\mathcal{P}} = [-\bar{L}^{\mathcal{P}}, A^b + \bar{A}^{\mathcal{P}} - \bar{L}^{\mathcal{P}}]$, respectively.

   It holds that $\tilde{E} \in \mathcal{E}$. We need $\tilde{E} \in \mathcal{E}^{\mathcal{P}}$ before showing that $\tilde{E}$ is a fixed point of $\Phi^{\mathcal{P}}$. First, note that the PTN-constraint implies that $\mathcal{E}^{\mathcal{P}} = [-\bar{L}^{\mathcal{P}}, A^b + \bar{A} - \bar{L}]$. Hence, $\mathcal{E}$ and $\mathcal{E}^{\mathcal{P}}$ have the same upper bound but different lower bounds. To see that $\tilde{E} \in \mathcal{E}^{\mathcal{P}}$, note that for all $i \in \mathcal{N} \setminus \mathcal{P}$ it holds that $\bar{L}_i = \bar{L}^{\mathcal{P}}_i$ and hence

[2] As mentioned before, the optimal PTN-optimisation problem in Definition 2.2.4 is identical to the non-conservative compression problem in D'Errico & Roukny (2021) when $\mathcal{P} = \mathcal{N}$.

the corresponding lower bound for $\tilde{E}_i$ is the same in $\mathcal{E}$ and $\mathcal{E}^{\mathcal{P}}$. Furthermore, by assumption (2.6), $\tilde{E}_i \geq 0$ for all $i \in \mathcal{P}$ and hence the lower bound does not matter. Therefore, $\tilde{E} \in \mathcal{E}^{\mathcal{P}}$.

Since $\tilde{E}$ is a fixed point of Φ, we have

$$\tilde{E}_i = \Phi_i(\tilde{E}) = A_i^b + \sum_{j \in \mathcal{M}} L_{ji} \mathbb{V}\left(\frac{\tilde{E}_j + \bar{L}_j}{\bar{L}_j}\right) - \bar{L}_i \quad \forall\, i \in \mathcal{N}.$$

We show that $\tilde{E}$ is also a fixed point of $\Phi^{\mathcal{P}}$.

First, let $i \in \mathcal{N} \setminus \mathcal{P}$. Then, $\bar{L}_i = \bar{L}_i^{\mathcal{P}}$ and

$$\begin{aligned}
\tilde{E}_i &= A_i^b + \sum_{j \in \mathcal{M} \setminus \mathcal{P}} L_{ji} \mathbb{V}\left(\frac{\tilde{E}_j + \bar{L}_j}{\bar{L}_j}\right) + \sum_{j \in \mathcal{M} \cap \mathcal{P}} L_{ji} \mathbb{V}\left(\frac{\tilde{E}_j + \bar{L}_j}{\bar{L}_j}\right) - \bar{L}_i^{\mathcal{P}} \\
&= A_i^b + \sum_{j \in \mathcal{M}^{\mathcal{P}} \setminus \mathcal{P}} L_{ji}^{\mathcal{P}} \mathbb{V}\left(\frac{\tilde{E}_j + \bar{L}_j}{\bar{L}_j}\right) + \sum_{j \in \mathcal{M} \cap \mathcal{P}} L_{ji}^{\mathcal{P}} \mathbb{V}\left(\frac{\tilde{E}_j + \bar{L}_j}{\bar{L}_j}\right) - \bar{L}_i^{\mathcal{P}},
\end{aligned}$$

where the last equality holds because $\mathcal{M} \setminus \mathcal{P} = \mathcal{M}^{\mathcal{P}} \setminus \mathcal{P}$ and $L_{ji} = L_{ji}^{\mathcal{P}}$ for all j. By assumption,

$$\mathbb{V}\left(\frac{\tilde{E}_j + \bar{L}_j}{\bar{L}_j}\right) = 1 \quad \forall\, j \in \mathcal{M} \cap \mathcal{P}, \qquad \mathbb{V}\left(\frac{\tilde{E}_j + \bar{L}_j^{\mathcal{P}}}{\bar{L}_j^{\mathcal{P}}}\right) = 1 \quad \forall\, j \in \mathcal{M}^{\mathcal{P}} \cap \mathcal{P}.$$

It follows that

$$\begin{aligned}
\tilde{E}_i &= A_i^b + \sum_{j \in \mathcal{M}^{\mathcal{P}} \setminus \mathcal{P}} L_{ji}^{\mathcal{P}} \mathbb{V}\left(\frac{\tilde{E}_j + \bar{L}_j^{\mathcal{P}}}{\bar{L}_j^{\mathcal{P}}}\right) + \sum_{j \in \mathcal{M}^{\mathcal{P}} \cap \mathcal{P}} L_{ji}^{\mathcal{P}} - \bar{L}_i^{\mathcal{P}} \\
&= A_i^b + \sum_{j \in \mathcal{M}^{\mathcal{P}} \setminus \mathcal{P}} L_{ji}^{\mathcal{P}} \mathbb{V}\left(\frac{\tilde{E}_j + \bar{L}_j^{\mathcal{P}}}{\bar{L}_j^{\mathcal{P}}}\right) + \sum_{j \in \mathcal{M}^{\mathcal{P}} \cap \mathcal{P}} L_{ji}^{\mathcal{P}} \mathbb{V}\left(\frac{\tilde{E}_j + \bar{L}_j^{\mathcal{P}}}{\bar{L}_j^{\mathcal{P}}}\right) - \bar{L}_i^{\mathcal{P}} \\
&= A_i^b + \sum_{j \in \mathcal{M}^{\mathcal{P}}} L_{ji}^{\mathcal{P}} \mathbb{V}\left(\frac{\tilde{E}_j + \bar{L}_j^{\mathcal{P}}}{\bar{L}_j^{\mathcal{P}}}\right) - \bar{L}_i^{\mathcal{P}} = \Phi_i^{\mathcal{P}}(\tilde{E}).
\end{aligned}$$

Second, let $i \in \mathcal{P}$. Then,

$$\begin{aligned}\tilde{E}_i &= A_i^b + \sum_{j \in \mathcal{M} \setminus \mathcal{P}} L_{ji}^{\mathcal{P}} \mathbb{V}\left(\frac{\tilde{E}_j + \bar{L}_j}{\bar{L}_j}\right) + \sum_{j \in \mathcal{M} \cap \mathcal{P}} L_{ji} \mathbb{V}\left(\frac{\tilde{E}_j + \bar{L}_j}{\bar{L}_j}\right) - \bar{L}_i \\ &= A_i^b + \sum_{j \in \mathcal{M}^{\mathcal{P}} \setminus \mathcal{P}} L_{ji}^{\mathcal{P}} \mathbb{V}\left(\frac{\tilde{E}_j + \bar{L}_j}{\bar{L}_j}\right) + \sum_{j \in \mathcal{M} \cap \mathcal{P}} L_{ji} - \bar{L}_i,\end{aligned}$$

where the last equality uses the fact that $\mathbb{V}\left(\frac{\tilde{E}_j + \bar{L}_j}{\bar{L}_j}\right) = 1$ for all $j \in \mathcal{M} \cap \mathcal{P}$. Using equation (A.2.2) and $\mathbb{V}\left(\frac{\tilde{E}_j + \bar{L}_j^{\mathcal{P}}}{\bar{L}_j^{\mathcal{P}}}\right) = 1$ for all $j \in \mathcal{M}^{\mathcal{P}} \cap \mathcal{P}$, we obtain

$$\begin{aligned}\tilde{E}_i &= A_i^b + \sum_{j \in \mathcal{M}^{\mathcal{P}} \setminus \mathcal{P}} L_{ji}^{\mathcal{P}} \mathbb{V}\left(\frac{\tilde{E}_j + \bar{L}_j}{\bar{L}_j}\right) + \sum_{j \in \mathcal{M}^{\mathcal{P}} \cap \mathcal{P}} L_{ji}^{\mathcal{P}} - \bar{L}_i^{\mathcal{P}} \\ &= A_i^b + \sum_{j \in \mathcal{M}^{\mathcal{P}} \setminus \mathcal{P}} L_{ji}^{\mathcal{P}} \mathbb{V}\left(\frac{\tilde{E}_j + \bar{L}_j^{\mathcal{P}}}{\bar{L}_j^{\mathcal{P}}}\right) + \sum_{j \in \mathcal{M}^{\mathcal{P}} \cap \mathcal{P}} L_{ji}^{\mathcal{P}} \mathbb{V}\left(\frac{\tilde{E}_j + \bar{L}_j^{\mathcal{P}}}{\bar{L}_j^{\mathcal{P}}}\right) - \bar{L}_i^{\mathcal{P}} \\ &= A_i^b + \sum_{j \in \mathcal{M}^{\mathcal{P}}} L_{ji}^{\mathcal{P}} \mathbb{V}\left(\frac{\tilde{E}_j + \bar{L}_j^{\mathcal{P}}}{\bar{L}_j^{\mathcal{P}}}\right) - \bar{L}_i^{\mathcal{P}} = \Phi_i^{\mathcal{P}}(\tilde{E}).\end{aligned}$$

Hence, $\tilde{E}$ is a fixed point of $\Phi^{\mathcal{P}}$.

2. We next show that if $\tilde{E}$ satisfying (2.6) is the greatest fixed point of Φ, then it is also the greatest fixed point of $\Phi^{\mathcal{P}}$. Let $\tilde{E}^{\mathcal{P}}$ be the greatest fixed point of $\Phi^{\mathcal{P}}$. Since $\tilde{E}$ is a fixed point of $\Phi^{\mathcal{P}}$, we have $\tilde{E} \leq \tilde{E}^{\mathcal{P}}$ and $0 \leq \tilde{E}_i \leq \tilde{E}_i^{\mathcal{P}}$ for all $i \in \mathcal{P}$ by (2.6). Therefore, $\{i \in \mathcal{P} \mid \tilde{E}_i^{\mathcal{P}} < 0\} = \emptyset$. It follows that $\tilde{E}^{\mathcal{P}}$ is also a fixed point of Φ (see the proof of Proposition 2.4.5) and hence $\tilde{E}^{\mathcal{P}} \leq \tilde{E}$. This implies $\tilde{E} = \tilde{E}^{\mathcal{P}}$. Furthermore, under these greatest re-valuated equities,

$$\mathcal{D}(L, A^b; \mathbb{V}) = \{i \in \mathcal{N} \mid \tilde{E}_i < 0\} = \mathcal{D}(L^{\mathcal{P}}, A^b; \mathbb{V}),$$

so there is systemic risk reduction but no strong reduction.

□

A.2.4 Proof of Theorem 2.5.1

We use Lemma A.2.5 to prove Theorem 2.5.1.

Lemma A.2.5. Consider the FPA (Algorithm 1) and the LA (Algorithm 2) for a given financial network. Fix an iteration $t \in \mathbb{N}_0$. Then

$$\bigcup_{s=0}^{t+1} \mathcal{A}(s) = \mathcal{S}^{(t)}, \tag{A.2.4}$$

i.e., the banks that make payments in the FPA up to time $t+1$ are identical to those that make payments in the LA up to time $t+1$.

Proof of Lemma A.2.5. We prove the result by induction. Let $t = 0$. By plugging the initial values of Algorithm 1 into equations (A.1.1) and (A.1.2), we get

$$\bigcup_{s=0}^{1} \mathcal{A}(s) = \mathcal{A}(0) \cup (\mathcal{A}(1) \setminus \mathcal{A}(0)) = \mathcal{A}(1) = \{i \in \mathcal{N} \mid e_i(1) \geq \bar{L}_i\} = \{i \in \mathcal{N} \mid A_i^b \geq \bar{L}_i\}$$

and

$$\mathcal{S}^{(0)} = \{i \in \mathcal{N} \mid A_i^b - \bar{L}_i \geq 0\}.$$

Therefore, $\bigcup_{s=0}^{1} \mathcal{A}(s) = \mathcal{S}^{(0)}$.

Now suppose (A.2.4) holds for a fixed $t \in \mathbb{N}$. We show that it also holds for $t+1$, i.e., $\bigcup_{s=0}^{t+2} \mathcal{A}(s) = \mathcal{S}^{(t+1)}$. Because

$$\bigcup_{s=0}^{t+2} \mathcal{A}(s) = \bigcup_{s=0}^{t+1} \mathcal{A}(s) \cup \mathcal{A}(t+2), \quad \mathcal{S}^{(t+1)} = \mathcal{S}^{(t)} \cup \left(\mathcal{S}^{(t+1)} \setminus \mathcal{S}^{(t)}\right),$$

it is sufficient to prove $\mathcal{A}(t+2) = \mathcal{S}^{(t+1)} \setminus \mathcal{S}^{(t)}$. According to Algorithm 1, we can write

$e_i(t+1)$ as

$$\begin{aligned} e_i(t+1) &= e_i(t) + \sum_{j\in\mathcal{N}} l_j(t)\Pi_{ji} - l_i(t) \\ &= e_i(t-1) + \sum_{j\in\mathcal{N}} l_j(t-1)\Pi_{ji} - l_i(t-1) + \sum_{j\in\mathcal{N}} l_j(t)\Pi_{ji} - l_i(t) \\ &= \cdots \\ &= A_i^b + \sum_{j\in\mathcal{N}} \Pi_{ji} \sum_{s=0}^{t} l_j(s) - \sum_{s=0}^{t} l_i(s). \end{aligned}$$

By steps 3-7 in Algorithm 1, $\sum_{s=0}^{t} l_j(s) > 0$ implies $j \in \bigcup_{s=0}^{t} \mathcal{A}(s)$. It follows that

$$e_i(t+1) = A_i^b + \sum_{j\in\bigcup_{s=0}^{t}\mathcal{A}(s)} \Pi_{ji} \sum_{s=0}^{t} l_j(s) - \sum_{s=0}^{t} l_i(s).$$

Because $\sum_{s=0}^{t} l_j(s) = \bar{L}_j$ for all $j \in \bigcup_{s=0}^{t} \mathcal{A}(s)$, the equation above can be rewritten as

$$e_i(t+1) = A_i^b + \sum_{j\in\bigcup_{s=0}^{t}\mathcal{A}(s)} \bar{L}_j\Pi_{ji} - \sum_{s=0}^{t} l_i(s).$$

First, we show that $\mathcal{S}^{(t+1)} \setminus \mathcal{S}^{(t)} \subseteq \mathcal{A}(t+2)$. Let $i \in \mathcal{S}^{(t+1)} \setminus \mathcal{S}^{(t)}$. By the induction hypothesis, $i \notin \bigcup_{s=0}^{t+1} \mathcal{A}(s)$, which implies that $\sum_{s=0}^{t+1} l_i(s) = 0$. Note that equation (A.1.3) at $t+1$ is written as

$$v_i^{(t+1)} = A_i^b + \sum_{j\in\mathcal{N}} l_j^{(t+1)}\Pi_{ji} - \bar{L}_i = A_i^b + \sum_{j\in\mathcal{S}^{(t)}} \bar{L}_j\Pi_{ji} - \bar{L}_i.$$

Therefore, we obtain

$$\begin{aligned} 0 \leq v_i^{(t+1)} &= A_i^b + \sum_{j \in \mathcal{S}^{(t)}} \bar{L}_j \Pi_{ji} - \bar{L}_i - \sum_{s=0}^{t+1} l_i(s) \\ &= A_i^b + \sum_{j \in \bigcup_{s=0}^{t+1} \mathcal{A}(s)} \bar{L}_j \Pi_{ji} - \sum_{s=0}^{t+1} l_i(s) - \bar{L}_i \\ &= e_i(t+2) - \bar{L}_i. \end{aligned}$$

Hence, $i \in \mathcal{A}(t+2)$.

Second, we show that $\mathcal{A}(t+2) \subseteq \mathcal{S}^{(t+1)} \setminus \mathcal{S}^{(t)}$. Let $i \in \mathcal{A}(t+2)$. Again, by the induction hypothesis, $i \notin \bigcup_{s=0}^{t+1} \mathcal{A}(s)$, which implies that $\sum_{s=0}^{t+1} l_i(s) = 0$. It follows that

$$\begin{aligned} 0 \leq e_i(t+2) - \bar{L}_i = A_i^b + \sum_{j \in \bigcup_{s=0}^{t+1} \mathcal{A}(s)} \bar{L}_j \Pi_{ji} - \sum_{s=0}^{t+1} l_i(s) - \bar{L}_i \\ = A_i^b + \sum_{j \in \mathcal{S}^{(t)}} \bar{L}_j \Pi_{ji} - \bar{L}_i = v_i^{(t+1)}. \end{aligned}$$

Hence, $i \in \mathcal{S}^{(t+1)} \setminus \mathcal{S}^{(t)}$. □

Proof of Theorem 2.5.1. Suppose that $\mathcal{A}(t) = \emptyset$ at iteration $t > 0$. Then $\tilde{l}_\star = \sum_{s=0}^{t-1} l(s)$, where $\tilde{l}_{\star,i} = \bar{L}_i$ if $i \in \bigcup_{s=0}^{t-1} \mathcal{A}(s)$ and 0 otherwise. Since $\bigcup_{s=0}^{t-1} \mathcal{A}(s) = \mathcal{S}^{(t-2)}$ by Lemma A.2.5, $\mathcal{A}(t) = \emptyset$ is equivalent to $\mathcal{D}^{(t)} = \mathcal{D}^{(t-1)}$ in the LA. Furthermore, the LA returns $l_\star = l^{(t-1)}$, where $l_{\star,i} = \bar{L}_i$ if $i \in \mathcal{S}(t-2)$ and 0 otherwise.

Therefore, both algorithms terminate when the same set of banks are selected, leading to the identical clearing payment vector. According to Rogers & Veraart (2013), the LA generates a sequence of vectors increasing to the least clearing vector, so the statement follows immediately. □

A.2.5 Proof of Theorem 2.5.3

We use Lemma A.2.6 to prove Theorem 2.5.3. Its proof is based on a modification of the proof of Proposition 4.12 in Veraart (2022).

Lemma A.2.6. Consider a PTN-exercise $(L, \mathcal{P}, L^{\mathcal{P}})$ that satisfies (2.10). Let $E^{(n)} \in \mathcal{E}$ and $E^{\mathcal{P}(n)} \in \mathcal{E}^{\mathcal{P}}$ be such that $E^{\mathcal{P}(n)} \geq E^{(n)}$. Then,

$$\Phi_i^{\mathcal{P}}(E^{\mathcal{P}(n)}; \mathbb{V}^{\text{zero}}) \geq \Phi_i(E^{(n)}; \mathbb{V}^{\text{zero}}) \quad \forall\, i \in \mathcal{N}.$$

Proof of Lemma A.2.6. Note that if $E^{\mathcal{P}(n)} \geq E^{(n)}$, then

$$\mathbb{1}_{\{E_j^{\mathcal{P}(n)} \geq 0\}} \geq \mathbb{1}_{\{E_j^{(n)} \geq 0\}} \quad \forall\, j \in \mathcal{N}. \tag{A.2.5}$$

First, let $i \in \mathcal{N} \setminus \mathcal{P}$. Then,

$$\begin{aligned}
\Phi_i^{\mathcal{P}}(E^{\mathcal{P}(n)}; \mathbb{V}^{\text{zero}}) &= A_i^b + \sum_{j \in \mathcal{M}^{\mathcal{P}}} L_{ji}^{\mathcal{P}} \mathbb{V}^{\text{zero}} \left(\frac{E_j^{\mathcal{P}(n)} + \bar{L}_j^{\mathcal{P}}}{\bar{L}_j^{\mathcal{P}}} \right) - \bar{L}_i^{\mathcal{P}} \\
&= A_i^b + \sum_{j \in \mathcal{N}} L_{ji} \mathbb{1}_{\{E_j^{\mathcal{P}(n)} \geq 0\}} - \bar{L}_i.
\end{aligned}$$

Inequality (A.2.5) leads to

$$\begin{aligned}
\Phi_i^{\mathcal{P}}(E^{\mathcal{P}(n)}; \mathbb{V}^{\text{zero}}) &\geq A_i^b + \sum_{j \in \mathcal{N}} L_{ji} \mathbb{1}_{\{E_j^{(n)} \geq 0\}} - \bar{L}_i \\
&= A_i^b + \sum_{j \in \mathcal{M}} L_{ji} \mathbb{V}^{\text{zero}} \left(\frac{E_j^{(n)} + \bar{L}_j}{\bar{L}_j} \right) - \bar{L}_i \\
&= \Phi_i(E^{(n)}; \mathbb{V}^{\text{zero}}).
\end{aligned}$$

Second, let $i \in \mathcal{P}$. Then by (A.2.5),

$$\Phi_i^{\mathcal{P}}(E^{\mathcal{P}(n)}; \mathbb{V}^{\text{zero}}) = A_i^b + \sum_{j \in \mathcal{N}} L_{ji}^{\mathcal{P}} \mathbb{1}_{\{E_j^{\mathcal{P}(n)} \geq 0\}} - \bar{L}_i^{\mathcal{P}} \geq A_i^b + \sum_{j \in \mathcal{N}} L_{ji}^{\mathcal{P}} \mathbb{1}_{\{E_j^{(n)} \geq 0\}} - \bar{L}_i^{\mathcal{P}}.$$

Moreover, by (A.2.2),

$$\begin{aligned}
\Phi_i^{\mathcal{P}}(E^{\mathcal{P}(n)}; \mathbb{V}^{\text{zero}}) &\geq A_i^b + \sum_{j \in \mathcal{N} \setminus \mathcal{P}} \underbrace{L_{ji}^{\mathcal{P}}}_{=L_{ji}} \mathbb{1}_{\{E_j^{(n)} \geq 0\}} + \sum_{j \in \mathcal{P}} L_{ji}^{\mathcal{P}} \mathbb{1}_{\{E_i^{(n)} \geq 0\}} - \bar{L}_i^{\mathcal{P}} \\
&= A_i^b + \sum_{j \in \mathcal{N} \setminus \mathcal{P}} L_{ji} \mathbb{1}_{\{E_j^{(n)} \geq 0\}} + \sum_{j \in \mathcal{P}} L_{ji}^{\mathcal{P}} \mathbb{1}_{\{E_j^{(n)} \geq 0\}} - \bar{L}_i + \sum_{j \in \mathcal{P}} L_{ji} - \sum_{j \in \mathcal{P}} L_{ji}^{\mathcal{P}} \\
&= A_i^b + \sum_{j \in \mathcal{N}} L_{ji} \mathbb{1}_{\{E_j^{(n)} \geq 0\}} - \bar{L}_i + \sum_{j \in \mathcal{P}} \underbrace{(L_{ji} - L_{ji}^{\mathcal{P}})}_{\geq 0 \text{ by (2.10)}} (1 - \mathbb{1}_{\{E_j^{(n)} \geq 0\}}) \\
&\geq A_i^b + \sum_{j \in \mathcal{N}} L_{ji} \mathbb{1}_{\{E_j^{(n)} \geq 0\}} - \bar{L}_i \\
&= A_i^b + \sum_{j \in \mathcal{N}: \bar{L}_j > 0} L_{ji} \mathbb{V}^{\text{zero}} \left(\frac{E_j^{(n)} + \bar{L}_j}{\bar{L}_j} \right) - \bar{L}_i = \Phi_i(E^{(n)}; \mathbb{V}^{\text{zero}}).
\end{aligned}$$

Taken together, $\Phi_i^{\mathcal{P}}(E^{\mathcal{P}(n)}; \mathbb{V}^{\text{zero}}) \geq \Phi_i(E^{(n)}; \mathbb{V}^{\text{zero}})$ for all $i \in \mathcal{N}$. □

Proof of Theorem 2.5.3. First, we prove inequality (2.11) for the greatest equilibrium. As in the proof of Proposition 4.12 in Veraart (2022), we consider a fixed point iteration. Let $\tilde{E}^{(0)} = E^{\text{initial}}(L)$ and $\tilde{E}^{\mathcal{P}(0)} = E^{\text{initial}}(L^{\mathcal{P}})$. We define the sequences $(\tilde{E}^{(n)})_{n \in \mathbb{N}_0}$ and $(\tilde{E}^{\mathcal{P}(n)})_{n \in \mathbb{N}_0}$ recursively under $\mathbb{V} = \mathbb{V}^{\text{zero}}$ as in Lemma A.2.3. Then, using Lemma A.2.6, we can show by induction that $\tilde{E}^{\mathcal{P}(n)} \geq \tilde{E}^{(n)}$ for all $n \in \mathbb{N}_0$. Finally, Lemma A.2.3 implies that for all $i \in \mathcal{N}$, $E_i^{\mathcal{P};*} = \lim_{n \to \infty} \tilde{E}_i^{\mathcal{P}(n)} \geq \lim_{n \to \infty} \tilde{E}_i^{(n)} = E_i^*$, where E^* and $E^{\mathcal{P};*}$ are the greatest re-valuated equity in the original network and the PTN-network, respectively.

Second, we prove inequality (2.11) for the least equilibrium. Let $E^{(0)} = A^b - \bar{L}$. Define the sequence $(E^{(n)})_{n \in \mathbb{N}_0}$ recursively by $E^{(n)} = \Phi(E^{(n-1)}; \mathbb{V}^{\text{zero}})$. We show by

induction that it is a non-decreasing sequence, i.e.,

$$E_i^{(n+1)} \geq E_i^{(n)} \quad \forall\, i \in \mathcal{N}. \tag{A.2.6}$$

Let $n = 0$. It follows directly from the definition of Φ that for all $i \in \mathcal{N}$,

$$E_i^{(1)} = \Phi_i(E^{(0)}; \mathbb{V}^{\text{zero}}) = A_i^b + \underbrace{\sum_{j \in \mathcal{N}: \bar{L}_j > 0} L_{ji} \mathbb{V}^{\text{zero}} \left(\frac{E_j^{(0)} + \bar{L}_j}{\bar{L}_j} \right)}_{\geq 0} - \bar{L}_i \geq E_i^{(0)}.$$

Now fix $n \in \mathbb{N}$ and assume that $E^{(n)} \geq E^{(n-1)}$. Then for all $i \in \mathcal{N}$,

$$E_i^{(n+1)} = A_i^b + \sum_{j \in \mathcal{N}: \bar{L}_j > 0} L_{ji} \underbrace{\mathbb{V}^{\text{zero}} \left(\frac{E_j^{(n)} + \bar{L}_j}{\bar{L}_j} \right)}_{\geq \mathbb{V}^{\text{zero}} \left(\frac{E_j^{(n-1)} + \bar{L}_j}{\bar{L}_j} \right)} - \bar{L}_i \geq \Phi_i(E^{(n-1)}; \mathbb{V}^{\text{zero}}) = E_i^{(n)}, \tag{A.2.7}$$

which completes the induction proof. Then, let $E^{\mathcal{P}(0)} = A^b - \bar{L}^{\mathcal{P}}$. As above, we can show that the sequence $(E^{\mathcal{P}(n)})_{n \in \mathbb{N}_0}$ defined by $E^{\mathcal{P}(n)} = \Phi^{\mathcal{P}}(E^{\mathcal{P}(n-1)}; \mathbb{V}^{\text{zero}})$ is non-decreasing (we omit the details). Hence, both $(E^{(n)})_{n \in \mathbb{N}_0}$ and $(E^{\mathcal{P}(n)})_{n \in \mathbb{N}_0}$ converge to a limit because they are non-decreasing and bounded from above.

Next, we prove by induction that

$$E^{\mathcal{P}(n)} \geq E^{(n)} \quad \forall\, n \in \mathbb{N}_0. \tag{A.2.8}$$

For $n = 0$, since the PTN-exercise satisfies (2.10), we have $\bar{L}^{\mathcal{P}} \leq \bar{L}$ and therefore $E^{\mathcal{P}(0)} = A^b - \bar{L}^{\mathcal{P}} \geq A^b - \bar{L} = E^{(0)}$. Now fix $n \in \mathbb{N}$. The induction step follows directly from Lemma A.2.6. Hence, we obtain that

$$\lim_{n \to \infty} E_i^{\mathcal{P}(n)} \geq \lim_{n \to \infty} E_i^{(n)} \quad \forall\, i \in \mathcal{N}.$$

If $\lim_{n\to\infty} E^{\mathcal{P}(n)}$ is a fixed point of $\Phi^{\mathcal{P}}$ and $\lim_{n\to\infty} E^{(n)}$ is a fixed point of $\Phi^{\mathcal{P}}$, then there is nothing left to prove. However, since $\mathbb{V}^{\text{zero}}$ is not left-continuous, there is no guarantee that $\lim_{n\to\infty} E^{(n)}$ is a fixed point of Φ or that $\lim_{n\to\infty} E^{\mathcal{P}(n)}$ is a fixed point of $\Phi^{\mathcal{P}}$.

As discussed in Section 3.1 in Rogers & Veraart (2013), if one of the limit is not a fixed point, then one will need to restart the iteration from this limit. For $n \in \mathbb{N}_0$, we set

$$\hat{E}_{(0)} = \lim_{m\to\infty}(E^{(m)}), \quad \hat{E}_{(n+1)} = \Phi(\hat{E}_{(n)}),$$
$$\hat{E}_{\mathcal{P}(0)} = \lim_{m\to\infty}(E^{\mathcal{P}(m)}), \quad \hat{E}_{\mathcal{P}(n+1)} = \Phi(\hat{E}_{\mathcal{P}(n)}).$$

Then, we repeat the previous arguments. If the initial element of such a sequence ($\hat{E}_{(0)}$ or $\hat{E}_{\mathcal{P}(0)}$) is a fixed point, then the sequence is just constant. The situation that the limit is not a fixed point can only occur at a point where a bank just becomes solvent in the limit. This can happen at most N times since there are N banks, meaning at most $N-1$ restarts of this fixed point iteration could become necessary, as discussed in Rogers & Veraart (2013). Then, after at most $N-1$ restarts, the limits of the iterations are indeed the least fixed points. If we need to restart the iteration, the same argument can be used to show the equivalence of (A.2.8) for the next two sequences. This sequence of arguments can be repeated until the fixed points are obtained. □

Appendix B

Appendix for Chapter 3

B.1 An index for mutual funds

This section demonstrates how to construct an index of vulnerability for mutual funds. It builds on the Cetorelli et al. (2016) model, which applies the setting of Greenwood et al. (2015) in the context of fund redemptions.

Specifically, there are N funds and K asset classes; each fund has total assets a_n, average duration d_n, and flow-performance sensitivity b_n.[1] After an interest rate shock Δr, fund n experiences a negative return of $d_n \Delta r$ on its total assets. Since the investors are sensitive to funds' performance, fund n with decreasing asset values suffers from investors' redemptions, i.e., outflows $b_n d_n \Delta r$. In response, fund n sells its assets proportionately to its original holdings, represented by the asset matrix $M = (m_{nk})$, where m_{nk} is the fraction of asset k in fund n's total assets. By assumption, the price impact of asset k's liquidation is linear and has no effect on other asset classes, so the matrix L that characterises price impacts is diagonal, i.e., $L = \text{diag}(l_1, \ldots, l_N)$. Finally,

[1] The use of b_n follows the notation in Cetorelli et al. (2016). The notation in this section should not be confused with that of the Greenwood et al. (2015) model; the meaning is clear from the context.

the total spillover losses in the system is given by

$$\mathrm{SL} = \mathbf{1}^\top AMLM^\top ABDF,$$

where $A = \mathrm{diag}(a_1, \ldots, a_N)$, $B = \mathrm{diag}(b_1, \ldots, b_N)$, $D = \mathrm{diag}(d_1, \ldots, d_N)$, and $F = (\Delta r)\mathbf{1}$.

Next, I show how to derive an index similar to what have been done in Section 3.2. Consider a system with homogeneous portfolio allocations by setting

$$m_{nk}^{\mathrm{H}} = \frac{v_k}{\sum_j v_j} =: m_k \quad \forall\, k,$$

where $v_k = \sum_n a_n m_{nk}$ is the value of asset k. Then, the decomposition of SL can be written as

$$\mathrm{SL} = \sum_n a_n \times \sum_n a_n b_n d_n \times \sum_k l_k m_k^2 \times \frac{\mathrm{SL}}{\mathrm{SL}^{\mathrm{H}}},$$

where SL^{H} is the total spillover losses in the hypothetical system. (The constant shock Δr is dropped from the expression.) Accordingly, the vulnerability index can be defined as $\sum_n a_n \times \sum_n a_n b_n d_n \times \sum_k l_k m_k^2$, where the three terms capture system size, fund characteristics, and illiquidity concentration, respectively. Again, the index does not depend on portfolio composition at the individual level.[2]

[2]The decomposition in Cetorelli et al. (2016) follows Duarte & Eisenbach (2021). See Footnote 5.

B.2 FR Y-9C variables

Category		Consolidated (Schedual HC), Securites (Schedule HC-B), and Loans (Schedule HC-C)	Trading assets (Schedule HC-D)
Total assets	Entire sample	BHCK2170	
Equity	Up to 2013Q4	BHCK8274	
	2014Q1 - Present	BHCK8274 or BHCA8274	
Cash	Entire sample	BHCK0081 + BHCK0395 + BHCK0397	
U.S. Treasuries	Up to 2007Q4	BHCK0211 + BHCK1287	BHCK3531
	2008Q1 - Present	BHCK0211 + BHCK1287	BHCM3531
Agency securities	Up to 2007Q4	BHCK1289 + BHCK1293 + BHCK1294 + BHCK1298	BHCK3532
	2008Q1 - 2018Q1	BHCK1289 + BHCK1293 + BHCK1294 + BHCK1298	BHCM3532
	2018Q2 - Present	BHCKHT50 + BHCKHT53	BHCM3532
Municipal securities	Up to 2000Q4	BHCK8531 + BHCK8534 + BHCK8535 + BHCK8538	BHCK3533
	2001Q1 - 2007Q4	BHCK8496 + BHCK8499	BHCK3533
	2008Q1 - Present	BHCK8496 + BHCK8499	BHCM3533
Agency MBS	Up to 2007Q4	BHCK1698 + BHCK1702 + BHCK1703 + BHCK1707 + BHCK1714 + BHCK1717 + BHCK1718 + BHCK1732	BHCK3534 + BHCK3535
	2008Q1 - 2009Q1	BHCK1698 + BHCK1702 + BHCK1703 + BHCK1707 + BHCK1714 + BHCK1717 + BHCK1718 + BHCK1732	BHCM3534 + BHCM3535

	2009Q2 - 2010Q4	BHCKG300 + BHCKG303 + BHCKG304 + BHCKG307 + BHCKG312 + BHCKG315 + BHCKG316 + BHCKG319 + (BHCKG324 + BHCKG327 + BHCKG328 + BHCKG331)/2	BHCKG379 + BHCKG380 + (BHCKG382)/2
	2011Q1 - Present	BHCKG300 + BHCKG303 + BHCKG304 + BHCKG307 + BHCKG312 + BHCKG315 + BHCKG316 + BHCKG319 + BHCKK142 + BHCKK145 + BHCKK150 + BHCKK153	BHCKG379 + BHCKG380 + BHCKK197
Nonagency MBS	Up to 2007Q4	BHCK1709 + BHCK1713 + BHCK1733 + BHCK1736	BHCK3536
	2008Q1 - 2009Q1	BHCK1709 + BHCK1713 + BHCK1733 + BHCK1736	BHCM3536
	2009Q2 - 2010Q4	BHCKG308 + BHCKG311 + BHCKG320 + BHCKG323 + (BHCKG324 + BHCKG327 + BHCKG328 + BHCKG331)/2	BHCKG381 + (BHCKG382)/2
	2011Q1 - Present	BHCKG308 + BHCKG311 + BHCKG320 + BHCKG323 + BHCKK146 + BHCKK149 + BHCKK154 + BHCKK157	BHCKG381 + BHCKK198
ABS & other debt securities	Up to 2000Q4	BHCK8539 + BHCK8542 + BHCK8545 + BHCK8548	BHCK3537
	2001Q1 - 2005Q4	BHCKB838 + BHCKB841 + BHCKB842 + BHCKB845 + BHCKB846 + BHCKB849 + BHCKB850 + BHCKB853 + BHCKB854 + BHCKB857 + BHCKB858 + BHCKB861 + BHCK1737 + BHCK1741 + BHCK1742 + BHCK1746	BHCK3537
	2006Q1 - 2007Q4	BHCKC026 + BHCKC027 + BHCK1737 + BHCK1741 + BHCK1742 + BHCK1746	BHCK3537

	2008Q1 - 2009Q1	BHCKC026 + BHCKC027 +	BHCM3537
		BHCK1737 + BHCK1741 + BHCK1742 + BHCK1746	
	2009Q2 - 2018Q1	BHCKC026 + BHCKC027 + BHCKG336 + BHCKG339 +	BHCKG383 + BHCKG384 +
		BHCKG340 + BHCKG343 + BHCKG344 + BHCKG347 +	BHCKG385 + BHCKG386
		BHCK1737 + BHCK1741 + BHCK1742 + BHCK1746	
	2018Q2 - Present	BHCKC026 + BHCKC027 + BHCKHT58 + BHCKHT61 +	BHCKHT62 + BHCKG386
		BHCK1737 + BHCK1741 + BHCK1742 + BHCK1746	
Equities & other securities	Up to 2000Q4	BHCK8544 + BHCK8550 + BHCKA511	BHCK3541
	2001Q1 - 2007Q4	BHCKA511	BHCK3541
	2008Q1 - 2020Q3	BHCKA511	BHCM3541
	2020Q4 - Present		BHCM3541
Repo and fed funds sold	Up to 1996Q4	BHCK0276 + BHCK0277	
	1997Q1 - 2001Q4	BHCK1350	
	2002Q1 - Present	BHDMB987 + BHCKB989	
Residential real estate loans	Up to 2007 Q4	BHDM1797 + BHDM5367 + BHDM5368	
	2008Q1 - 2018Q1	BHDM1797 + BHDM5367 + BHDM5368	BHDMF606 + BHDMF607 + BHDMF611
	2018Q2 - Present	BHDM1797 + BHDM5367 + BHDM5368	BHCKHT63
Commercial real estate loans	Up to 2007Q4	BHDM1415 + BHDM1460 + BHDM1480	
	2008Q1 - 2018Q1	BHCKF158 + BHCKF159 + BHDM1460 + BHCKF160 + BHCKF161	BHDMF604 + BHDMF612 + BHDMF613

	2018Q2 - Present	BHCKF158 + BHCKF159 + BHDM1460 + BHCKF160 + BHCKF161	
Other real estate loans	Up to 2007Q4	BHCK1410 - all real estate loans above (from HC-C)	
	2008Q1 - 2018Q1	BHCK1410 - all real estate loans above (from HC-C)	BHCKF610 - all real estate loans above (from HC-D)
	2018Q2 - Present	BHCK1410 - all real estate loans above (from HC-C)	BHCKHT64
C & I loans	Up to 2007Q4	BHCK1763 + BHCK1764	
	2008Q1 - 2019Q3	BHCK1763 + BHCK1764	BHCKF614
	2019Q4 - Present	BHCK1763 + BHCK1764 + BHCKKX56	BHCKF614
Consumer loans	Up to 2000Q4	BHCK2008 + BHCK2011	
	2001Q1 - 2007Q4	BHCKB538 + BHCKB539 + BHCK2011	
	2008Q1 - 2010Q4	BHCKB538 + BHCKB539 + BHCK2011	BHCKF615 + BHCKF616 + BHCKF617
	2011Q1 - 2018Q1	BHCKB538 + BHCKB539 + BHCKK137 + BHCKK207	BHCKF615 + BHCKF616 + BHCKK199 + BHCKK210
	2018Q2 - Present	BHCKB538 + BHCKB539 + BHCKK137 + BHCKK207	BHCKHT65
Lease financings	Up to 2006Q4	BHCK2182 + BHCK2183	
	2007Q1 - 2019Q3	BHCKF162 + BHCKF163	
	2019Q4 - Present	BHCKF162 + BHCKF163 + BHCKKX58	
Residual loans	Up to 2007Q4	BHCK2122 - all loans above (from HC-C)	
	2008Q1 - Present	BHCK2122 - all loans above (from HC-C)	BHCKF618
Residual securities	Up to 2000Q4	BHCK1754 + BHCK1773 + BHCK8553 + BHCK8556 -	BHCK3545 - all securities above (from HC-D)

		all securities above (from HC-B)	
	2001Q1 - Present	BHCK1754 + BHCK1773 -	BHCK3545 - all securities above (from HC-D) -
		all securities above (from HC-B)	all loans above (from HC-D)
Residual assets	Entire sample	BHCK2170 - all assets above	

Notes: The following abbreviations are used: "Repo" is securities purchased under agreements to resell, "MBS" is mortgage-backed securities, "ABS" is agency-backed securities, "RRE" is residential real estate, and "C & I" is commercial and industrial. Firms that are required to report also include savings and loan holding companies, securities holding companies, etc. The report form is completed by firms on a quarterly basis with total assets over $150 million before 2006Q1, over $500 million between 2006Q1 and 2014Q4, over $1 billion between 2014Q4 and 2018Q3, and over $3 billion thereafter. I use amortised cost for held-to-maturity securities and fair value for available-for-sale securities. I categorise trading assets - securities from Schedule HC-D into corresponding categories under securities (HC-B). I categorise trading assets - loans from Schedule HC-D into corresponding categories under loans (HC-C). During 2009Q2–2010Q4, I follow Duarte & Eisenbach (2021) in allocating commercial MBS to agency MBS and nonagency MBS 50-50. I replace negative values of "ABS & other debt securities" and "Residual loans" with zero. The sample period is 1996Q1–2021Q4.

Bibliography

Acharya, V. V., Pedersen, L. H., Philippon, T. & Richardson, M. (2017). Measuring systemic risk. *The Review of Financial Studies* **30**, 2–47.

Adrian, T., Boyarchenko, N. & Giannone, D. (2019). Vulnerable growth. *American Economic Review* **109**, 1263–89.

Adrian, T. & Brunnermeier, M. K. (2016). CoVaR. *American Economic Review* **106**, 1705–1747.

Adrian, T., Covitz, D. & Liang, N. (2015). Financial stability monitoring. *Annual Review of Financial Economics* **7**, 357–395.

Adrian, T. & Shin, H. S. (2010). Liquidity and leverage. *Journal of Financial Intermediation* **19**, 418–437.

Aikman, D., Beale, D., Brinley-Codd, A., Hüser, A.-C., Covi, G. & Lepore, C. (2023). Macro-prudential stress test models: A survey. Bank of England Staff Working Paper No. 1037.

Allen, F. & Gale, D. (1994). Limited market participation and volatility of asset prices. *American Economic Review* **84**, 933–955.

Allen, F. & Gale, D. (2000). Financial contagion. *Journal of Political Economy* **108**, 1–33.

Amini, H. & Feinstein, Z. (2023). Optimal network compression. *European Journal of Operational Research* **306**, 1439–1455.

Amini, H., Filipović, D. & Minca, A. (2016). To fully net or not to net: Adverse effects of partial multilateral netting. *Operations Research* **64**, 1135–1142.

Amini, H. & Minca, A. (2020). Clearing financial networks: Impact on equilibrium asset prices and seniority of claims. In *Pushing the Boundaries: Frontiers in Impactful OR/OM Research*, 154–175, INFORMS.

Anderson, H., Paddrik, M. & Wang, J. J. (2019). Bank networks and systemic risk: Evidence from the National Banking Acts. *American Economic Review* **109**, 3125–3161.

Bai, J., Krishnamurthy, A. & Weymuller, C.-H. (2018). Measuring liquidity mismatch in the banking sector. *The Journal of Finance* **73**, 51–93.

Bank of England (2023). The Financial Policy Committee's approach to setting the countercyclical capital buffer – Policy Statement. Available at https://www.bankofengland.co.uk/paper/2023/ps/the-financial-policy-committees-approach-to-setting-the-countercyclical-capital-buffer.

Bardoscia, M., Ferrara, G., Vause, N. & Yoganayagam, M. (2019). Full payment algorithm. Available at SSRN: https://dx.doi.org/10.2139/ssrn.3344580.

Bardoscia, M., Ferrara, G., Vause, N. & Yoganayagam, M. (2021). Simulating liquidity stress in the derivatives market. *Journal of Economic Dynamics and Control* **133**.

Baron, M., Verner, E. & Xiong, W. (2021). Banking crises without panics. *The Quarterly Journal of Economics* **136**, 51–113.

Basel Committee on Banking Supervision (2010). Guidance for national authorities operating the countercyclical capital buffer. Bank for International Settlements.

Basel Committee on Banking Supervision (2014). Basel III: the net stable funding ratio. Bank for International Settlements.

Basel Committee on Banking Supervision (2017). Range of practices in implementing the countercyclical capital buffer policy. Bank for International Settlements. Available at https://www.bis.org/bcbs/publ/d407.pdf.

Basel Committee on Banking Supervision (2021). Early lessons from the Covid-19 pandemic on the Basel reforms. Bank for International Settlements. Available at https://www.bis.org/bcbs/publ/d521.pdf.

Bekaert, G., Engstrom, E. C. & Xu, N. R. (2022). The time variation in risk appetite and uncertainty. *Management Science* **68**, 3975–4004.

Benoit, S., Colliard, J.-E., Hurlin, C. & Pérignon, C. (2017). Where the risks lie: A survey on systemic risk. *Review of Finance* **21**, 109–152.

Berger, A. N. & Bouwman, C. H. (2009). Bank liquidity creation. *The Review of Financial Studies* **22**, 3779–3837.

Bernanke, B. S. (2012). Some reflections on the crisis and the policy response. Presented at the Russell Sage Foundation and The Century Foundation Conference on "Rethinking Finance", April 13, New York. https://www.federalreserve.gov/newsevents/speech/files/bernanke20120413a.pdf.

Bernanke, B. S. & Gertler, M. (1989). Agency costs, net worth, and business fluctuations. *American Economic Review* **79**, 14–31.

Bisias, D., Flood, M., Lo, A. W. & Valavanis, S. (2012). A survey of systemic risk analytics. *Annual Review of Financial Economics* **4**, 255–296.

Black, F. & Scholes, M. (1973). The pricing of options and corporate liabilities. *Journal of Political Economy* **81**, 637–654.

Borio, C. & Drehmann, M. (2009). Towards an operational framework for financial stability: "fuzzy" measurement and its consequences. BIS Working Paper No 284.

Borio, C., Drehmann, M. & Tsatsaronis, K. (2014). Stress-testing macro stress testing: does it live up to expectations? *Journal of Financial Stability* **12**, 3–15.

Borio, C. & Lowe, P. (2002). Asset prices, financial and monetary stability: exploring the nexus. BIS Working Papers, No 114.

Borio, C. & Zhu, H. (2012). Capital regulation, risk-taking and monetary policy: a missing link in the transmission mechanism? *Journal of Financial Stability* **8**, 236–251.

Börner, L. & Hatfield, J. W. (2017). The design of debt-clearing markets: Clearinghouse mechanisms in preindustrial Europe. *Journal of Political Economy* **125**, 1991–2037.

Brave, S. A. & Butters, R. A. (2012). Diagnosing the financial system: Financial conditions and financial stress. *International Journal of Central Banking* **8**, 191–239.

Brownlees, C. & Engle, R. F. (2017). SRISK: A conditional capital shortfall measure of systemic risk. *The Review of Financial Studies* **30**, 48–79.

Brunnermeier, M. K. (2009). Deciphering the liquidity and credit crunch 2007-2008. *Journal of Economic Perspectives* **23**, 77–100.

Brunnermeier, M. K., Gorton, G. & Krishnamurthy, A. (2012). Risk topography. In *NBER Macroeconomics Annual 2011* (eds. D. Acemoglu & M. Woodford), vol. 26, 149–176, University of Chicago Press, Chicago.

Brunnermeier, M. K. & Pedersen, L. H. (2009). Market liquidity and funding liquidity. *The Review of Financial Studies* **22**, 2201–2238.

Burns, A. F. & Mitchell, W. C. (1946). *Measuring Business Cycles*. National Bureau of Economic Research, New York.

Calomiris, C. W. (1993). Financial factors in the Great Depression. *Journal of Economic Perspectives* **7**, 61–85.

Calomiris, C. W. & Gorton, G. (1991). The origins of banking panics: models, facts, and bank regulation. In *Financial Markets and Financial Crises* (ed. R. G. Hubbard), 109–174, University of Chicago Press, Chicago.

Calomiris, C. W. & Wilson, B. (2004). Bank capital and portfolio management: The 1930s "capital crunch" and the scramble to shed risk. *The Journal of Business* **77**, 421–455.

Cetorelli, N., Duarte, F. & Eisenbach, T. M. (2016). Are asset managers vulnerable to fire sales? Liberty Street Economics blog, Federal Reserve Bank of New York, February 18.

Cifuentes, R., Ferrucci, G. & Shin, H. S. (2005). Liquidity risk and contagion. *Journal of the European Economic Association* **3**, 556–566.

Committee on the Global Financial System (2012). Operationalising the selection and application of macroprudential instruments. CGFS Papers No 48.

Cont, R. & Schaanning, E. (2019). Monitoring indirect contagion. *Journal of Banking & Finance* **104**, 85–102.

Csóka, P. & Herings, P. J.-J. (2018). Decentralized clearing in financial networks. *Management Science* **64**, 4681–4699.

Demirgüç-Kunt, A. & Detragiache, E. (2005). Cross-country empirical studies of systemic bank distress: a survey. *National Institute Economic Review* **192**, 68–83.

D'Errico, M. & Roukny, T. (2021). Compressing over-the-counter markets. *Operations Research* **69**, 1660–1679.

Detken, C., Weeken, O., Alessi, L., Bonfim, D., Boucinha, M. M., Castro, C., Frontczak, S., Giordana, G., Giese, J., Jahn, N., Kakes, J., Klaus, B., Lang, J. H., Puzanova, N. & Welz, P. (2014). Operationalising the countercyclical capital buffer: indicator selection, threshold identification and calibration options. ESRB Occasional Paper Series No. 5.

Drehmann, M., Borio, C. & Tsatsaronis, K. (2011). Anchoring countercyclical capital buffers: the role of credit aggregates. *International Journal of Central Banking* **7**, 189–240.

Duarte, F. & Eisenbach, T. M. (2021). Fire-sale spillovers and systemic risk. *The Journal of Finance* **76**, 1251–1294.

Duffie, D. (2018). Financial regulatory reform after the crisis: An assessment. *Management Science* **64**, 4835–4857.

Duffie, D. & Zhu, H. (2011). Does a central clearing counterparty reduce counterparty risk? *The Review of Asset Pricing Studies* **1**, 74–95.

Eisenberg, L. & Noe, T. H. (2001). Systemic risk in financial systems. *Management Science* **47**, 236–249.

Elenev, V., Landvoigt, T. & Van Nieuwerburgh, S. (2021). A macroeconomic model with financially constrained producers and intermediaries. *Econometrica* **89**, 1361–1418.

European Securities and Markets Authority (2020). Consultation Paper, Report on post trade risk reduction services with regards to the clearing obligation (EMIR Article 85(3a)). Available at https://www.esma.europa.eu/sites/default/files/library/esma70-151-2852_consultation_report_ptrr_services_-_article_853a_of_emir.pdf.

European Systemic Risk Board (2017). The macroprudential use of margins and haircuts. Available at https://www.esrb.europa.eu/pub/pdf/reports/170216_macroprudential_use_of_margins_and_haircuts.en.pdf.

European Systemic Risk Board (2018). The ESRB handbook on operationalising macroprudential policy in the banking sector. Available at https://www.esrb.europa.eu/pub/pdf/reports/esrb.report180115_handbook~c9160ed5b1.en.pdf.

Favara, G., Gilchrist, S., Lewis, K. F. & Zakrajšek, E. (2016). Updating the recession risk and the excess bond premium. FEDS Notes. Washington: Board of Governors of the Federal Reserve System, https://doi.org/10.17016/2380-7172.1836.

Financial Stability Board (2021). FSB Financial Stability Surveillance Framework. Available at https://www.fsb.org/wp-content/uploads/P300921.pdf.

Fisher, I. (1933). The debt-deflation theory of great depressions. *Econometrica* **1**, 337–357.

Friedman, M. & Schwartz, A. J. (1963). *A Monetary History of the United States, 1867-1960*. Princeton University Press, Princeton.

Frydman, C. & Xu, C. (2023). Banking crises in historical perspective. *Annual Review of Financial Economics* **15**, 265–290.

Gertler, M. & Gilchrist, S. (2018). What happened: Financial factors in the Great Recession. *Journal of Economic Perspectives* **32**, 3–30.

Ghamami, S., Glasserman, P. & Young, H. P. (2022). Collateralized networks. *Management Science* **68**, 2202–2225.

Giglio, S., Kelly, B. & Pruitt, S. (2016). Systemic risk and the macroeconomy: An empirical evaluation. *Journal of Financial Economics* **119**, 457–471.

Gilchrist, S. & Zakrajšek, E. (2012). Credit spreads and business cycle fluctuations. *American Economic Review* **102**, 1692–1720.

Glasserman, P., Moallemi, C. C. & Yuan, K. (2016). Hidden illiquidity with multiple central counterparties. *Operations Research* **64**, 1143–1158.

Glasserman, P. & Young, H. P. (2015). How likely is contagion in financial networks? *Journal of Banking & Finance* **50**, 383–399.

Glasserman, P. & Young, H. P. (2016). Contagion in financial networks. *Journal of Economic Literature* **54**, 779–831.

Gorton, G. & Metrick, A. (2012). Securitized banking and the run on repo. *Journal of Financial Economics* **104**, 425–451.

Greenwood, R., Hanson, S. G., Shleifer, A. & Sørensen, J. A. (2022). Predictable financial crises. *The Journal of Finance* **77**, 863–921.

Greenwood, R., Landier, A. & Thesmar, D. (2015). Vulnerable banks. *Journal of Financial Economics* **115**, 471–485.

International Monetary Fund (2009). *Global Financial Stability Report, April 2009*. International Monetary Fund, Washington, D.C.

International Monetary Fund (2010). The IMF-FSB Early Warning Exercise - design and methodological toolkit.

International Swaps and Derivatives Association (2012). Interest Rate Swaps Compression: A Progress Report. Available at https://www.isda.org/a/BeiDE/irs-compression-progress-report-feb-2012.pdf.

International Swaps and Derivatives Association (2022). ISDA letter on EMIR review. Available at https://www.isda.org/a/UE5gE/ISDA-Letter-on-EMIR-Review.pdf.

Jackson, J. P. & Manning, M. J. (2007). Comparing the pre-settlement risk implications of alternative clearing arrangements. Bank of England Working Paper No. 321.

Jordà, Ò., Richter, B., Schularick, M. & Taylor, A. M. (2021). Bank capital redux: solvency, liquidity, and crisis. *The Review of Economic Studies* **88**, 260–286.

Jurado, K., Ludvigson, S. C. & Ng, S. (2015). Measuring uncertainty. *American Economic Review* **105**, 1177–1216.

Kaminsky, G. L. & Reinhart, C. M. (1999). The twin crises: the causes of banking and balance-of-payments problems. *American Economic Review* **89**, 473–500.

Kindleberger, C. P. (1978). *Manias, Panics, and Crashes: A History of Financial Crises*. Basic Books, New York.

Kiyotaki, N. & Moore, J. (2002). Balance-sheet contagion. *American Economic Review* **92**, 46–50.

Koenker, R. & Bassett, G., Jr. (1978). Regression quantiles. *Econometrica* **46**, 33–50.

Koopmans, T. C. (1947). Measurement without theory. *The Review of Economics and Statistics* **29**, 161–172.

Krishnamurthy, A. & Muir, T. (2020). How credit cycles across a financial crisis. NBER Working Paper No. 23850.

Laeven, L. & Valencia, F. (2020). Systemic banking crises database II. *IMF Economic Review* **68**, 307–361.

Leontief, W. W. (1936). Quantitative input and output relations in the economic systems of the United States. *The Review of Economic Statistics* **18**, 105–125.

Lorenzoni, G. (2008). Inefficient credit booms. *The Review of Economic Studies* **75**, 809–833.

Mason, J. W. & Jayadev, A. (2014). "Fisher dynamics" in US household debt, 1929–2011. *American Economic Journal: Macroeconomics* **6**, 214–234.

Mian, A. & Sufi, A. (2018). Finance and business cycles: The credit-driven household demand channel. *Journal of Economic Perspectives* **32**, 31–58.

Minsky, H. P. (1964). Longer waves in financial relations: Financial factors in the more severe depressions. *American Economic Review* **54**, 324–335.

Mishkin, F. S. (1978). The household balance sheet and the Great Depression. *The Journal of Economic History* **38**, 918–937.

Mitchener, K. J. & Richardson, G. (2019). Network contagion and interbank amplification during the Great Depression. *Journal of Political Economy* **127**, 465–507.

O'Kane, D. (2017). Optimising the multilateral netting of fungible OTC derivatives. *Quantitative Finance* **17**, 1523–1534.

Paddrik, M., Rajan, S. & Young, H. P. (2020). Contagion in derivatives markets. *Management Science* **66**, 3603–3616.

Rajan, R. & Ramcharan, R. (2015). The anatomy of a credit crisis: The boom and bust in farm land prices in the United States in the 1920s. *American Economic Review* **105**, 1439–1477.

Reinhart, C. M. & Rogoff, K. S. (2009). *This Time Is Different : Eight Centuries of Financial Folly*. Princeton University Press, Princeton.

Rogers, L. C. G. & Veraart, L. A. M. (2013). Failure and rescue in an interbank network. *Management Science* **59**, 882–898.

Schularick, M. & Taylor, A. M. (2012). Credit booms gone bust: Monetary policy, leverage cycles, and financial crises, 1870-2008. *American Economic Review* **102**, 1029–61.

Schuldenzucker, S. & Seuken, S. (2020). Portfolio compression in financial networks: Incentives and systemic risk. Available at SSRN: https://dx.doi.org/10.2139/ssrn.3135960.

Shin, H. S. (2014). Procyclicality and the search for early warning indicators. In *Financial Crises: Causes, Consequences, and Policy Responses* (eds. S. Claessens, A. Kose, L. Laeven & F. Valencia), 157–171, International Monetary Fund, Washington, D.C.

Shleifer, A. & Vishny, R. W. (1992). Liquidation values and debt capacity: A market equilibrium approach. *The Journal of Finance* **47**, 1343–1366.

Shleifer, A. & Vishny, R. W. (2011). Fire sales in finance and macroeconomics. *Journal of Economic Perspectives* **25**, 29–48.

Stone, R. (1947). Definition and measurement of the national income and related totals. In *Measurement of National Income and the Construction of Social Accounts*, 21–113, United Nations, Geneva.

Sufi, A. & Taylor, A. M. (2022). Financial crises: a survey. In *Handbook of International Economics: International Macroeconomics* (eds. G. Gopinath, E. Helpman & K. Rogoff), vol. 6, 291–340, Elsevier, Amsterdam.

Tarski, A. (1955). A lattice-theoretical fixpoint theorem and its applications. *Pacific Journal of Mathematics* **5**, 285–309.

Upper, C. (2011). Simulation methods to assess the danger of contagion in interbank markets. *Journal of Financial Stability* **7**, 111–125.

Van Oordt, M. R. (2023). Calibrating the magnitude of the countercyclical capital buffer using market-based stress tests. *Journal of Money, Credit and Banking* **55**, 465–501.

Vause, N. (2010). Counterparty risk and contract volumes in the credit default swap market. BIS Quarterly Review, December.

Veraart, L. A. M. (2020). Distress and default contagion in financial networks. *Mathematical Finance* **30**, 705–737.

Veraart, L. A. M. (2022). When does portfolio compression reduce systemic risk? *Mathematical Finance* **32**, 727–778.

Wagner, W. (2011). Systemic liquidation risk and the diversity–diversification trade-off. *The Journal of Finance* **66**, 1141–1175.

White, E. N. (1983). *The Regulation and Reform of the American Banking System, 1900-1929*. Princeton University Press, Princeton.

Wicker, E. (1996). *The Banking Panics of the Great Depression*. Cambridge University Press, Cambridge.